



Norwegian University of
Science and Technology

Analysis of district heating systems integrating distributed sources

Mohammad Shakerin

Master of Science in Mechanical Engineering

Submission date: May 2017

Supervisor: Natasa Nord, EPT

Co-supervisor: Vittorio Verda, Politecnico di Torino

Norwegian University of Science and Technology
Department of Energy and Process Engineering

EPT-M-2016-178

MASTER THESIS

for

Mohammad Shakerin

Autumn 2016

Analysis of district heating systems integrating distributed sources

*Analyse av fjernvarmesystemer med distribuerte kilder***Background and objective**

Use of renewable energies and waste energy is highly necessary and required by national and international regulations. Future district heating and cooling systems will be based on completely renewable energies from solar, waste heat, and geothermal energy. This will imply that many distributed systems have to be available to deliver their heat to the central system. In this new situation, a building will be able to be user and supplier at the same time and therefore it may be called “prosumer”. The introduction of prosumers to the district heating (DH) system will affect both the DH network and the users. Therefore, models to explain interfaces between the energy supply and demand are critically important to enable transition to the renewable energy society. At the beginning these models should include DH network, heat users, and heat deliverers models. Within this project, the student should start with the network model for pressure and temperature distribution. The model should enable bidirectional flow. The model should be able to treat heat load changes on time frequency scale. Further development of the model, including different components and control in a simple way would be highly desirable. To work on the master thesis, the student should use MATLAB. As a start point, the student may analyze the DH ring at the university campus.

The objective is to develop the DH network model enabling connection of distributed heat sources. Primary, the work should focus on the network modeling together with the pressure and flow control.

The following tasks are to be considered:

1. Literature review on the following topic would be necessary: modelling DH network, modelling of bidirectional flow in a network, prosumers in the DH systems, distributed heat sources and storages, etc.
2. Develop the DH network model in MATLAB. A general model would be desirable. A model of the DH ring at the university campus would be also desirable.
3. Analysis the model by testing the model on different heat load profiles and different share of the distributed heat sources.
4. Analyse and discuss in detail problems with the pressure and flow control when including a high share of the distributed heat sources.
5. If possible, include simple models for the heat source and storage components.

6. Perform uncertainty analysis of the most critical parameters.
7. Analyse the results and define the most critical issues in the operation of the distributed systems.
8. Prepare material for a draft article.

-- ” --

Within 14 days of receiving the written text on the master thesis, the candidate shall submit a research plan for his project to the department.

When the thesis is evaluated, emphasis is put on processing of the results, and that they are presented in tabular and/or graphic form in a clear manner, and that they are analyzed carefully.

The thesis should be formulated as a research report with summary both in English and Norwegian, conclusion, literature references, table of contents etc. During the preparation of the text, the candidate should make an effort to produce a well-structured and easily readable report. In order to ease the evaluation of the thesis, it is important that the cross-references are correct. In the making of the report, strong emphasis should be placed on both a thorough discussion of the results and an orderly presentation.

The candidate is requested to initiate and keep close contact with his/her academic supervisor(s) throughout the working period. The candidate must follow the rules and regulations of NTNU as well as passive directions given by the Department of Energy and Process Engineering.

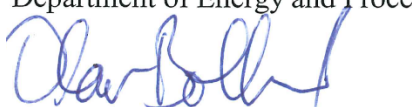
Risk assessment of the candidate's work shall be carried out according to the department's procedures. The risk assessment must be documented and included as part of the final report. Events related to the candidate's work adversely affecting the health, safety or security, must be documented and included as part of the final report. If the documentation on risk assessment represents a large number of pages, the full version is to be submitted electronically to the supervisor and an excerpt is included in the report.

Pursuant to “Regulations concerning the supplementary provisions to the technology study program/Master of Science” at NTNU §20, the Department reserves the permission to utilize all the results and data for teaching and research purposes as well as in future publications.

The final report is to be submitted digitally in DAIM. An executive summary of the thesis including title, student's name, supervisor's name, year, department name, and NTNU's logo and name, shall be submitted to the department as a separate pdf file. Based on an agreement with the supervisor, the final report and other material and documents may be given to the supervisor in digital format.

- Work to be done in lab (Water power lab, Fluids engineering lab, Thermal engineering lab)
- Field work

Department of Energy and Process Engineering, 16. September 2016



Olav Bolland
Department Head



Natasa Nord
Academic Supervisor

Research Advisor: Vittorio Verda, vittorio.verda@polito.it

Preface

This project is submitted as MSc Thesis at Norwegian University of Science and Technology. The research presented herein was conducted under supervision of Professor Natasa Nord in the department of Department of Energy and Process Engineering, Norwegian University of Science and Technology.

I would like to thank my supervisor Professor Natasa Nord for endless help, knowledge and support through every step of this project.



Mohammad Shakerin

Trondheim, May 2017

Abstract

Renewable energies sources are found to be the promising solution toward the prospect of environmental friendly and energy efficient societies. District heating systems play an important role concerning utilization of distributed renewable energy sources, as if national and international regulations are set for both decreasing heat energy demand and development of renewable energy production and efficient distribution in district heating and cooling systems. Waste heat from cooling datacentres and server aisles are considered to be reliable to utilize for district heating purposes, however there are still limitations in efficient integrating waste heat sources to main distribution networks. Therefore the aim of this study was to develop a general physical model of a district heating distribution network connected to various consumers and central heat production unit, able to carry bidirectional flow. Based on fundamental equations derived from continuum mechanics, two one dimensional models for hydraulic part and thermal part of the system was built. These models were coded in MATLAB software. As a case study district heating ring network of Gløshaugen campus of NTNU in Trondheim which has utilized the waste heat from a datacentre with annual 1 MW heat base load was used. Hourly quasi-static simulation of different cases which reflect different shares of integrating the waste heat source was done for analysing the network in presence of higher shares of distributed waste heat. Two scenarios were introduced in order to analyse and compare performance of the system when supply temperature and pumping system are controlled. The result showed that increasing contribution of waste heat source as a secondary heat provider could cause pressure balance problem in consumer substations near to it. However adopting variable speed control for the pump together with utilizing flow control valve at consumer substation could lower the pressure level within the network and decrease the pressure fluctuations near waste heat source. Lowering temperature levels lead to considerable heat energy saving in distribution pipes from 10% to 7%. Also average annual heat load and consequently annual energy obtained from the waste heat was significantly increased by 45%. Low temperature levels however was shown to have a drawback on the temperature of the heat harvested from the waste heat source and resulted in heat with up to 8°C lower temperature which is difficult to utilize. Despite of the assumptions and simplifications applied, the result still indicates main features, advantages and disadvantages of integrating waste heat sources.

Table of Contents

Preface	i
Abstract	ii
Figures	vi
Tables	viii
Abbreviations	ix
Symbols	x
1 Introduction.....	1
1.1 Importance of renewable heat sources in district heating systems	1
1.2 Future of district heating systems	4
1.3 Objective.....	6
1.4 Scope of the work	6
2 Literature review.....	7
2.1 Issues in integrating renewable heat sources to district heating systems	7
2.2 Introduction of prosumer	8
2.3 Modelling approaches in district heating systems	8
2.4 Simulation of district heating systems in presence of prosumer	10
3 Methodology	13
4 Theoretical background for modelling of district heating systems.....	15
4.1 Theory and principles	15
4.2 Conservation law	16
4.2.1 Continuity equation.....	16
4.2.2 Momentum equation	17

4.2.3	Internal energy equation.....	18
4.3	One dimensional model of a district heating network.....	20
4.3.1	Graph theory.....	21
4.3.2	Fluid dynamic model.....	23
4.3.3	Thermal model.....	26
4.3.4	Steady state condition.....	27
4.3.5	Solution methods.....	29
4.3.6	Unsteady state model.....	33
5	Case Study.....	36
5.1	Preliminary design.....	37
5.1.1	Thermal energy demand.....	37
5.1.2	Waste heat from datacenter.....	44
5.1.3	Mass flow rate of consumer substations in design condition.....	47
5.1.4	Pipe sizing.....	48
5.1.5	Incidence Matrix of Network.....	49
5.2	Assumption and constraints for fluid dynamic problem.....	52
5.3	Assumption and constraints for thermal problem.....	56
5.4	Scenarios for improvement of district heating control.....	58
5.4.1	Outdoor temperature compensation.....	59
5.4.2	Pressure difference control.....	60
5.4.3	Pump control.....	61
5.5	Waste heat integration measurement cases.....	63
6	Results.....	65
6.1	Reference scenario.....	65
6.1.1	Thermal characteristics of the network.....	65
6.1.2	Hydraulic analysis of the network.....	70
6.2	Outdoor temperature compensation scenario.....	75
6.3	Pump and valve control scenario.....	84
7	Discussion.....	87
8	Conclusion.....	89
9	Further work.....	91

Reference.....	93
10 Appendix.....	95
Implementation of SIMPLE algorithm and FIXED-POINT loop.....	95

Figures

Figure 1-1 Main parts of a district heating system [3]	2
Figure 1-2 Net production of district heating in Norway by type of heat central	3
Figure 4-1	16
Figure 4-2 Connection of nodes through directed branches	21
Figure 4-3 Control volume around the branch	24
Figure 4-4 Control volume at the junction of branches - Node	25
Figure 4-5	32
Figure 5-1 Gløshaugen campus of NTNU	36
Figure 5-2 Statistics of outdoor temperature and heat consumption from 2010 to 2016	38
Figure 5-3 Overall heat consumption of campus and out door temperature in 2016	39
Figure 5-4 Ground temperature and thermal energy loss	40
Figure 5-5 Hourly heat demand and out door temperature in 2016	40
Figure 5-6 Duration curve of outdoor temperature and heat load for NTNU	41
Figure 5-7 Heat demand of the campus Vs. Outdoor temperature in 2016	42
Figure 5-8 Location number and type of each building sorted by distance	43
Figure 5-9 Profile of heat request of users	44
Figure 5-10 Waste heat recovery through heat pump cycle	45
Figure 5-11 Molier diagram of heat pump cycle for Ammonia as refrigerant	46
Figure 5-12 Numeration of nodes an branches of supply pipe line	50
Figure 5-13 Numeration of nodes an branches of return pipe line	51
Figure 5-14 Characteristic curve of the pump, total head Vs. flow rate	54
Figure 5-15 System curve and charecteristic curve relation	54
Figure 5-16 Best efficiency point in charecteristic curve of the selected pump.	55
Figure 5-17 Adjustment of supply temperature proportional to outdoor temperature	59
Figure 5-18 Hydraulic resistances due to additional components	60
Figure 5-19 Working points of variable speed controlled pump	62
Figure 6-1 Temperature distribution for Reference scenario	66

Figure 6-2 Hourly temperature drop variation at user substation no. 24	66
Figure 6-3 Hourly heat power from waste heat source (Reference scenario)	67
Figure 6-4 Duration curve of heat power at datacenter substation (Reference scenario)	68
Figure 6-5 Temperature of the return water redirected to datacenter substation for al the cases of waste heat share (Reference scenario)	68
Figure 6-6 Hourly temperature levels at main heat production building	69
Figure 6-7 Hourly variation of heat power loss in the pipes (Reference scenario)	69
Figure 6-8 Pressure distribution Vs. nodes arranged by distance in design condition (Reference scenario)	70
Figure 6-9 Pumping power vs. number of hours.....	71
Figure 6-10 Hourly supply pressure variations at CHDB	72
Figure 6-11 Hourly variation of pumping power required by network (Reference scenario) .	72
Figure 6-12 Hourly Pressure gradient at node 37 (user substation no. 17) in reference scenario	73
Figure 6-13 Frequency of fail hydraulic balance at node 37 (user substation no. 17)	73
Figure 6-14 Hourly variation of waste heat outlet connection pressure	74
Figure 6-15 Hourly variation of waste heat inlet connection pressure	75
Figure 6-16 Temperature distribution vs. distance in OTCscenario	75
Figure 6-17 Hourly variation of temperature drop at user substation no.50	76
Figure 6-18 Temperature drop variation at user substation no.50	76
Figure 6-19 Hourly variation of heat power absorbed by waste heat source for OTC scenario	77
Figure 6-20 Hourly variation of temperature of redirected water to waste heat source	78
Figure 6-21 Heat power vs. number of hours.....	79
Figure 6-22 Hourly variation of water temperature at the outlet of waste heat source	80
Figure 6-23 Annual renewable waste heat production comparison	81
Figure 6-24 Hourly variation of supply and return temperature at main heat production building OTC scenario.....	82
Figure 6-25 Hourly variation of heat power loss in the pipes OTC scenario	83
Figure 6-26 Annual heat loss comparison.....	83
Figure 6-27 Pressure distribution in design condition for PC scenario.....	84
Figure 6-28 Waste heat inection pressure for PC scenario	84
Figure 6-29 Duration curve of pump input power for reference and PC scenario	85
Figure 6-30 Hourly pressure gradient at user substation (PC scenario).....	86

Tables

Table 5-1 thermal characteristics of buildings 43

Table 5-2 Important nodes reference 52

Table 5-3 Design parameters of the pump at best efficiency point (BEP)..... 55

Table 5-4 Test cases for reflecting different share of renewable energy source 63

Table 6-1 Waste heat recovery in Reference scenario 67

Table 6-2 Distribution energy losses in three cases 70

Table 6-3 Distribution energy losses in three cases OTC scenario 82

Table 6-4 Pump energy consumption in two scenarios 85

Abbreviations

Abbreviation	Definition
CHDB	Central Heat Distribution Building
DHS	District Heating Systems
OTC	Outdoor Temperature Compensation
PC	Pressure Control
RES	Renewable Energy Source
DHC	District Heating and Cooling
LTDH	Low Temperature District Heating

Symbols

Symbol	Definition	Unit
ρ	Density	kg/m ³
v	Velocity	m/s
P	Total pressure	bar
p	Static pressure	bar
T	Temperature	°C
g	Gravity	m/s ²
c_p	Specific heat capacity	kJ/kg.K
L	Length	m
S	Area	m ²
D	Diameter	m
A	Incidence matrix	-
β	Local loss factor	-
f	Friction factor	-
G	Mass flow rate	kg/s
M	Mass	kg
R	Hydraulic resistance	bar
Y	Hydraulic conductance	1/bar
Ω	perimeter	m
U	Overall heat transfer coefficient	W/m ² . °C
λ	Under-relaxation coefficient	-
φ	Heat load	W
V	Volume	m ³
\dot{V}	Volumetric flow rate	m ³ /h
η_p	Pump efficiency	-
η_t	Heat exchanger efficiency	-
w	Pump power	W
k	Heat exchanger hydraulic loss coefficient	1/m.kg
k_v	Valve hydraulic loss coefficient	[m.kg] ^{1/2}

N	Valve authority	-
n	Rotation speed	rpm
Q	Waste heat flux	W
r	Heat exchanger fluid ratio	-
t	Time	S
τ	Shear stress	bar
σ	Stress tensor	bar
h	Enthalpy	W/kg
z	Height	m

CHAPTER 1

Introduction

1.1 Importance of renewable heat sources in district heating systems

Increasing rate of greenhouse gas emissions together with scarcity of fossil based energy sources and prospect of future buildings role in energy sector have projected national and international regulations to put renewable energy sources into practice in order to achieve sustainable energy systems in the future. According to directive of the European parliament and the council on the promotion of the use of energy from renewable sources, the framework has been set an EU 20% target for renewable energy utilization until 2020. As a result of National Renewable Energy Action Plans for promoting investors and other economic operators, the rapid increase in the share of renewables from 10.4% in 2007 to 17% in 2015 is evident. The energy efficiency in the heating and cooling sector is generally planned through energy savings and renovation, especially in the building sector. In parallel, the heating and cooling options would motivate the fuel switching from fossil fuels to renewable energy in the heating and cooling sector, also covering the existing building stock [1].

District heating and cooling systems play a determinative role regarding new policies. In recent years the effect of DHC in future energy systems is consistently studied whether in a statistical or analytical approach with focus on parameters such as buildings heat energy demand, possibilities to use local renewable energy sources, design, control and management, etc. [2].

District heating system means the distribution of thermal energy in the form of steam or hot water from a central source of production to multiple buildings or sites. Thermal energy is used for space heating and domestic hot water or process heating. A DHS is consisted of a heat producer, a transmission network of pipelines for supply and return, and local substations in which heat from the DH water is transferred to the radiator circuit and the hot water circuit of the heat consumer. The DH network is called the primary side, and the consumer circuit including heat exchange utilities connected to DH are called the secondary side. Every substation is connected both to the supply and the return circuits of the DH system. Figure 1-1 shows three main parts of a DH system.

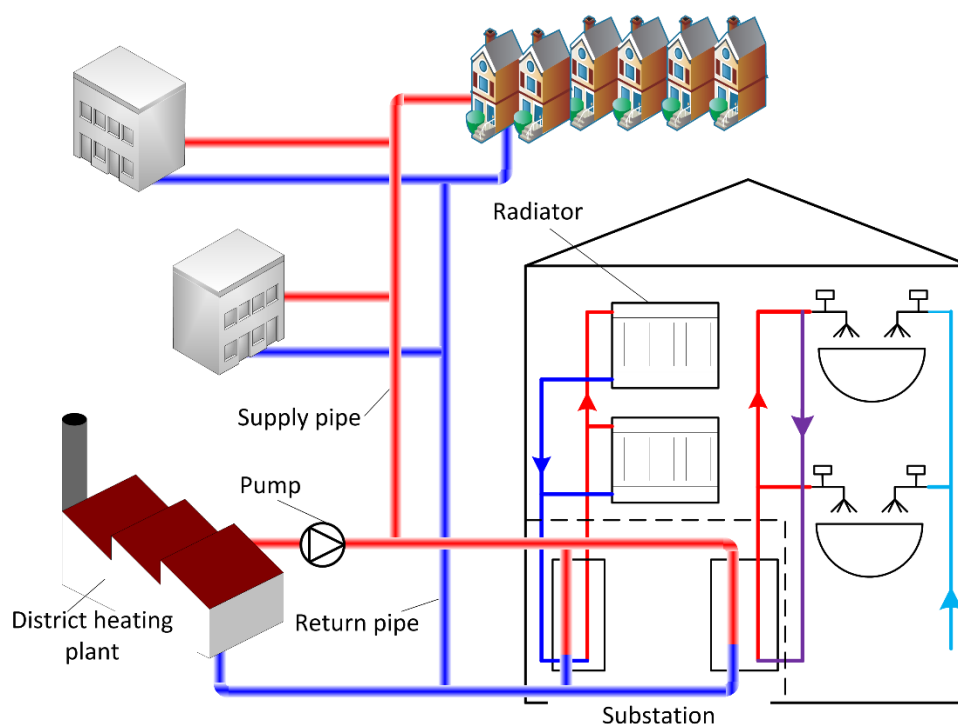


Figure 1-1 Main parts of a district heating system [3]

In 2012 the main fuel used in Europe was gas (40%), followed by coal (29%) and biomass (16%). District heating can integrate renewable electricity (through heat pumps), geothermal and solar thermal energy, waste heat and municipal waste. It can offer flexibility to the energy system through synergies between waste-to-energy processes and district heating/cooling which finally could provide a secure, renewable, and in some cases, more affordable energy comparing to fossil fuels [4]. Future of DHS is depicted as sustainable energy systems using 100% Renewable energy sources such as wind, solar, geothermal, waste heat, biomass energy,

etc. The new actor called "prosumer" are energy consumers able to act as distributed heat sources and cooperate in energy production by delivering heat into the main system. In this situation due to fluctuating energy sources a flexible energy management is needed [5].

Compared to individual heat production by end users, DHS are considered as a more reliable and efficient, and environmentally friendlier alternative solution for meeting space heating and domestic hot water demand of households, offices and industries. For example, a comparison of heat production by DHS and by individual heat production using electric boilers in Norway shows that DH solution will result in lower CO₂ emission [6]. Request for district heating in Norwegian buildings will be less in all types of buildings by up to 18% in 2050 [7]. This makes the efficient utilization of RES in DHS essential because DHS not only will still be the promising solution for most users but also should meet newly executed energy and environmental regulations as well. The statistics in Figure 1-2 shows production and consumption of district heating and district cooling in Norway in the past 10 years [8].

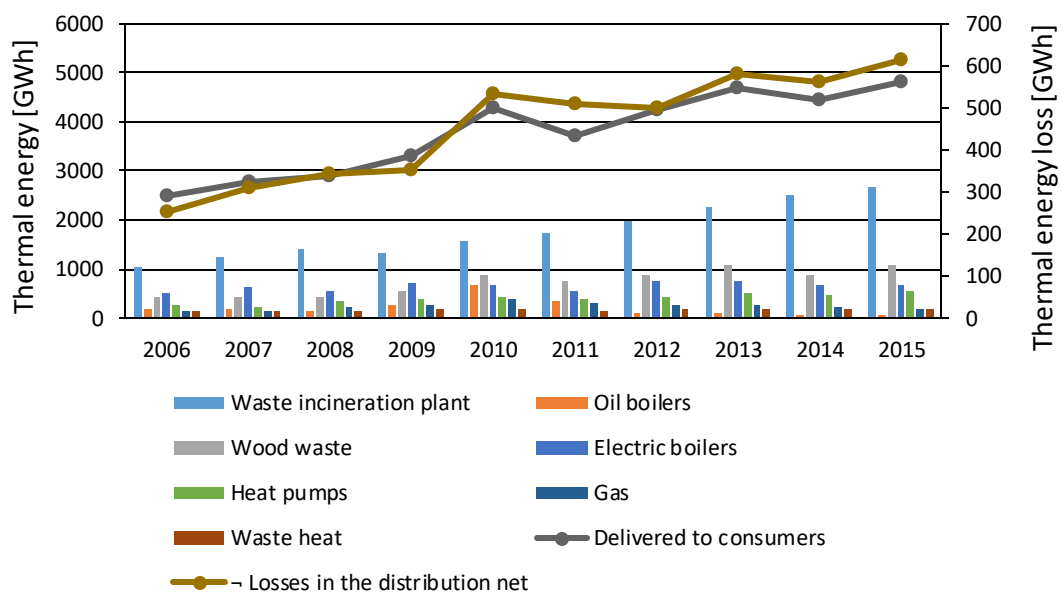


Figure 1-2 Net production of district heating in Norway by type of heat central

During the past ten years district heat energy consumptions has considerably increased, however heat produced by clean energy sources had a slight increase. Heating and cooling represents nearly half of the EU final energy use. The share of renewable energy in electricity has increased more than 8% points between 2009 and 2015, while the share of renewables in

the heating and cooling sector has only expanded by less than 3% in the same period. Therefore, an ambitious, but flexible, measure in this sector seem to be highly demanded [1].

1.2 Future of district heating systems

DHC are an enabler for higher shares of renewable energy in the EU energy system. There is a vast untapped potential for using industrial scale heat pumps in district heating and it is estimated that over 25% of the EU population live in areas suitable for geothermal district heating applications. Furthermore, DHS represents an important infrastructural technology to facilitate increased total conversion efficiencies of waste-to-energy plants.[4]

An option to increase renewable energy in the heating is to facilitate the uptake of renewable energy and waste heat in District Heating systems by utilizing best production sharing and energy performance measures to enable a better access to local heat sources. A close consideration to an additional reinforced consumer rights framework is also necessary. This option empowers consumers to produce renewable heat locally and use a renewable district heating system to create local synergies with other users and possibly disconnection of prosumer with additional local renewable heat production from previous DHS, thereby having a positive social impact. Analysis of the future application of such strategies shows the disconnection between 2020 and 2030 further contributing to climate change issues. Even though allowing disconnection could have negative effect on the economic planning of local district heating companies, these impacts would be compensated by the positive social and environmental impacts. In this option administrative burden will be directly associated to the level of penetration of district heating systems at national level. In particular, EU Member States with low share of district heating will face confined administrative burden and likely moderate disconnection probabilities [1].

The older district heating and cooling systems must develop to accommodate the increase of renewable energy shares. However, the current cost in district heating and cooling does not allow a transition to efficient and renewable energy supply. Energy management will require administrative supports in order to increase the profitability of integration of RES. Heat generation as a by-product from industries, waste heat from power stations, the service sector

and infrastructure such as metros or low grade waste heat from other reliable resources such as waste heat from cooling datacentres could be reused within plants or sold to heat buildings nearby. Heat-creating operations like datacentres might be paired with heat-consuming operations like district heating systems, creating a closed-loop system that has minimized waste. Datacentres act as huge electrical heaters fed with electrical energy and all this electrical energy is converted to thermal energy inside the datacentre and finally heats up the outdoor air. A growing number of datacentres are redirecting this excess heat to nearby facilities such as district heating plants or directly in heat distribution operations. The ability to re-use excess heat from servers is being built into new datacentres, helping to improve the energy efficiency profile of these facilities.

There are two considerable technical issues with datacentre waste heat reuse: the relatively low temperatures involved and the difficulty of transporting heat.

Many of the reuse applications to date have used the low-grade server exhaust heat in an application physically adjacent to the datacentre. To increase the temperature level datacentres operate with mechanical cooling such as heat pumps and provide more valuable, and marketable thermal energy as hot refrigerant at temperatures far better for heat recovery. Waste heat coming out of heat pumps at temperatures in the range of 55°C to 80°C can be transferred to a liquid medium for easier transport and can be used in district heating. The heat pumps appropriate for this type of work are highly efficient, and the energy used by the heat pumps gets added to the stream of energy moving to the heat user. A common design approach is to recover the rejected heat is using heat recovery condensers added to other cooling equipment. Depending on the application requirements such water temperatures combined with the quantity supplied may offer significant economic advantages.

The second problem is producer-consumer. A link between the producer of the thermal energy, the datacentre, and the consumer, applications that need the thermal energy for heating, is practically and in a large scale hardly possible today DHS could be a possibility, but there are not too many available and those operate with high temperature levels, however trend through all generations of district heating systems was mainly to reduce the distribution temperature in order to reduce heat losses within the pipe lines and thus more efficient heat production system. Therefore, a new generation of DHS should be LTDH in order to be able to comply with integrating such clean energy resources. The barriers to the use of these resources are lack of awareness; information on the resource available; insufficient business models and

motivations; a lack of heat networks; and lack of cooperation between waste heat generator unit and district heating companies.

1.3 Objective

Based on the future trends in DHS transition to renewable energy society depends on in depth understanding of the effect of prosumers and distributed heat production on the whole performance and efficiency of DHS.

By introducing the concept of prosumer in the mathematical models the interaction of centralized heat production with presence of a distributed heat source and consequent technical characteristics of the whole network such as time variant pressure and temperature distributions will be investigated. Further on different components and controls will be introduced to the model. The aim is to first develop the models for DHS that could treat the pressure and temperature distribution in the network and analyse possibilities of integrating different shares of distributed waste heat source.

1.4 Scope of the work

Gløshaugen university campus of NTNU in Trondheim Norway is considered as a case study to analyse the developed model, because the university has established its own heat distribution network. Gløshaugen campus DHS is a separated ring network which is connected to the main network of Trondheim by utilizing heat exchangers to receive heat from the main network and distribute it through the whole campus. This way, it is possible to control the supply and return temperature within the DH ring. Within this small-scale network it is also possible to utilize waste heat from cooling the datacentre by using heat pumps. The mathematical model will be implemented in MATLAB and different scenarios will be examined and compared.

CHAPTER 2

Literature review

During recent years integration of RES and distributed heat sources has been vastly studied with focus on different aspects.

2.1 Issues in integrating renewable heat sources to district heating systems

Future DHS integrated with RES must supply necessary heat with lower temperature grade in order to experience less grid losses and production cost. This is predictable, since general trend of buildings energy demand is decreasing and also new standards on renovation and fabricating methods are being applied in different countries. In this context interfaces between energy supply and demand could play an important role toward the transition to smart grid DHS. Interfaces in DHS are linkages between energy supply and consumer demand. Issues concerning enhancement of interfaces to be enabled to utilize are classified in hard and soft issues in [7]. Hard issues are structural aspects of DHS including energy supply models, pressure and temperature levels in the network, adaptability of consumer's substation and configuration of decentralized energy sources connection. Soft issues are related to pricing and business models, control concepts, optimization of energy supply and demand and energy measurements [7].

Decentralized systems are defined as system in which heat supply is distributed between several plants but centrally managed. Regarding problems with distribution of energy, studies on pipes

are highly necessary because in this situation pipes must be able to carry production fluxes in addition to consumption fluxes. Despite of limited range of available data for different operation conditions investigated in this research [7] it was revealed that heat losses through pipes in a DHS is less in bigger networks and is more when heat density is lower.

2.2 Introduction of prosumer

Within the scope of smart grid DHS, it is highly necessary to take into account the possibilities for available distributed RES to get integrated with the main systems. In this situation each building could be able to deliver its production into the grid which affects the business models and plans of DHS. The new actor “prosumer” who actually is a consumer able to export heat to main distribution network is introduced. In this situation characteristics of prosumer must be studied both in technical and financial aspects.

Introduction of prosumer and its effects was studied in [7] while a research on technical challenges of integrating prosumers with an already existed DHS in Malmö Sweden was conducted in [9]. DHS with presence of prosumers will have lower temperature levels because heat produced from RES has high thermal efficiency but at low temperature levels. Also utilization of RES and waste heat is more efficient with lower temperature levels within DHS. Increase in velocity within pipes are predictable when prosumers produce at their maximum, why pipe dimensioning is of a great importance in smart grid DHS.

Introduction of prosumer heat to the system causes pressure cones which dramatically affect consumers both near and far from prosumer substation. In order to be able to harvest more heat from prosumer it is suggested to maintain lower initial pressure gradient from main plant but this consideration may cause low pressure at customers not affected from prosumers [9].

2.3 Modelling approaches in district heating systems

Operation of the DHS is analysable once the physical characteristics involved in a DHS are modelled in a proper way. Including details and assumptions aligned with the reality of the operation leads to more accurate description of DHS and consequently better decision making. General theory behind the all researches concerning technical characteristics and behaviour of

DHS is based on hypotheses from continuum mechanics, however proper assumptions and design methods applied on each study.

A physical model in Matlab for dynamic analysis of a DHS was studied in [10]. Network structure consist of pipes, connections and substations is modelled using graph theory approach. Pressure drop and thermal losses are linked to pipes as flow and heat resistor. Considering constant return temperature controlled by flow control valve, consumer installations in the network are assumed as time varying thermal and hydraulic resistances. In hydraulic part of their model computations were optimized by Proper orthogonal decomposition (POD) approach which based on finding a set of orthogonal data that explains most of the dynamic behaviour of system. These set is obtained by monitoring time instances of flow in branches over a time period. Dynamic simulation of thermal behaviour is separated from hydraulic part due to difference in response time. Hydraulic balance in DHS is typically achieved in few seconds, however temperature changes may take hours to propagate from plant to consumers. This duration depends on velocity of water in the pipes which consequently should be resulted from hydraulic balance in network. By applying nodal method approach and using implicit backward method thermal part was solved for a case study. Despite the small average error, simulation showed to be hardly able to follow dynamic pattern of the network, more sever at costumers further away. This might have been because of lack detailed information about pipes.

Another model of a DHS that utilizes geothermal resources as centralized heat production solution is presented in [11]. Steady state and dynamic models of a DHS is developed in this research. Models of radiators, water as heat carrier, hydraulic and thermal losses in pipes and building heat storage were integrated into one model block. Finally a case study were simulated in Matlab in order to study behaviour of one costumer building. At first system characteristics were obtained from steady state model. Results of dynamic simulation shows that at maximum flow rates increase in radiator size is needed in order to cope with the required heat demand. This effect is more significant if maximum flow rate must keep unchanged. These models could reflect the reality with low average error, number of costumers to be considered has strong impact on results though.

Models of a DHS which can be coupled with RES and building energy simulations is presented in [12]. In this research programme spheat consist of 5 sub-programme is introduced. With a quasi-dynamic approach flow and pressures were calculated using static flow model in one sub

programme, while temperature is calculated in time variant model in its proper sub programme. Another sub program carries on the structure model of network which is developed from graph theory. Analogy of Kirchhoff's law of electric circuits is applied to this model in order to define relations able to compute flow rate and pressure in the network. Developed equations then solved by the application of standard numerical approaches. Dynamic values of Temperatures likewise are obtained in related sub programme by solving first law of thermodynamics applied on different nodes with finite difference method. Finally models were structured in Matlab in order to study performance of an existing DHS. Further optimizations were outdoor temperature compensation by outdoor temperature and control strategies of pump. Static pump control which is based on constant pressure difference between supply and return lines seemed not to be so advantageous as if extra pumping cost during low demand seasons were evident, while dynamic control strategy resulted in 40% saving in pump energy cost. Another development of network achieved by investigating consumer's distributions. The closer the high demand consumers are to the plant, the more saving of heat and pumping energy cost is potential. In a different situation assistance of solar collector in increasing temperature in the pipes were studied. Re-heating the supply temperature in this situation might not be advantageous, since inlet temperature is high, and heating return temperature and introducing it to supply line struggles with pressure gradients between supply and return lines.

2.4 Simulation of district heating systems in presence of prosumer

Depend on temperature levels of DHS prosumers connections may have different approaches. Installation configurations of a Substation connected to a decentralized production unit and able to carry bidirectional thermal flux in a smart district heating network is simulated with I.H.E.N.A software in order to compare the effect of such installations on supply and temperature levels [13]. Results of four utility layouts (Supply- Return, Supply- Supply, Return - Return, Return- Supply) shows that circuits of Supply- Return and Return – Return cause increase in return temperature which consequently leads to decrease in main production efficiency, while two other circuits shows increase in Supply temperature which propagates also in return line but with lower level. In this case temperature rise by this utility might have negative effect on decentralized production of utilities downstream. Considering that in this study it was assumed that prosumers production is first used by user utility and excess of energy is directed into the network, the effect of prosumers more significant when higher shares of

distributed production is included in DHS. Being able to Obtain sufficient amount of decentralized energy production substations must allow bidirectional energy flow within a proper temperature levels, why utility substations in Smart DHS is important.

Impact of prosumers equipped with solar collectors on DHS of Malmö, Sweden is studied using the NetSim in [9]. In this simulation study scenarios were categorized by season, energy and production cases and then combined to reflect the reality. Results for both pressure and temperature distribution in network shows that costumers close to prosumer substation are significantly affected. Utilities near to prosumer might face changes in supply or return temperature (depend on where heat is introduced) which effects on flow rate within the pipes. it is resulted that when prosumers produce their maximum heat, due to higher energy flux, velocity in pipes increases, therefore greater attention to pipe dimensions and interfaces must be paid when dealing with DHS with decentralized production units. Also this study is resulted that when prosumers apply their own pressure cones (supply and return pressure gradient) pressure differential is higher and it's lower when supply water temperature is mixed with lower temperature water produced by prosumers. Later mostly happens when prosumer generates its pressure cone less frequently. Pressure differential is also affected by propagation of water from prosumer on the whole network which consequently depends on how pressure differential in the network is controlled.

Another similar simulation by NetSim on same DHS as previous one but focused on energy balance and carbon dioxide emission was done by [14]. Prosumers in this simulation was able to utilize excess heat from cooling machines. Results compare the reference case without prosumers and the case with prosumers. CO₂ emission saving was shown to be positive when cooling machine is able to provide higher supply temperature. This is because more electricity is converted to heat. Since cooling machines usually provide low grade heat, utilization of such units could have negative impact on whole network when higher share of these heats are available. This condition might be because of introduction of low temperature heat produced by cooling machine into supply line during warmer seasons. Results of pressure differentials and velocity gradients at users near prosumer was shown to be higher particularly when in warmer seasons main supply temperature is high. Regardless of Renewable energy type more delicate investigations of Impact of prosumers on DHS seems to be highly demanded, as if both of the two last mentioned studies were revealed some of such impacts.

All the mentioned studies are based on the common mathematical models, however include specific constraints or supplements depending on the aim of the research. Numerical design of thermal systems by [15] Represents one of the most comprehensive models of overall design of thermal system with application on DHS, hence it is used as a basis for the present thesis project, and will be further discussed.

CHAPTER 3

Methodology

Beside the importance of detailed representation of DHS in general, a delicate research on distributed RES is necessary for treating both parts simultaneously. First, the literature review identified areas with application of RES and DHS. It was found that all studies could be categorized in four subjects where each group was focused on a specific aspect of DHS and utilization of RES. The research activities were mainly focused on issues associated with connection of RES and DHS, introduction of the so called prosumer to the existing and future DHS, modelling and design approaches that are able to treat bidirectional flow in network grids and simulation methods that reflect the reality of utilizing RES in DHS.

According to majority of the reviewed literature concerning modelling of DHS with RES, continuum mechanics together with first and second laws of thermodynamic were found to be the most reasonable ways of physical process representation. Moreover, it was found that for the analysis of different variables in the DHS it is sufficient to describe the physical characteristics in macroscopic level.

Therefore, for this project a mathematical model was developed in order to find the performance of DHS Gløshaugen campus of NTNU. The aim was to model scenarios of RES use and identify their influence on DHS. The model employed conservation laws and was developed in MATLAB. Simplified sub-models of different components such as pumps, heat exchangers, flow control valves and prosumer substation were created and integrated to the main model.

The mechanical components were sized and selected according to criteria suggested in standards and manufactures brochures.

Independent data on energy inputs such as heat demands, building types and outdoor temperature were collected by using statistical information provided by university's energy monitoring platform and national statistics.

The hydraulic and thermal performance were the main parameters this study aimed to find out. Therefore, the outcome was identification of the temperature and pressure levels and mass flow rate in each pipe section of selected network. Appropriate boundary conditions that reflect the reality of the Gløshaugen campus were selected.

Hence, in order to discuss the pros and cons of integration of higher shares of RES to DHS, three test cases were defined accordingly. In addition, functionality and operation of the pump and flow control valve were analysed. The scenario for the supply temperature level control was developed and studied. Further, the found results were treated as reliable.

CHAPTER 3

Theoretical background for modelling of district heating systems

In this section first fundamental theories concerning design of thermal systems are explained then related equations are derived in order to analyse the DHS. Models for hydraulic and thermal parts are separately derived as it was suggested in the most reviewed literature.

4.1 Theory and principles

Design of thermal systems and DHS in particular compels one to deal with transport phenomena. Approach based on continuum mechanics allow one to explicitly study performance of a thermal system including propagation of physical characteristics while geometry of system is considered. Continuum hypothesis is relied on studying the system in macroscopic scale, means that discrete nature of physical quantities in microscopic scale is ignored by considering only average effect of system properties. Hence, physical quantities are assumed to be vary continuously in different points of the system. Density of the continuum body therefore can be defined as

$$\rho = \lim_{\Delta V \rightarrow 0} \frac{\Delta M}{\Delta V} \quad 4-1$$

4.2 Conservation law

In problems including isothermal and non-isothermal properties, equations that reflect the natural behaviour of systems must be applied. Such equations are called “conservation laws”. Equations “continuity equation” and “momentum equation” treat isothermal characteristics while “energy equation” deals with non-isothermal problems.

4.2.1 Continuity equation

Assume an infinitesimal volume of dV as shown in Figure 4-1.

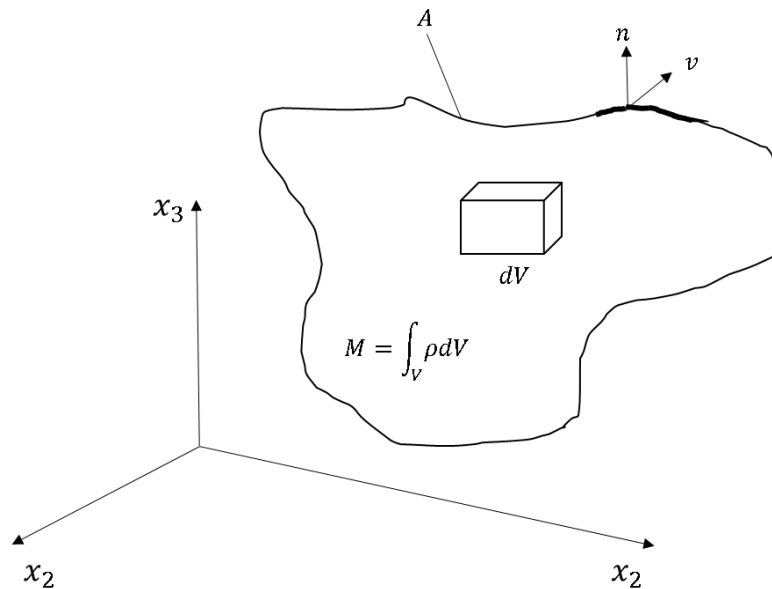


Figure 4-1

According to principle of mass conservation rate of change of mass inside dV is equal to rate of the mass flowing through surface boundaries of dV . The net rate of mass increase in volume dV is also obtained by considering time derivative of mass contained in infinitesimal volume.

$$\frac{\partial \rho}{\partial t} = -\left(\frac{\partial(\rho v_1)}{\partial x_1} + \frac{\partial(\rho v_2)}{\partial x_2} + \frac{\partial(\rho v_3)}{\partial x_3}\right) \quad 4-2$$

For the volume V surrounded by surface A , if n is the local normal of infinitesimal area dA , Divergence theorem for the flux W through surface A is defined as

$$\int_A W \cdot n dA = \int_V \nabla \cdot W dV \quad 4-3$$

Using the divergence theorem, 4-2 can be written as

$$\frac{\partial \rho}{\partial t} = -\nabla \cdot \rho v \quad 4-4$$

Integrating over the entire volume continuity equation is derived as

$$\frac{d}{dt} \int_V \rho dV = - \int_A \rho v \cdot n dA \quad 4-5$$

4.2.2 Momentum equation

Momentum equation expresses second law of Newton, applied to a fluid. This means rate of change of momentum of a fluid is equal to sum of all forces related to fluid. Here we assume infinitesimal volume dV again.

Forces acting on the fluids are divided in rate of momentum due to convection and external forces.

$$\begin{aligned} & [\textit{rate of change of momentum}] \\ &= [\textit{net rate of momentum due to convection}] \\ &+ [\textit{surface forces (pressure and viscous forces)}] \\ &+ [\textit{body forces (gravity, etc.)}] \end{aligned}$$

Change in momentum due to convection is because fluid is crossing momentum of ρv to boundary of dV . Momentum flux if considered on all boundaries in three dimensional representation is a tensor quantity. This generally can be expressed as

$$\rho v v = \rho v_i v_j \quad 4-6$$

j^{th} component of momentum flow toward the normal of unit area in i^{th} direction

Using the divergence theorem 4-6 can be written as

$$-(\nabla \cdot \rho v v)_i = -\frac{\partial(\rho v_i v_j)}{\partial x_j} \quad 4-7$$

Hydraulic forces to be taken into account in momentum equation are surface and body forces.

Surface forces are related to pressure and viscous forces acting on fluid body.

Surface forces could be defined considering Deviatoric stress tensor τ :

$$\sigma = PI + \tau \quad 4-8$$

Where first right hand side term is static pressure and second term represents shear stress on fluid that can be interpreted as viscous effects.

Fluid at rest experiences only normal stresses which is independent of surface orientation while moving fluid builds up additional pressure due to viscosity of fluid and deformation of control volume. Hence, static pressure can be approximated by considering average of diagonal terms. This approximation is valid since static pressure is purely applied when flow is idle. Taylor expansion relates shear forces in opposite faces of the fluid body and by summing surface forces due to viscosity on each direction viscous force is obtained. The only external body force we assume is gravity force which acts on elementary volume dV . Arranging all terms together it is possible to write momentum equation as

$$\frac{\partial \rho v}{\partial t} = -\nabla \cdot \rho v v - \nabla P - \nabla \cdot \tau + \rho g \quad 4-9$$

4.2.3 Internal energy equation

Internal energy equation is directly derived by subtracting mechanical energy equation from energy equation. Energy equation roots in first law of thermodynamics. Total energy is equal to the sum of kinetic and internal energy.

$$e = u + \frac{1}{2}v^2 \quad 4-10$$

Energy balance of infinitesimal volume dV gives

$$\frac{\partial}{\partial t} \left(\rho u + \frac{1}{2} \rho v^2 \right) = -\nabla \cdot \left(\left(\rho u + \frac{1}{2} \rho v^2 \right) v \right) - \nabla \cdot \mathbf{q} - \nabla \cdot P v - \nabla \cdot (\boldsymbol{\tau} \cdot v) + \rho g \cdot v \quad 4-11$$

Where left hand side takes rate of change of energy in the volume into account. The right hand side terms are convective flow rate of energy, net heat flux, work done by pressure, work done by viscous stress and work done by gravity respectively.

Mechanical energy equation (or conservation of kinetic energy) is derived directly from scalar product of velocity vector and momentum equation.

$$v \cdot \left(\frac{\partial \rho v}{\partial t} \right) = -\nabla \cdot \rho v v - \nabla P - \nabla \cdot \boldsymbol{\tau} + \rho g \quad 4-12$$

4-12 can be rearranged as

$$\frac{\partial}{\partial t} \left(\frac{1}{2} \rho v^2 \right) = -\nabla \cdot \left(\frac{1}{2} \rho v v^2 \right) - \nabla \cdot P v + P \nabla \cdot v - \nabla \cdot (\boldsymbol{\tau} v) + \boldsymbol{\tau} : \nabla v + \rho v \cdot g \quad 4-13$$

As always on the left hand side there is rate of change of kinetic energy within the volume. On the right hand side terms are convective kinetic energy flux, rate of work done by pressure, reversible conversion of kinetic energy into internal energy, work done by viscous stress, rate of conversion of kinetic energy into internal energy (energy dissipation) and work done by gravity respectively.

Having total energy equation and mechanical energy, internal energy equation is simply obtained by subtracting 4-13 from 4-11 which gives

$$\frac{\partial}{\partial t} (\rho u) = -\nabla \cdot (\rho u v) - \nabla \cdot \mathbf{q} - P \nabla \cdot v - \boldsymbol{\tau} : \nabla v \quad 4-14$$

In continuum mechanics fluid motion can be describe either by using Eulerian or Lagrangian approach. Substantial derivative indicated by $\frac{D}{Dt}$ represents is composed of two terms: the partial time derivative ($\frac{\partial}{\partial t}$) and the advection term $v \cdot \nabla$. for any quantity Z :

$$\rho \frac{DZ}{Dt} = \frac{\partial(\rho Z)}{\partial t} + \rho v \cdot \nabla Z \quad 4-15$$

Using the definition of enthalpy $h = u + \left(\frac{1}{\rho}\right)p$, and Lagrangian approach to write substantial derivative we can rewrite 4-15 as

$$\rho \frac{Dh}{Dt} = -\nabla \cdot q - \tau : \nabla v + \frac{DP}{Dt} \quad 4-16$$

But still this equation is not able to give temperature explicitly. Variation of specific enthalpy could be formulated as

$$dh = T ds + \left(\frac{1}{\rho}\right) dP \quad 4-17$$

Heat flux could be described by expression of Fourier's law $q = -K\nabla T$. Finally energy equation in a simpler way is defined by neglecting viscous heating and considering constant thermal conductivity.

$$\rho c_p \frac{\partial T}{\partial t} + \rho c_p v \cdot \nabla T = K\nabla^2 T + \phi_s \quad 4-18$$

Last term of right hand side takes heat generation in the volume into account.

Now that necessary equations to analyse a thermal system are acquired we can consider the model of a DHS.

4.3 One dimensional model of a district heating network

In order to model a DHS first network topology must be defined. Systems including flow distribution are often complicated and vast number of details are to be considered. One of the

useful tools for description of is based on graph theory. Previously illustrated equations must be then formulated accordingly.

4.3.1 Graph theory

Graph is a mathematical representation of a set of connected objects. Conceptually graph is built by nodes which are connected through edges (lines that connect two nodes).

In the case of DHS, nodes could be interpreted as junctions and edges are corresponding to pipe branches in the network. Central heat distribution building and costumer substations are also treated as nodes. An example of such representation is shown in Figure 4-2.

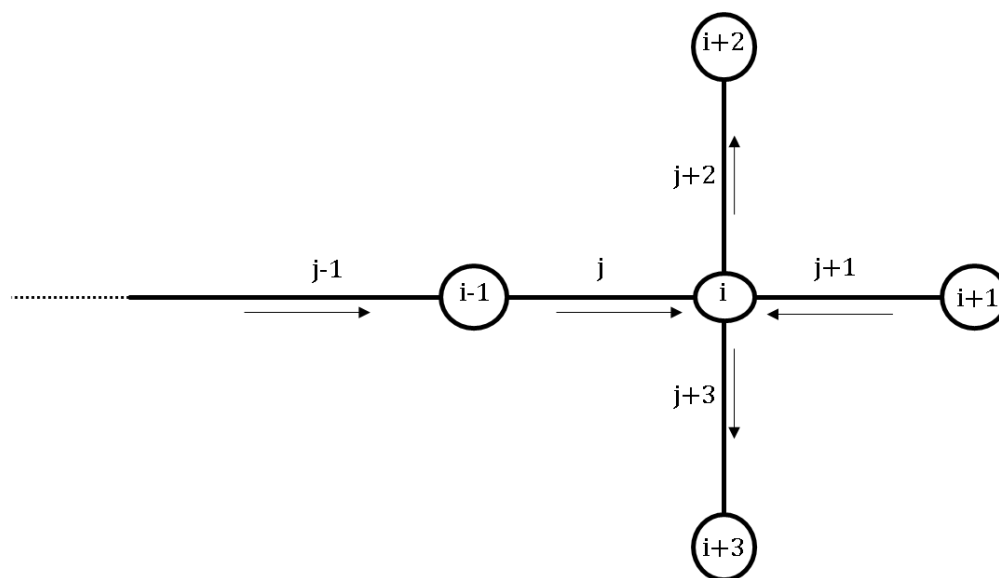


Figure 4-2 Connection of nodes through directed branches

Interconnection of nodes and branches is expressed by means of the so called “incidence matrix” A . Rows equal to number of nodes and columns equal to number of branches form matrix A . Generic element (i,j) of the matrix A could have the value of $(+1)$ if i^{th} node is an inlet for j^{th} branch, (-1) if i^{th} node is an outlet for j^{th} branch or zero in other cases. Incidence matrix associated with network is shown in Figure 4-2 is

$$A = \begin{bmatrix} -1 & 1 & 0 & 0 & 0 \\ 0 & -1 & -1 & 1 & 1 \\ 0 & 0 & 1 & 0 & 0 \\ 0 & 0 & 0 & -1 & 0 \\ 0 & 0 & 0 & 0 & -1 \end{bmatrix} \quad 4-19$$

Using graph illustration for a DHS, it is possible to define state properties such as pressure and temperature at each node. Also mass flow rates and velocities are defined in each branch of the network which will be explained later. Following simplifications are to be considered:

- One-dimensional model

Fluid systems in which fluids are distributed in pipe lines are often considered in one predominant dimension (usually along the pipe length when $L \gg D$). This approach allows one to significantly reduce complexity and computation burdens and investigate larger systems thoroughly, however three-dimensional models give more delicate description of system. Therefore, first simplification of DHS model is to consider propagation of state properties along the length of the pipes.

- Specific heat capacity

District heating network supplies water with at most 120°C which makes it possible to assume constant specific heat capacity for water of 4.187 kJ/kg·K at all temperatures for sake of simplicity.

- Incompressible fluid

At Mach numbers below 0.4 fluid can be considered incompressible, therefore density doesn't change with pressure changes. In this case, the coupling between pressure and velocity introduces a constraint on the solution: one should find the pressure field which makes the resulting velocity field satisfy the continuity equation.

Hydraulic behaviour and thermal behaviour of the DHS are separately modelled.

4.3.2 Fluid dynamic model

Iso-thermal characteristics of thermal systems such as hydraulic behaviour of DHS could be explained through momentum and continuity equations, therefore 4-4 and 4-9 are expanded to:

$$\frac{\partial \rho}{\partial t} + \left(\frac{\partial(\rho v_1)}{\partial x_1} + \frac{\partial(\rho v_2)}{\partial x_2} + \frac{\partial(\rho v_3)}{\partial x_3} \right) = 0 \quad 4-20$$

$$\begin{cases} \rho \left(\frac{\partial v_1}{\partial t} + v_1 \frac{\partial v_1}{\partial x_1} + v_2 \frac{\partial v_1}{\partial x_2} + v_3 \frac{\partial v_1}{\partial x_3} \right) = -\frac{\partial P}{\partial x_1} - (\nabla \cdot \tau)_1 + F_1 \\ \rho \left(\frac{\partial v_2}{\partial t} + v_1 \frac{\partial v_2}{\partial x_1} + v_2 \frac{\partial v_2}{\partial x_2} + v_3 \frac{\partial v_2}{\partial x_3} \right) = -\frac{\partial P}{\partial x_2} - (\nabla \cdot \tau)_2 + F_2 \\ \rho \left(\frac{\partial v_3}{\partial t} + v_1 \frac{\partial v_3}{\partial x_1} + v_2 \frac{\partial v_3}{\partial x_2} + v_3 \frac{\partial v_3}{\partial x_3} \right) = -\frac{\partial P}{\partial x_3} - (\nabla \cdot \tau)_3 + F_3 \end{cases} \quad 4-21$$

In case of one-dimensional model it would be assume

$$v \equiv v(x_1, t)$$

$$P \equiv P(x_1, t)$$

Therefore, 4-20 and 4-21 are reduced to

$$\frac{\partial \rho}{\partial t} + \frac{\partial(\rho v_1)}{\partial x_1} = 0 \quad 4-22$$

$$\rho \frac{\partial v_1}{\partial t} + \rho v_1 \frac{\partial v_1}{\partial x_1} = -\frac{\partial P}{\partial x_1} - (\nabla \cdot \tau)_1 + F_1 \quad 4-23$$

Where $(\nabla \cdot \tau)_1$ takes viscous force into account and must then be formulated. F_1 However, includes local fluid resistance and effect of pumps and gravity.

$$F_1 = \rho g_{x_1} - F_{LOCAL} + F_{PUMP} \quad 4-24$$

At this point proper control volumes must be defined in order to derive integration form of momentum and continuity equations. Hence, a generic branch of network is now considered as shown in Figure 4-3.

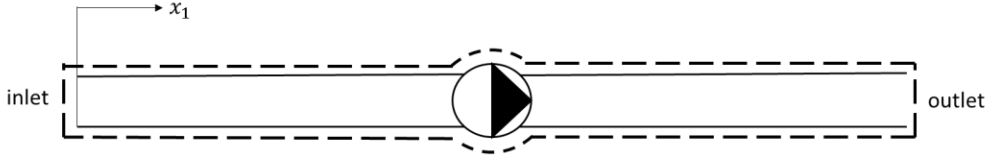


Figure 4-3 Control volume around the branch

Integrating 4-23 over control volume gives

$$\int_{cv} \rho \frac{\partial v_1}{\partial t} dV + \int_{cv} \rho v_1 \frac{\partial v_1}{\partial x_1} dV = \int_{cv} -\frac{\partial P}{\partial x_1} dV - \int_{cv} (\nabla \cdot \tau)_1 dV + \int_{cv} F_{x_1} dV \quad 4-25$$

dV can be converted to SdX where S is the cross section of pipe.

$$\rho \frac{dv_1}{dt} SL + \rho \left[\frac{(v_{out,1})^2 - (v_{in,1})^2}{2} \right] S = (p_{in} - p_{out})S - \rho g(z_{out} - z_{in})S - \Delta P_{FRICT}S - \Delta P_{LOCAL}S + \Delta P_{PUMP}S \quad 4-26$$

Total pressure is defined as

$$P = p + \rho \frac{v^2}{2} + \rho g z \quad 4-27$$

Equation 4-26 is reformulated to

$$\rho \frac{dv_1}{dt} L + (P_{out} - P_{in}) = -\Delta P_{FRICT} - \Delta P_{LOCAL} + \Delta P_{PUMP} \quad 4-28$$

The Darcy-Weisbach equation is now considered the best empirical relation for pipe-flow resistance [16]:

$$\Delta P_{FRICT} = \frac{1}{2} f \frac{L}{D} \rho (v_1)^2 \quad 4-29$$

Similarly minor loss is formulated as:

$$\Delta P_{LOCAL} = \frac{1}{2} \sum_k \beta_k \rho (v_1)^2 \quad 4-30$$

f the friction factor and β_k the local loss coefficient must be selected properly according to pipe and connection types. These are values usually provided in literature or producers catalogue.

ΔP_{PUMP} is usually expressed by characteristic curve which can be approximated by polynomial functions. Same procedure is applied to mass conservation equation considering appropriate cv as shown in Figure 4-4. Current cv includes a generic junction connected to branches.

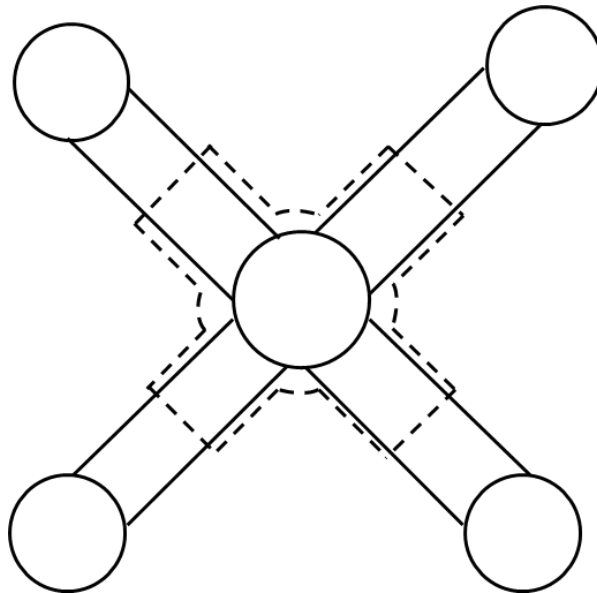


Figure 4-4 Control volume at the junction of branches - Node

$$\int_{cv} \frac{\partial \rho}{\partial t} dV + \int_{cv} \frac{\partial(\rho v_1)}{\partial x_1} dV = 0 \quad 4-31$$

Using divergence theorem and integrating over CV

$$\frac{d}{dt} M + \sum_j \rho_j v_{1,j} S_j + G_{ext} = 0 \quad 4-32$$

Where M is the mass of the fluid within cv . , Summation is over generic branches j and G_{ext} is possible extraction of fluid from junction to external environment.

4.3.3 Thermal model

In most applications including heat transfer the effect of viscous heating and compressibility is neglected.

$$\rho c_p \frac{\partial T}{\partial t} + \rho c_p \mathbf{v} \cdot \nabla T = \nabla \cdot K \nabla T + \varphi_s \quad 4-33$$

Which can be expanded to

$$\frac{\partial(\rho c_p T)}{\partial t} + \frac{\partial(\rho c_p v_1 T)}{\partial x_1} + \frac{\partial(\rho c_p v_2 T)}{\partial x_2} + \frac{\partial(\rho c_p v_3 T)}{\partial x_3} = K \frac{\partial^2 T}{\partial x_1^2} + K \frac{\partial^2 T}{\partial x_2^2} + K \frac{\partial^2 T}{\partial x_3^2} + \varphi_s \quad 4-34$$

Here again one-dimensional approach holds $T \equiv T(x_1, t)$

$$\frac{\partial(\rho c_p T)}{\partial t} + \frac{\partial(\rho c_p v_1 T)}{\partial x_1} = K \frac{\partial^2 T}{\partial x_1^2} + \varphi_s \quad 4-35$$

Where $\varphi_s = \varphi_v - \varphi_l$

φ_v Takes volumetric heat generation into account and φ_l considers non adiabatic walls. Heat exchange at the walls are perpendicular to assumed direction in this one dimensional analysis and it's not possible to analyse them. Therefore, this heat exchange is considered by φ_l as a volumetric sink term. It is positive in case of heat loss and negative when heat is supplied through walls.

cv shown in Figure 4-4 includes the junction and branch ducts connected to it. Water with different temperatures join in junction and leave with equal temperatures. Integrating 4-35 and using divergence theorem gives

$$\frac{\partial(\rho c_p T)}{\partial t} \Delta V + \sum_j p_j c_{p,j} v_{1,j} T_j S_j = K \frac{\partial T}{\partial x_1} |_j S_j + \varphi_v - \varphi_l \quad 4-36$$

First term on the right hand side is heat transfer due to conduction and can be neglected, because convection heat transfer (second term in left hand side 4-36) is dominant.

4.3.4 Steady state condition

Models for thermal systems are often proposed in steady state condition in order to obtain essential characteristics of the system.

4.3.4.1 Steady state fluid dynamic problem

Equation 4-32 is considered for steady state condition. Mass flow rate G in generic j^{th} branch is equal to $\rho v s$. G_{ext} is associated with i^{th} node according to cv .

$$\sum_j \rho_j v_{1,j} S_j + G_{ext} = 0 \quad 4-37$$

In order to write mass conservation for each node 4-37 must be formulated in matrix form as

$$A \cdot G + G_{ext} = 0 \quad 4-38$$

Where A incidence matrix and G is a column vector that contains flow rates of each branch. G_{ext} is a column vector sized by number of nodes and its values are positive when G is extracted and negative if injected.

Considering a generic branch connecting nodes i^{th} and $i-1^{\text{th}}$ as cv .momentum equation 4-28 can be written for steady state condition:

$$(P_i - P_{i-1}) = -\frac{1}{2} \rho_j (v_{1,j})^2 \left(f_j \frac{L_j}{D_j} + \sum_k \beta_{k,j} \right) + \Delta P_{PUMP,j} \quad 4-39$$

Using $G = \rho v s$

$$(P_{i-1} - P_i) = \frac{1}{2} \frac{G_j^2}{\rho_j (S_j)^2} \left(f_j \frac{L_j}{D_j} + \sum_k \beta_{k,j} \right) - \Delta P_{PUMP,j} \quad 4-40$$

Previous equation can be reformulated as

$$(P_{i-1} - P_i) = R_j G_j - \Delta P_{PUMP,j} \quad 4-41$$

Where the term R_j stands for hydraulic resistance

$$R_j = \frac{1}{2} \frac{G_j}{\rho_j (S_j)^2} \left(f_j \frac{L_j}{D_j} + \sum_k \beta_{k,j} \right) \quad 4-42$$

Momentum equation must be solved for each branch. in matrix form B set of equations are obtained as

$$A^T \cdot P = R \cdot G - t \quad 4-43$$

Where R is a diagonal matrix, P is a column vector contains pressure of each node. Product of $A^T \cdot P$ defines pressure difference between inlet and outlet of each node. t Contains effect of pumps. Rearranging 4-43 gives

$$G = Y \cdot A^T \cdot P + Y \cdot t \quad 4-44$$

Where $Y = R^{-1}$, is hydraulic conductance.

4.3.4.2 Steady state thermal problem

Thermal problem in steady state condition involves calculation of temperature when time rate of change in thermal energy is neglected. Equation 4-36 is simplified for steady state condition as:

$$\sum_j p_j c_{p,j} v_{1,j} T_j S_j = K \frac{\partial T}{\partial x_1} |_j S_j + \varphi_v - \varphi_l \quad 4-45$$

As it mentioned before conductive term can be neglected and we assume there is no volumetric heat generation in *cv*. φ_l Could be formulated in order to take heat transfer to surrounding through the walls into account.

$$\varphi_{l,i} = \sum_j \frac{L_j}{2} \Omega_j U_j (T_i - T_\infty) \quad 4-46$$

Where Ω_j is perimeter of the branch and U_j is global heat transfer coefficient. T_∞ is fixed temperature of ground in this formulation half of the branch length according to Figure 5-12 is considered. Therefore 4-45 is rewritten as

$$\sum_j G_j c_{p,j} T_j = \sum_j \frac{L_j}{2} \Omega_j U_j (T_i - T_\infty) \quad 4-47$$

Set of N equations in matrix form can be defined as

$$K \cdot T = f \quad 4-48$$

K is called stiffness matrix and f is the known vector.

Since flow rates in the network are forced convectively by components such as pumps, continuity and momentum equation must be solved in order to define P and G . Thermal problem (Linear system of equations 4-48) then can be solved using proper numerical approach.

4.3.5 Solution methods

4.3.5.1 Simple and Fixed-Point Algorithms

There are some issues concerning solution of 4-38 and 4-44. Due to term Y momentum equation is non-linear and two equations are coupled. The vector G appears in both equations

Therefore if G is unknown momentum equation cannot be solved explicitly. An iterative method called ‘‘SIMPLE-algorithm’’ (semi-implicit algorithm) is adopted to find values of P and G .

SIMPLE algorithm starts by guessing values of P and G and solves 4-38 and 4-44.

$$G^* = Y^* \cdot A^T \cdot P^* + Y^* \cdot t \quad 4-49$$

Correction values of P' and G' can be defined as difference between corrected values and guess values

$$\begin{cases} P = P^* + P' \\ G = G^* + G' \end{cases} \quad 4-50$$

For sake of simplicity it is assumed that the difference between hydraulic conductance Y and Y^* is negligible. Subtracting 4-49 from 4-44 gives

$$G' = Y^* \cdot A^T \cdot P' \quad 4-51$$

Using 4-50, continuity equation can be written as

$$A \cdot G' = -A \cdot G^* - G_{ext} \quad 4-52$$

By substituting 4-51 in 4-52

$$A \cdot Y^* \cdot A^T \cdot P' = -A \cdot G^* - G_{ext} \quad 4-53$$

Equation 4-53 can be written as

$$H \cdot P' = b \quad 4-54$$

A set of linear equations can be solved to obtain P' . Having P' correction of mass flow rate G' can be found from 4-51. Due to approximation of hydraulic conductance, resulted values are still different from the correct value, therefore previous steps must be iterated.

SIMPLE algorithm needs to solve 4-49. At each iteration and find the guess value of mass flow rate. A numerical scheme called fixed-point method is then adopted to treat non-linearity of momentum equation.

$$G^* = \Psi(G^*) = Y(G^*) \cdot A^T \cdot P^* + Y(G^*) \cdot t \quad 4-55$$

Fixed-point is an iterative method that is expressed as

$$G_{(k+1)}^* = \Psi(G_{(k)}^*) \quad 4-56$$

According to 4-56 an updated value of G^* is obtained by iteratively solving $\Psi(G^*)$ with previous value of G^* , therefore an initial guess $G_{(0)}^*$ must be made to start the computation. Convergence of the method severely depends on proper guess. Practically by using under relaxation coefficients this problem can be prevented. Following adjustments are considered:

$$G_{(k+1)}^* = \Psi(G_{(r)}^*) \quad 4-57$$

$$G_{(r)}^* = \lambda_1 G_{(k)}^* + \lambda_2 G_{(k-1)}^* \quad 4-58$$

Under relaxation coefficients are selected so that $\lambda_1 + \lambda_2 = 1$

4.3.5.2 Nodal method and upwind scheme

Upwind scheme is adopted to solve equation 4-47 for thermal problem. T_i in 4-47 represents temperature of the i^{th} node while T_j is the temperature at the boundary of control volume surrounding node i . since temperatures are actually defined at the nodes, by means of upwind scheme temperatures at the boundary are defined in accordance to the nodes. According to upwind scheme method, temperature at each boundary is assumed equal to temperature in upstream node. Control volume in Figure 4-5 is assumed as an example.

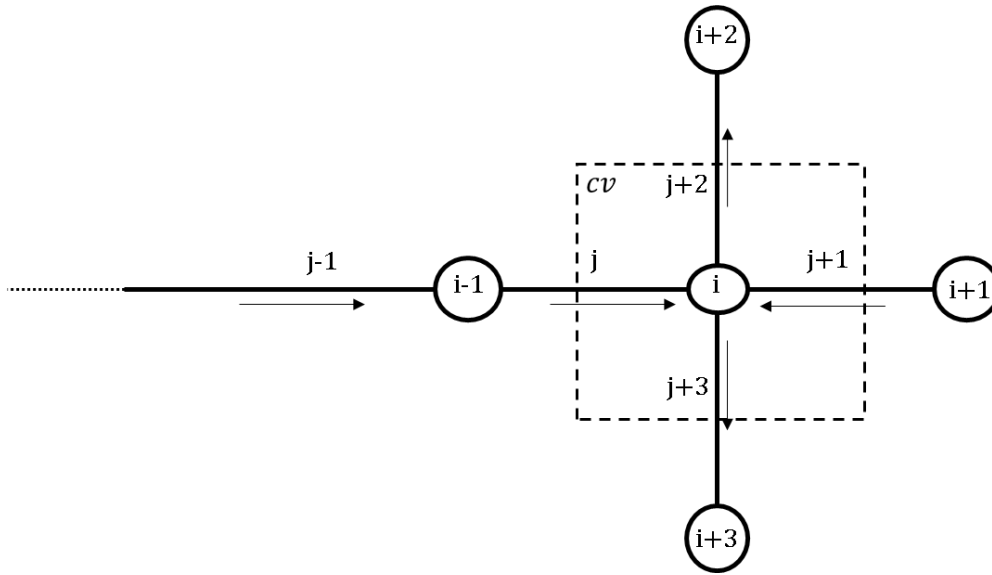


Figure 4-5

Temperatures corresponding to branches when the fluid is moving in its positive direction are:

$$\begin{aligned} T_j &= T_{i-1} \\ T_{j+1} &= T_{i+1} \\ T_{j+2} &= T_i \\ T_{j+3} &= T_i \end{aligned}$$

In a more explicit form the equation $K \cdot T = f$ for each node could be written in a general form:

$$a_n T_n + \sum_{i=1}^m b_i T_i = f_n \quad 4-59$$

Where diagonal term of K , a_n is:

$$a_n = \sum_{k=1}^p c_p G_k + \frac{1}{2} \sum_{j=1}^{p+m} L_j \Omega_j U_j \quad 4-60$$

And forcing element f_n is:

$$f_n = \frac{1}{2} T_g \sum_{j=1}^{p+m} L_j \Omega_j U_j \quad 4-61$$

Non-diagonal element b_i is:

$$b_i = -c_p G_i \quad 4-62$$

Where m indicates all the nodes connected by means of a branch to node n with a flow-rate directed toward n , while p indicates all the nodes connected by means of a branch to node n with a flow-rate exiting from n .

Where K ($N \times N$ for N number of nodes) is the stiffness matrix containing the elements a_n on the main diagonal and the elements b_i in other sparse position, T ($N \times 1$) is the vector of the unknown temperature and f ($N \times 1$) is the vector containing the terms f_n .

4.3.6 Unsteady state model

Transient operation of DHS can be illustrated in order to take time variation of temperature and velocities into account.

Equations of continuity, momentum and energy must be modified in this case.

Recalling unsteady state formulation of continuity equation

$$\frac{d}{dt} M + \sum_j \rho_j v_{1,j} S_j + G_{ext} = 0 \quad 4-63$$

Since control volume is fixed,

$$\frac{d\rho_i}{dt} \Delta V_i + \sum_j G_j + G_{ext} = 0 \quad 4-64$$

Adopting a backward Euler method 4-64 can be discretized with time steps of Δt .

$$\frac{\rho_i^t - \rho_i^{t-\Delta t}}{\Delta t} \Delta V_i + \sum_j G_j^t + G_{ext,i}^t = 0 \quad 4-65$$

Since no concentration occurs in the system and according to assumption of incompressible fluid $\rho_i^t = \rho_i^{t-\Delta t}$. Therefore, continuity equation remains unchanged. Momentum equation for unsteady state condition is defined as

$$\rho_j \frac{dv_{1,j}}{dt} L_j + (P_{i-1} - P_i) = \frac{1}{2} \frac{G_j^2}{\rho_j (S_j)^2} \left(f_j \frac{L_j}{D_j} + \sum_k \beta_{k,j} \right) - \Delta P_{PUMP,j} \quad 4-66$$

Using $G = \rho v s$ and adopting backward Euler method for time discretization gives

$$-\rho_j^t \frac{L_j}{S_j \Delta t} \left(\frac{G_j^t}{\rho_j^t} - \frac{G_j^{t-\Delta t}}{\rho_j^{t-\Delta t}} \right) + (P_{i-1} - P_i)^t = \frac{1}{2} \frac{(G_j^t)^2}{\rho_j^t (S_j)^2} \left(f_j \frac{L_j}{D_j} + \sum_k \beta_{k,j} \right) - (\Delta P_{PUMP,j})^t \quad 4-67$$

Which in matrix notation would be

$$(P_{i-1} - P_i)^t = R_j^t G_j^t + C_j^t G_j^t - (\Delta P_{PUMP,j})^t - S_j^t \quad 4-68$$

Where newly produced terms are diagonal matrix C_j^t and vector S_j^t are

$$C_j^t = \rho_j^t \frac{L_j}{S_j \Delta t} \quad 4-69$$

$$S_j^t = -\rho_j^t \frac{L_j}{S_j \Delta t} \frac{G_j^{t-\Delta t}}{\rho_j^{t-\Delta t}} \quad 4-70$$

Modified form of momentum equation for unsteady state is finally achieved as

$$G^t = \bar{Y} \cdot A^T \cdot P^t + \bar{Y} \cdot t^t + \bar{Y} \cdot s^t \quad 4-71$$

Where $\bar{Y} = (R + C)^{-1}$

4.3.6.1 Thermal problem

Time derivative rate of change of energy in 4-36 cannot be neglected in this case.

$$\frac{d(\rho_j c_{p,i} T_i)}{dt} \Delta V_i + \sum_j p_j c_{p,j} v_{1,j} T_j S_j = K \frac{\partial T}{\partial x_1} |_j S_j + \varphi_{v,i} - \varphi_{l,i} \quad 4-72$$

Time discretization of previous equation according to backward Euler method gives

$$\frac{(\rho_j c_{p,i} T_i)^t - (\rho_j c_{p,i} T_i)^{t-\Delta t}}{\Delta t} \left(\sum_j \frac{S_j L_j}{2} \right) + \sum_j G_j^t T_j^t c_{p,j} = \varphi_{v,i}^t - \sum_j \frac{L_j}{2} \Omega_j U_j (T_i^t - T_\infty) \quad 4-73$$

The whole set of energy equation is finally a can be written in matrix form

$$(M^t + K^t) \cdot T^t = f^t + \varphi_v^t + M^{t-\Delta t} \cdot T^{t-\Delta t} \quad 4-74$$

Where diagonal matrix M is defined as $M(i, i) = \frac{\rho_i c_{p,i}}{\Delta t}$

CHAPTER 4

Case Study

In this chapter models illustrated in previous chapter were utilized to analyse DHS of NTNU university campus in Trondheim, Norway (Figure 5-1). Discussions about network thermal losses, decentralized heat production and performance of mechanical components could be done once the pressure and temperature distribution in the network is understood.



Figure 5-1 Gløshaugen campus of NTNU

Gløshaugen campus of NTNU, has established its own DHS separated from the main DHS of Trondheim in order to enable low grade excess heat from the datacentre at to be used. DHS of Gløshaugen campus utilizes two heat exchangers in order to supply heat with demanded temperature from 23 consumer buildings selected for this study and one building which can act as prosumer in the campus by utilizing heat pumps in order to capture waste heat from cooling a datacentre were analysed. These 23 buildings are departments, classrooms, laboratories and other offices of university and the prosumer is the building which datacentre is located. Prosumer of this DHS receives its total heat demand from CHDB. Its production is redirected to the return line, due to high centralized heat distribution water temperature.

5.1 Preliminary design

Before starting calculation of pressure and temperature distributions in the network it was necessary to perform preliminary design of the system in order to be able to define and size different component in the network. Statistical analysis for thermal energy consumption patterns of consumers and polynomial function fitting for formulating the performance curve of the pump are the most useful tools for this purpose.

5.1.1 Thermal energy demand

The first step of this preliminary design is the calculation of the heat requirement by the various buildings connected to the network. Thermal requirement of buildings was obtained by collecting thermal energy use history of each building from “energy operation monitoring platform” provided for the university campus from 2010 until 2016. DHS supplies heat for space heating and domestic hot water, however the energy meters provided for energy monitoring platform record the total value of the heat consumption. Therefore in this analysis heat demand includes total heat requirement of consumer and is supplied through one heat exchanger at user substation. Figure 5-2 reports seasonal thermal consumption in recent 6 years.

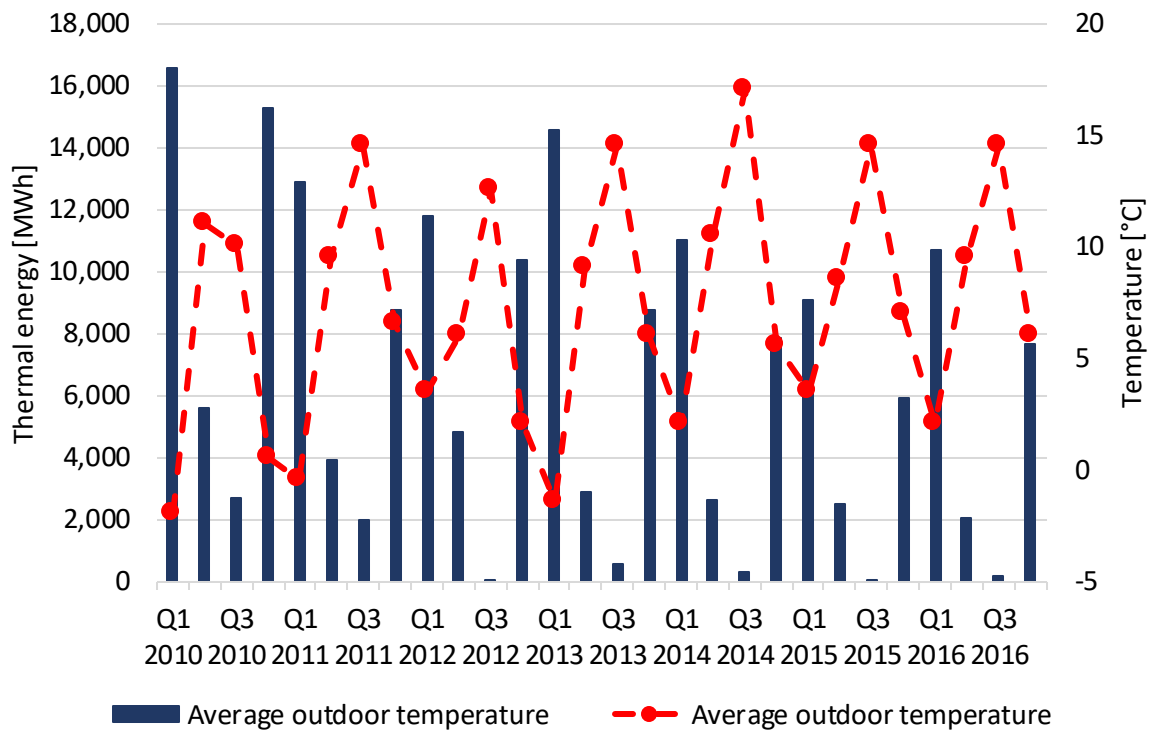


Figure 5-2 Statistics of outdoor temperature and heat consumption from 2010 to 2016

Reduction of thermal energy consumption in recent years might be because of higher average outdoor temperature and energy efficiency improvements and utilization of waste heat since 2012. The research in [17] gives detailed information about buildings energy use and demand load characteristics of buildings in campus, such as building area, functionality, construction year and overall heat transfer coefficient U-value of exterior walls. For this study the models were calibrated and tested according to thermal demand in 2016. The heat demand for 2016 is given in Figure 5-3.

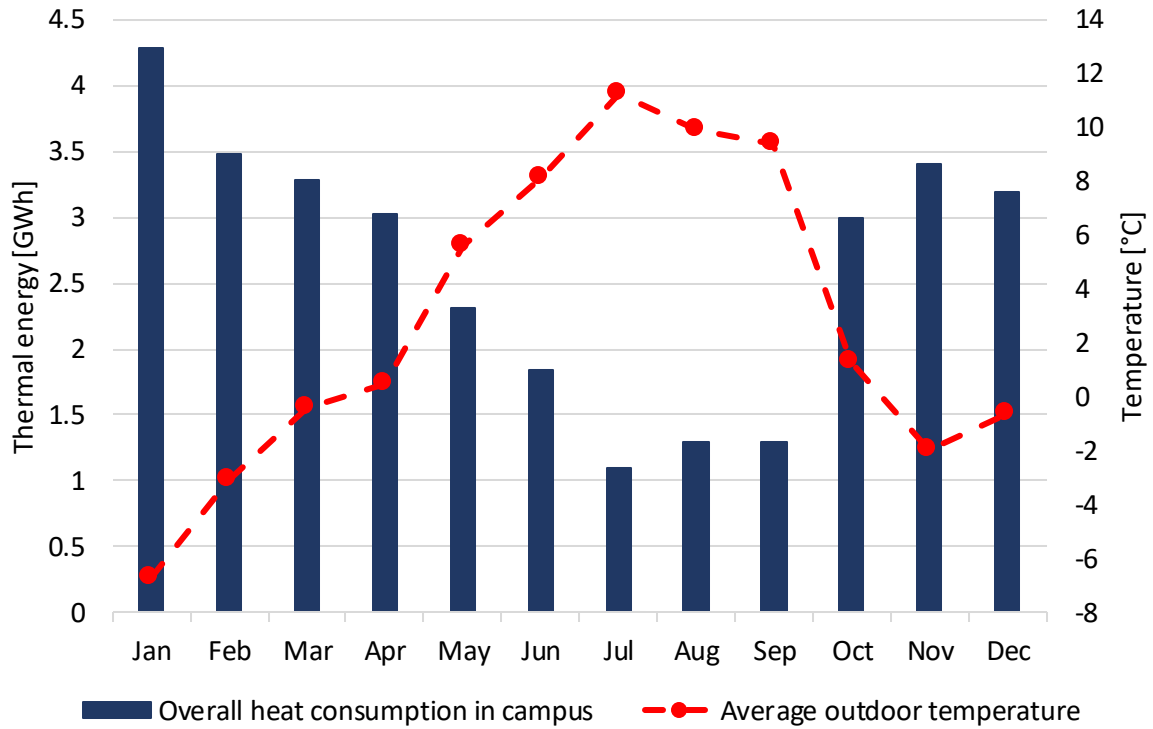


Figure 5-3 Overall heat consumption of campus and out door temperature in 2016

Heat load at CHDB is the sum of thermal request of all consumers together with distribution losses.

$$\varphi_{Load} = \varphi_{request} + \varphi_{Loss} \tag{5-1}$$

Heat losses due to conduction between pipe surface and soil is proportional to the temperature of the water flowing in the pipes and temperature of the soil as shown in Figure 5-4. Selection of proper pipe configuration and insulation type is of a great importance in order to minimizing thermal losses. Equation 4-47 was applied considering annual average supply and return temperature. For a single pipe insulated with polyurethane foam with thermal conductivity of maximum 0.026 W/m-K around 10% annual losses was assumed.

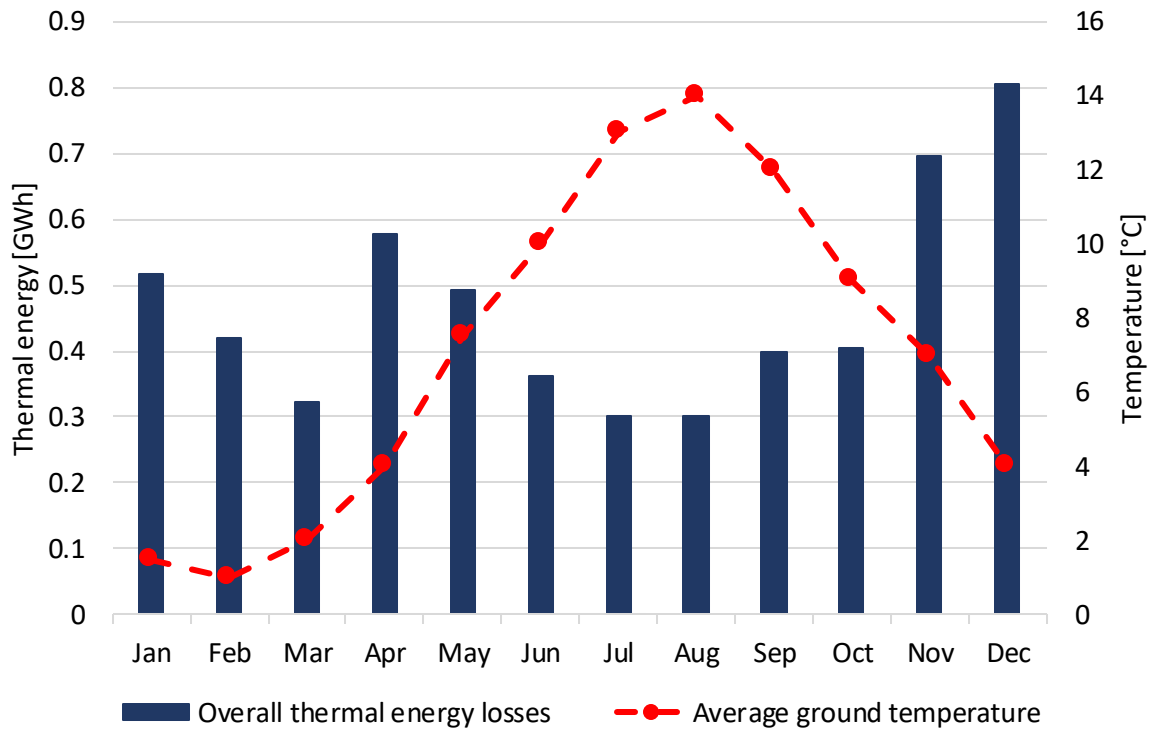


Figure 5-4 Ground temperature and thermal energy loss

The heat load in the campus was obtained using 5-1, Hourly heat demand of campus and outdoor temperature variations are shown in Figure 5-5.

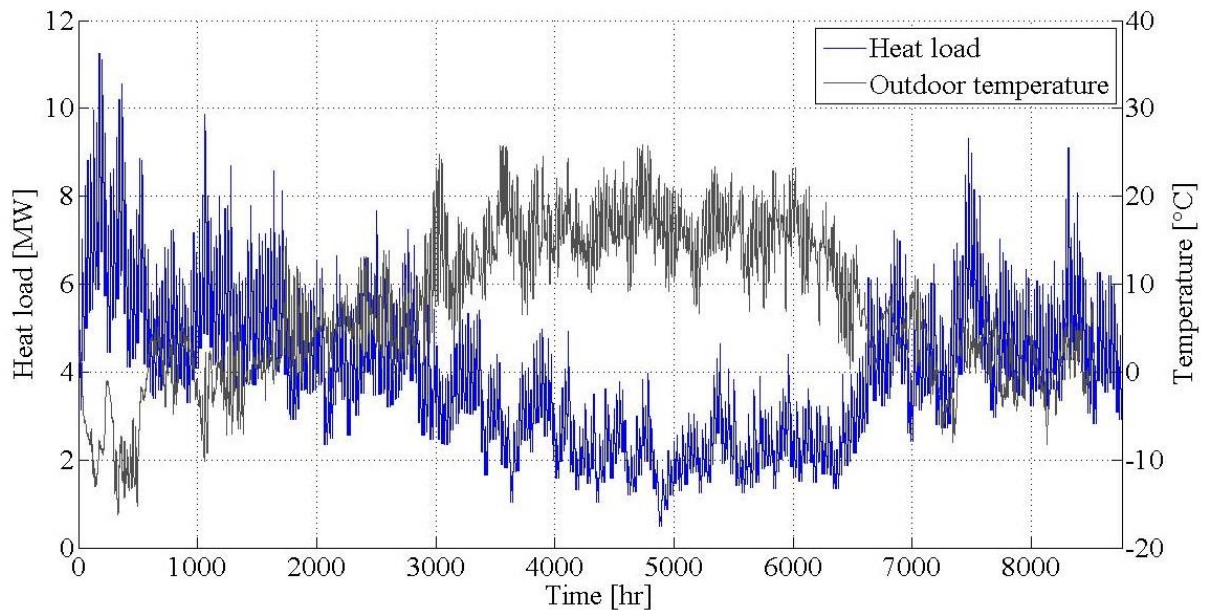


Figure 5-5 Hourly heat demand and out door temperature in 2016

The duration curve is considered as a useful tool for understanding the size of thermal plants. Figure 5-6 shows for how many hours production center has to meet required thermal request. Gløshaugen campus at its highest load requires nearly 11 MW heat power, hence the system must be designed in order to be able to work in such condition.

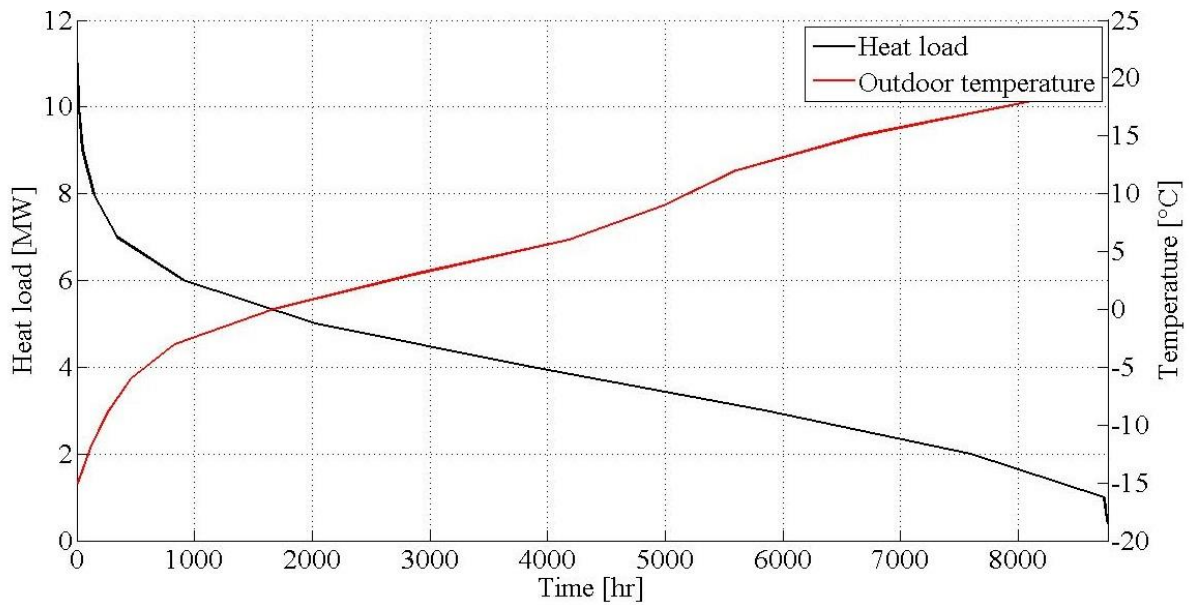


Figure 5-6 Duration curve of outdoor temperature and heat load for NTNU

The heat demand of the buildings is associated with outdoor temperature. As shown in Figure 5-7 by increasing outdoor temperature heat demand reduces from occasional peak loads to most frequent heat demands in warmer days.

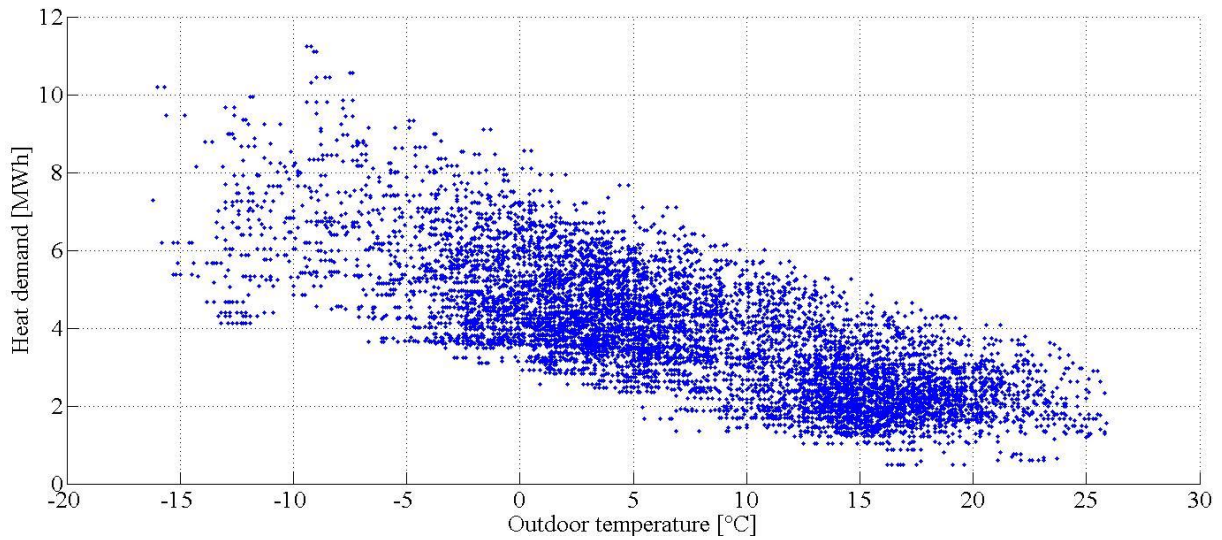


Figure 5-7 Heat demand of the campus Vs. Outdoor temperature in 2016

Despite of the fact that for most of the hours in the year thermal request is much lower than the maximum, the network design parameters such as pipe diameters, and pumps design characteristics were set for maximum thermal requirement. Highest heat load, 11 MW appeared only four hours in the year was then selected as design condition. Figure 5-8 shows the location of each building in the campus numbered according to the pipe distance of the building from central heat production centre. In the Table 5-1 there is heat demand of each building in design condition according to numeration of Figure 5-8.

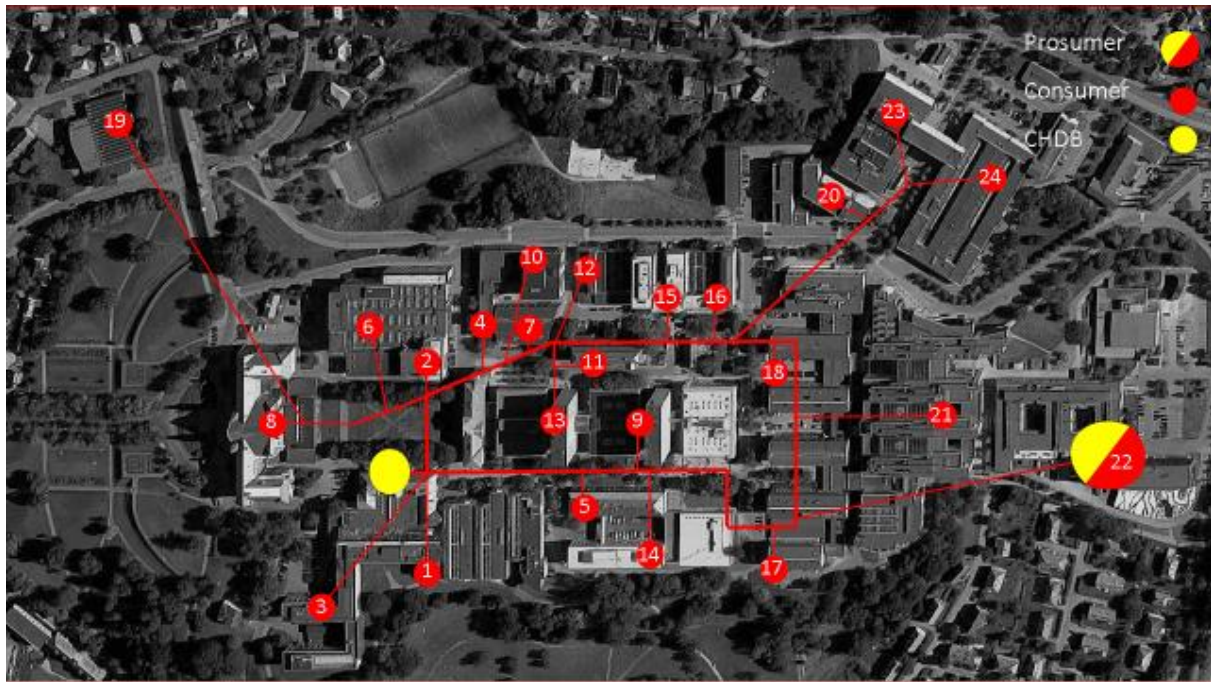


Figure 5-8 Location number and type of each building sorted by distance

Table 5-1 thermal characteristics of buildings

No.	Total area [m ²]	Distance [m]	Heat demand [kW]	No.	Total area [m ²]	Distance [m]	Heat demand [kW]
1	19468.6	92.5	742.1595	13	12860.69	250	213.5855
2	5053.22	101	254.3445	14	3684	290	298.7236
3	45342	149	429.6997	15	3955	325	335.0341
4	3030	152	159.6743	16	7598	345	254.27
5	4116	162.5	224.3542	17	6067	375	567.2586
6	15026	172.5	527.5961	18	4837	417	813.7315
7	4312	172.5	162.873	19	4046	437	159.6782
8	17360	190	686.2723	20	4781.21	475	164.8263
9	17936.36	215	508.0162	21	52773	512	2759.265
10	2476	215	110.8951	22	18595	523	567.1222
11	2353	220	124.219	23	11400	535	11400
12	2215	232	210.7057	24	12600	542	332.7508

Heat demand profile in design day was obtained by comparing the profile of all buildings in different days of the year. It was revealed that variations in demand of all buildings in a day were very similar to each other and almost constant during the year. Overall heat load on the CHDB was obtained by aggregating heat demand of all buildings in design day as shown in Figure 5-9.

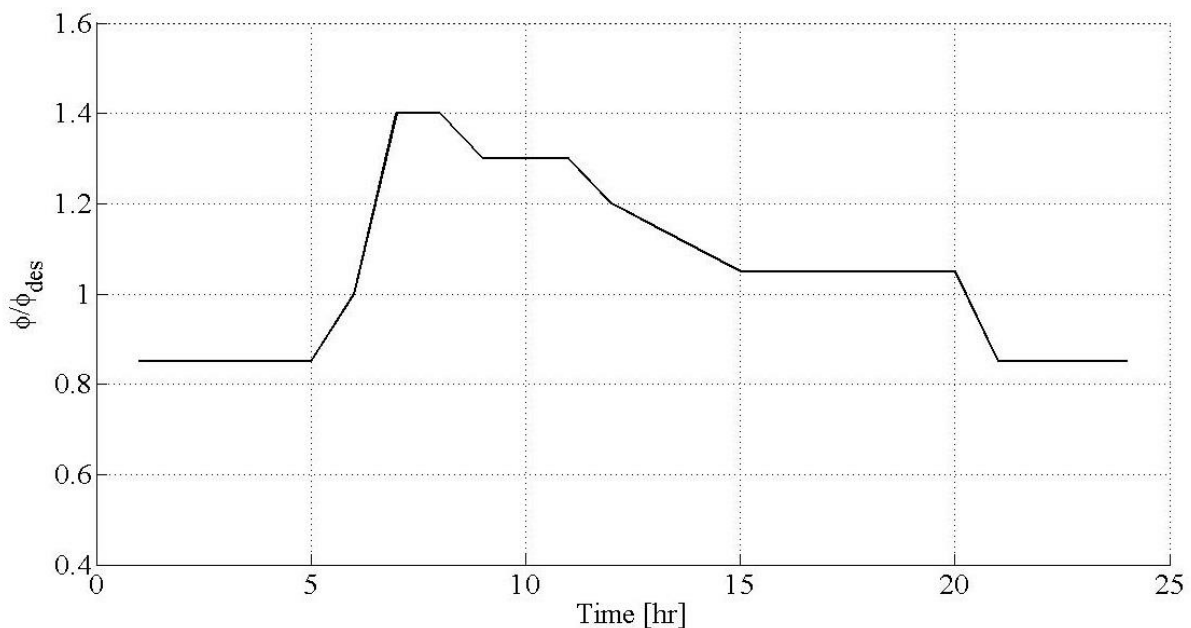


Figure 5-9 Profile of heat request of users

Heat is provided for the campus buildings during both day and night. At around 6:00 heat load of the CHDB is at its maximum which is 140% of the value estimated for that day according to the outdoor temperature and remains higher than the design value for most of the daytime. During the night heat demand of the campus is nearly 85% of the design.

5.1.2 Waste heat from datacenter

Heat pumps could increase the efficiency of the waste heat integration by maintaining higher temperature level of the product. As it was discussed in previous chapters, despite of low temperature level of heated water, cooling process in datacentre is done the entire year at fairly constant load. This makes the waste heat from cooling process to be always available, however recovering large amount of thermal energy requires low temperature of water from the main network. If the waste heat is not absorbed continuously then the financial pay-back quickly

fades away. An outlet branch redirects required flow rate to heat pump circuits where cooling the datacentre provides waste heat to be recovered.

In the datacentre substation a typical refrigeration machine working with ammonia rejects approximately 1 MW for each 650 kW of cooling at maximum temperature of 65°C. Heat recovery involves matching a source of waste heat to a practical sink. To recover the heat, a heat exchanger is installed in the hot-gas line between the compressor and the condenser as shown in Figure 5-10. Heat pumps, operating year-round for cooling or heating, offer a fine opportunity to use a hot-gas heat exchanger. Cold water is circulated through the heat exchanger by the circulating pump. In order to guarantee the efficiency of heat transfer process cold water is supplied for heat recovery with constant mass flow rate. The value was obtained for design condition where 1.2 MW is captured with maximum temperature.

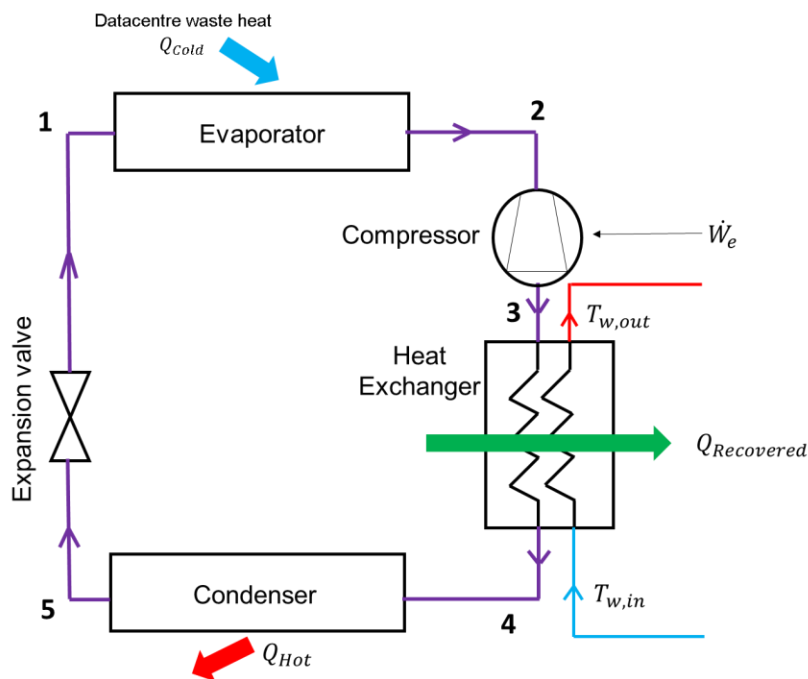


Figure 5-10 Waste heat recovery through heat pump cycle

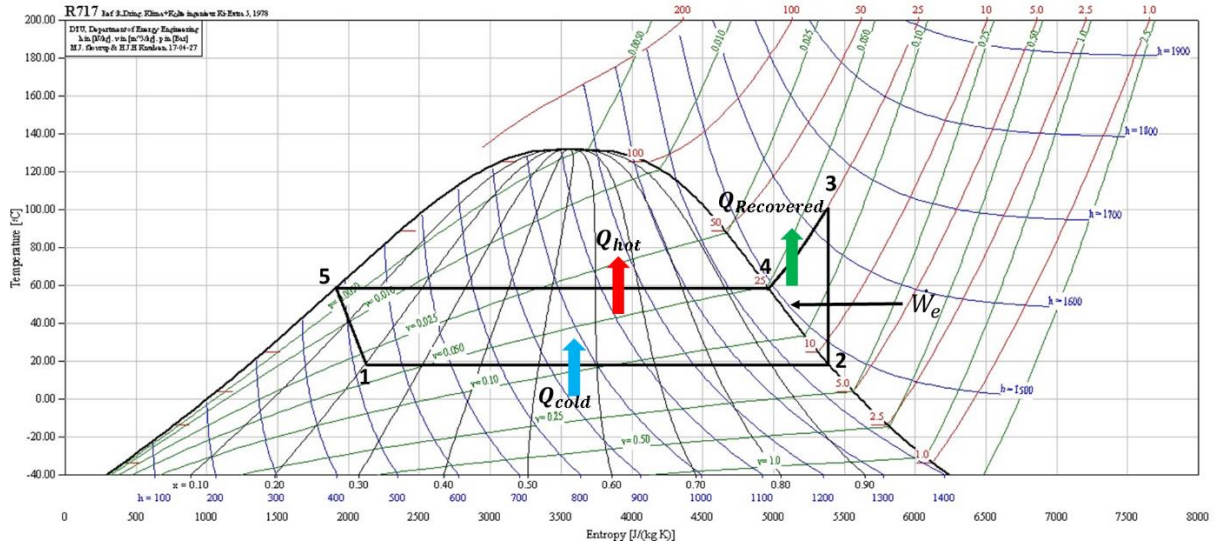


Figure 5-11 Molier diagram of heat pump cycle for Ammonia as refrigerant

Working fluid ammonia evaporates as a result of cooling purposes (1-2). Ammonia vapour then compressed to 25 bar and 100°C by consuming electric power W_e before entering the heat exchanger where cold water from return line is recirculated on the other side in order to capture heat from hot vapour until condensation temperature of ammonia (2-3). saturated ammonia exits from heat exchanger and condensed at constant temperature nearly 60°C (4-5). Thermodynamic processes 5-1 is associated with expansion valve in order to decrease pressure and temperature of liquid refrigerant (5-1). Mollier diagram of ammonia produced by “Coolpack simulation tool for refrigeration systems”. Heat load $Q_{Recovered}$ is calculated by performing heat transfer analysis in heat exchanger.

Heat transfer phenomena between ammonia-gas and water for counter-flow heat exchanger is analyzed. Logarithmic mean temperature difference is defined as:

$$LMTD = \frac{((T_{h,i}-T_{c,o})-(T_{h,o}-T_{c,i}))}{\ln((T_{h,i}-T_{c,o})-(T_{h,o}-T_{c,i}))} \quad 5-2$$

$$NTU = \frac{UA}{c_{p_h}G_{h,des}} \quad 5-3$$

where $UA = \frac{\dot{Q}_{des}}{LMTD}$ defines heat transfer area and overall heat transfer coefficient.

Efficiency is computed as

$$\eta_t = \frac{1 - e^{-NTU(1-r)}}{1 - r e^{-NTU(1-r)}} \quad 5-4$$

where the ratio $r = \frac{c_{p_h} G_{h,des}}{c_{p_c} G_{c,des}}$ is used.

Heat exchanger is designed to work in the following condition:

Hot side	Cold side
$T_{h,i} = 100^\circ\text{C}$	$T_{c,i} = 40^\circ\text{C}$
$T_{h,o} = 60^\circ\text{C}$	$T_{c,o} = 65^\circ\text{C}$

Having R and η_t and two known inlet temperatures at each current time the amount of heat transfer and temperatures at the outlet can be obtained:

$$Q_{Recovered} = AU \cdot LMTD = c_{p_c} G_{c,des} (T_{c,o} - T_{c,i}) = c_{p_h} G_{h,des} (T_{h,i} - T_{h,o}) \quad 5-5$$

$$(T_{c,o} - T_{c,i}) = r(T_{h,i} - T_{h,o}) = r\eta_t (T_{h,i} - T_{c,i}) \quad 5-6$$

5.1.3 Mass flow rate of consumer substations in design condition

Once the heat demand of all buildings were collected, the mass flow rates supplying for each building was obtained by

$$G = \frac{\varphi_d}{c_p (T_S - T_R)} \quad 5-7$$

where c_p stands for the specific heat of the fluid, T_S for the supply temperature and T_R for the return temperature in design conditions. Temperature level of the network was assumed 25K which is near to annual average observed from the records. This value was approximated as design value for sizing of the pipes and the consumer heat exchangers. Low temperature difference is the consequence of lower supply temperature. The reason for relatively low temperature level in this DHS is to increase the ability to integrate decentralized waste heat source. On the other hand, low temperature level demands higher mass flow rate in the network and consequently higher power consumption and larger pipes.

5.1.3.1 Mass flow rates in the network branches

The evaluation of the mass flow rates flowing through each branch of the network starts with the values of G at each branch belong to the users and using the analogy of Kirchhoff's current law:

“At any node in the network, the sum of mass flow rates flowing into that node is equal to the sum of mass flow rates flowing out of that node”

For any node i :

$$\sum_{j=1}^n G_j = 0 \quad 5-8$$

where n , is the number of branches flowing toward or away from i^{th} node.

Applying the continuity equation to the nodes mass flow rate at each branch is evaluated. These values will later be used as guess values to solve fluid dynamic problem.

5.1.4 Pipe sizing

Pipes must be sized such that the velocity of the water running through them will not be high enough to cause either vibration induced noise or erosion of the pipe material. In order to avoid these problems maximum velocity of 1.5 m/s in pipes is considered for sizing calculations. Knowing all values of the mass flow rates involved in the process, the diameters can be calculated from:

$$D = \sqrt{\frac{4G}{\rho v \pi}} \quad 5-9$$

Where v is the design velocity of flow and ρ is the fluid density. The results have been compared to commercial values of pipe diameters.

5.1.5 Incidence Matrix of Network

Following the principles of graph theory, incidence matrix of supply and return network is reached by constructing vectors of inlet and outlet nodes arranged by the number of branches. Inlets vector includes nodes that inlet for the branches, outlet vector includes nodes that are outlet for the branches. The references to the number of each branch and node are shown in the following layouts of network topology.

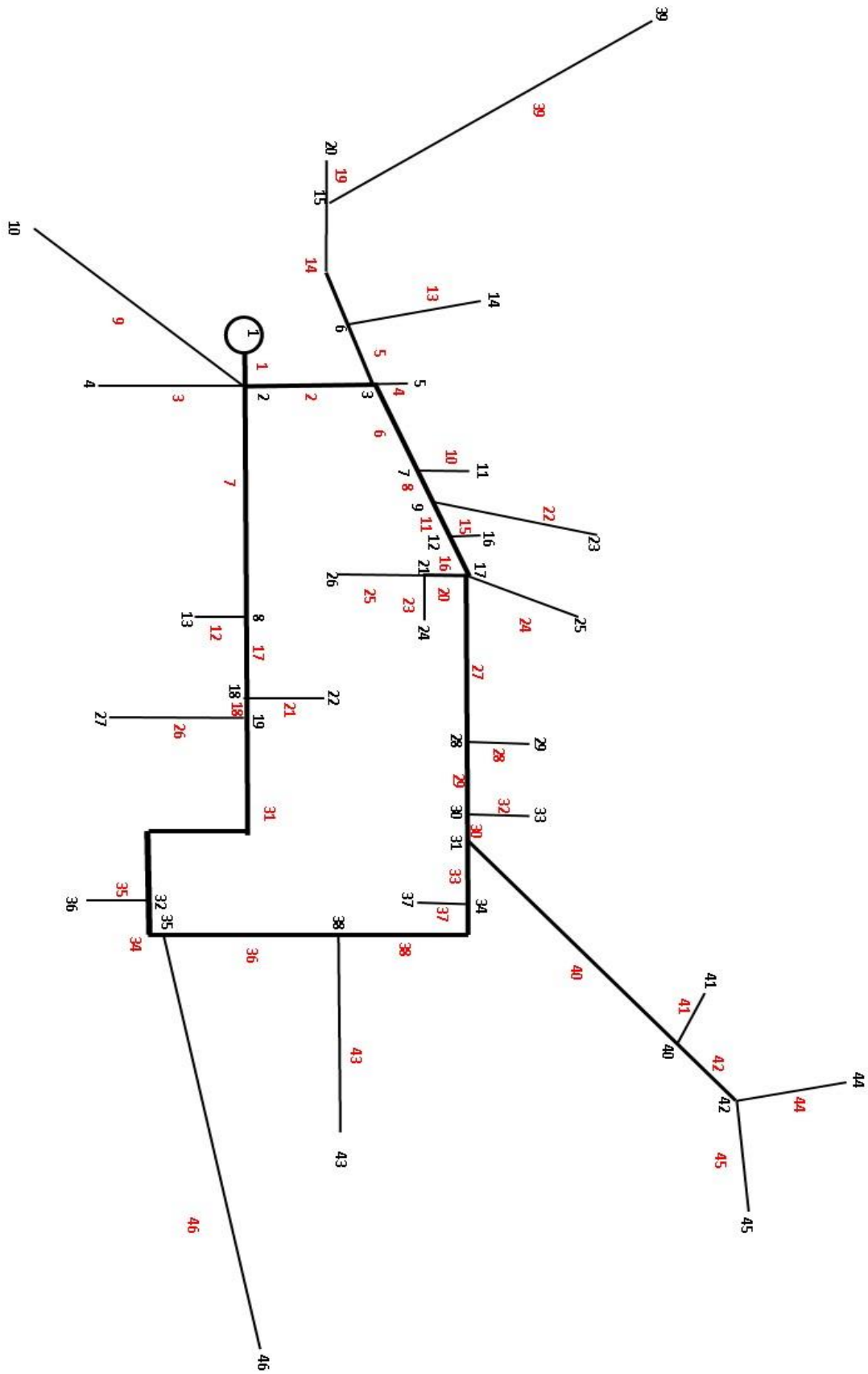


Figure 5-12 Numeration of nodes an branches of supply pipe line

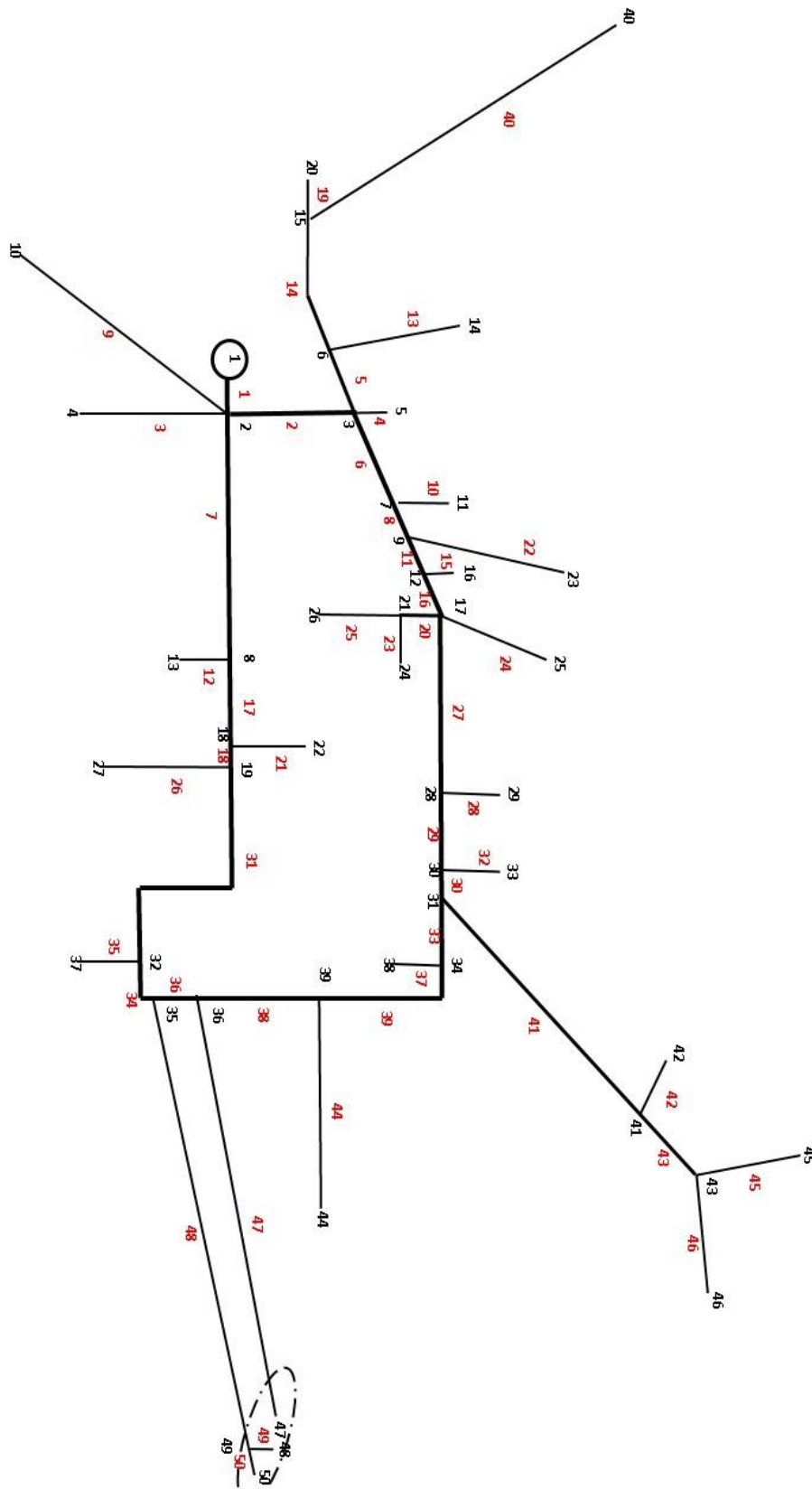


Figure 5-13 Numeration of nodes an branches of return pipe line

Nodes and branches are numbered with black and red numbers respectively. Node 1 is the central heat production building. As it can be seen, Due to introduction of heat from datacentre in the return line, Figure 5-12 and Figure 5-13 are slightly different. Therefore, analysis of supply and return distribution are separately done.

Two more branches in return line enables the connection of decentralized heat production unit to the main network (branches 49, 48). Branch 37 and 46 of supply line is therefore needed to be divided in two in return configuration. Hence, return line has four more nodes and branches comparing to supply line. Nodes 48, 49, 50 are located in the same building but due to difference in utility of substations in this building they are separately considered. Table 5-2 summarises the important nodes of the network in return line which will be addressed in later chapters.

Table 5-2 Important nodes reference

Node	Description
1	CHDB
47	Datacentre inlet
48	Datacentre outlet
37	Consumer node close to datacentre. Building no. 17
46	Last consumer substation. Building no. 24

5.2 Assumption and constraints for fluid dynamic problem

Considering the ring network, the momentum and the continuity equations must be solved to determine the mass flow rate in each branch and the pressure at each node of the network.

Following assumption and constraints were also considered for boundaries of system.

As it has been computed in the last section, each user extracts demanded mass flow rate from the network to substation in secondary side. Therefore for mass flow rate for boundaries associated with consumer substations:

$$G_{ext} = \frac{\varphi_d}{c_p(T_S - T_R)} \quad 5-10$$

Vector G_{ext} collects extracted and injected mass flow rates from/to each node (positive if extracted and minus if injected). Mass flow rate of water for reheating purpose G_d is also included in this equation for return calculations.

$$G_d = \frac{Q_{Recovered}}{c_p(T_{w,in} - T_{w,out})} \quad 5-11$$

Another boundary condition has been applied to the pressure at the first node which has been considered equal to 1 bar. It is considered that first node is perfectly able to maintain 1 bar pressure for injecting heat flux to first branch.

Only one pump has been considered in the network. It has been considered to belong to the first branch. Its head requirement is adjusted for design condition as it is corresponding to maximum flow rate in the network and therefore maximum hydraulic losses according to Darcy-Weisbach (4-29). In order to control the pump power requirement the value of pressure at the plant in the return line was assumed higher than 1 bar as

$$P_{1Ret} = P_{1Sup} + \Delta P_{PUMP} - 2\Delta P_{MAX} - \Delta P_{USER} \quad 5-12$$

Hydraulic losses ΔP_{MAX} were approximated as equal considering both supply and return line and is therefore written two times.

The performance of a centrifugal pump can be shown graphically on a characteristic curve. A typical characteristic curve shows head, efficiency, and power consumption plotted over the flow rate capacity range of the pump.

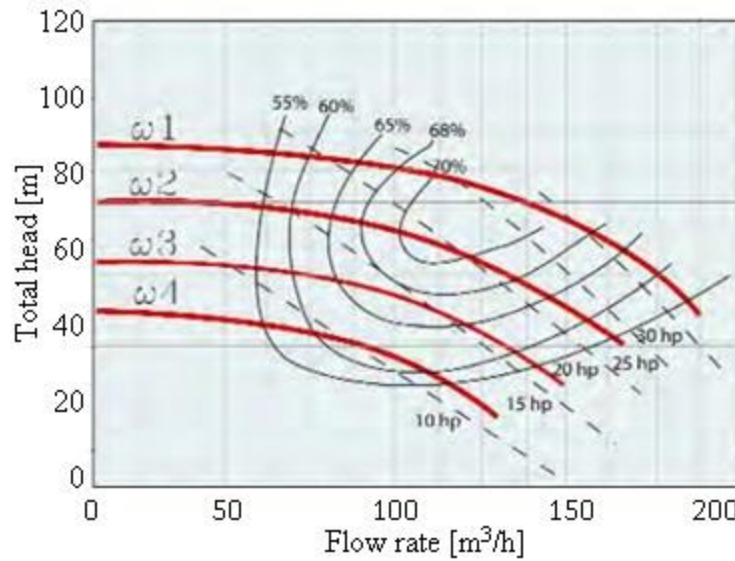


Figure 5-14 Characteristic curve of the pump, total head Vs. flow rate

A system characteristic curve represents the behaviour of the system in which the pump is operated. It defines the point on the pump characteristic curve on which the pump operates. Plotting the system and pump characteristic curve in the same diagram, the point of intersection is the operation point of the pump, operated at a certain speed in a given system.

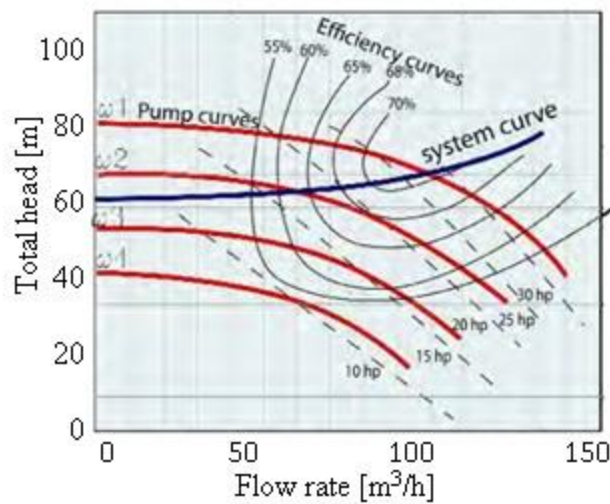


Figure 5-15 System curve and charecteristic curve relation

Generally pump head is reduced by increasing the flow rate, however hydraulic and friction pressure losses in pipes are at maximum when flow rate has its higher value.

Therefore the pump is dimensioned in order to cope with maximum pressure loss in pipes together with pressure drop at buildings substation.

$$\Delta P_{Pump} = 2\Delta P_{MAX} - \Delta P_{USER}$$

Sizing and selection of pump is done for the condition associated with maximum hydraulic losses. Sizing measures are based on flow rate, head requirement working temperature and application. The pump fit for the application of pressure boosting for distribution network selected from Grundfos Danish pump manufacturer with sizing parameters shown in Table 5-3.

Table 5-3 Design parameters of the pump at best efficiency point (BEP)

$\Delta P_{Pump,BEP}$ [bar]	\dot{V} [m ³ /h]	n [rpm]	Pump power at BEP [kW]	$\eta_{P,BEP}$ [%]
3.7	243	2620 (0.78 x n_{max})	28	78

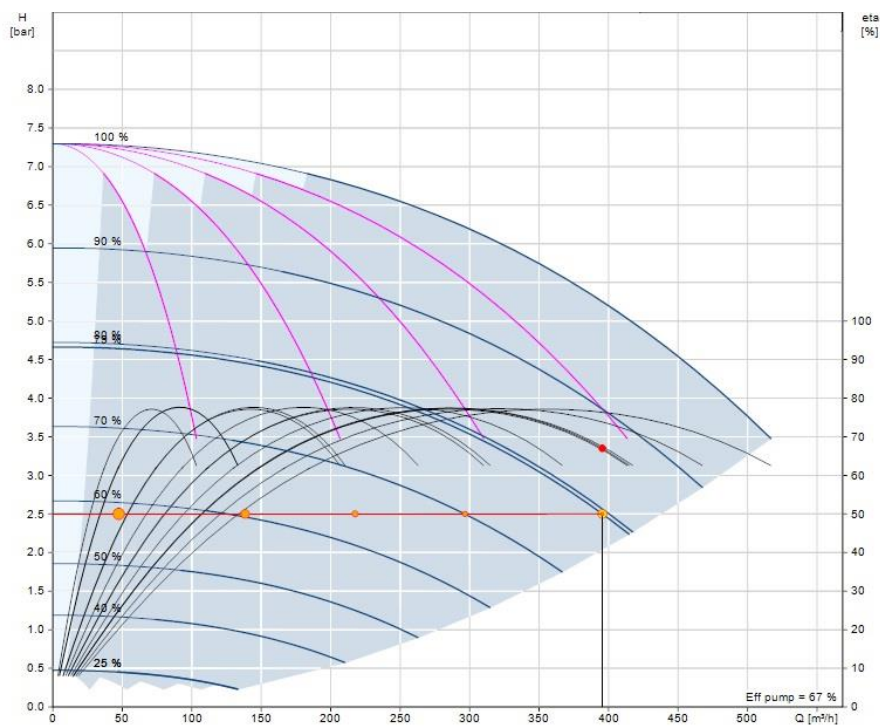


Figure 5-16 Best efficiency point in charecteristic curve of the selected pump.

Characteristic curve of the pump is approximated by a polynomial function. Using series of real data from the pump datasheet polynomial fitting coefficients between head and volumetric flow rate, and pump efficiency and volumetric flow rate are obtained:

$$\Delta P_{PUMP} = a(\dot{V}^2) + b(\dot{V}) + c \quad 5-14$$

$$\eta_p = x(\dot{V}^2) + y(\dot{V}) + z \quad 5-15$$

Input power of pump at constant rotation speed can be achieved by:

$$w = \frac{1}{\eta_p \rho} G \Delta P_{PUMP} \quad 5-16$$

ΔP_{USER} takes minimum pressure drop at the substation at furthest location from first node into account. This is due to ensure performance of heat exchangers at the user's substation. Furthest substation have lowest supply pressure in the network, therefore calculation of pressure in return line requires the boundary condition for this node as below

$$P_{end,Ret} = P_{end,Sup} - \Delta P_{USER} \quad 5-17$$

5.3 Assumption and constraints for thermal problem

The problem is solvable once the boundary conditions are imposed. Referring to the network the boundary conditions to apply are:

The inlet temperature, i.e. the temperature at node 1 is known, so the first equation became trivial and in particular $f(1) = T_{inlet}$ and the first row of K has a 1 in K (1, 1) and zeros in all other positions.

$$[1 \ 0 \ 0 \ \dots] \begin{bmatrix} T_{inlet} \\ 0 \\ 0 \\ \vdots \end{bmatrix} = \begin{bmatrix} T_{inlet} \\ 0 \\ 0 \\ \vdots \end{bmatrix} \quad 5-18$$

Outlet temperature, since the supply network must provide heat to the buildings, at those nodes which are users for the network the flow-rate is extracted from the network, so the balance equations for that nodes becomes

$$\frac{SL\rho c_p}{\Delta t} \left(\frac{(T_i^t + T_{i+1}^t)}{2} - \frac{(T_i^{t-\Delta t} + T_{i+1}^{t-\Delta t})}{2} \right) + Gc_p(T_{i+1}^t - T_i^t) = L * P * U(\bar{T}_b - T_g) \quad 5-19$$

Where T_{i+1}^t is the temperature of the node which is sending flow-rate to node n and $\bar{T}_b = \frac{(T_i^t + T_{i+1}^t)}{2}$ is the mean temperature of the branch. Therefore the row of the matrix problem corresponding to a user node must be modified to

$$f_n = -\frac{L_j P_j U_j T_g}{cpG_j} + \frac{SL\rho c_p (T_i^{t-\Delta t} + T_{i+1}^{t-\Delta t})}{\Delta t \cdot 2} \quad 5-20$$

$$K_{i,i} = -\left(1 + \frac{L_j P_j U_j}{2cpG_j} + \frac{SL\rho}{2\Delta t G_j}\right) \quad 5-21$$

$$K_{i,i+1} = 1 - \frac{L_j P_j U_j}{2cpG_j} + \frac{SL\rho}{2\Delta t G_j} \quad 5-22$$

Implementing this matrix problem in a proper software like Matlab it is possible to find the vector T of the temperatures at the nodes. For the return network boundary conditions has to change.

Boundary condition for the outlet must now be applied only at node 1, while user nodes are now inlet node with known temperature.

Temperature of return line at user nodes is computed by considering performance of heat exchangers at user's substations. Stating the same procedure illustrated in analysis of waste heat from datacentre efficiency of a heat exchanger is defined as

$$\eta_t = \frac{(T_{sp} - T_{rp})}{(T_{sp} - T_{rs})} \quad 5-23$$

Where T_{sp} , T_{rp} and T_{rs} stand for supply temperature at the primary side, return temperature at primary side and return temperature of secondary side respectively.

It is also possible to determine efficiency of heat exchangers by means of “means of logarithmic mean temperature difference” and “number of transfer units”.

$$LMTD = \frac{((T_{sp} - T_{ss}) - (T_{rp} - T_{rs}))}{\ln((T_{sp} - T_{ss}) - (T_{rp} - T_{rs}))} \quad 5-24$$

$$NTU = \frac{UA}{c_p G_{p,des}} \quad 5-25$$

where $UA = \frac{\phi_{des}}{LMTD}$. Finally efficiency is computed as

$$\eta_t = \frac{1 - e^{-NTU(1-r)}}{1 - Re^{-NTU(1-r)}} \quad 5-26$$

where the ratio $r = \frac{G_{p,des}}{G_{s,des}}$ is used. Heat exchangers are designed to work in following design condition:

Network side	User side
$T_{sp} = 90^\circ\text{C}$	$T_{ss} = 60^\circ\text{C}$
$T_{rp} = 65^\circ\text{C}$	$T_{rs} = 40^\circ\text{C}$

For any current load $\phi_c(t)$ other than design load, return temperature of the consumer side may be obtained by empirical relation as:

$$T_{rs}(t) = T_{ss}(t) - \left[1 + 0.3 \left(\frac{\phi_c(t)}{\phi_{des}} \right) \left(\frac{T_{ss}(t) - T_R}{(T_{ss} + T_{rs})/2} \right)^{-n_1} \right]^{\frac{2}{n_2}} (T_{ss}(t) - T_R) \quad 5-27$$

Indoor temperature T_R is suggested 20°C for summer and 22°C winter in standards published in [18].

Finally by having the efficiency it is possible to predict return temperature at primary side using 5-23.

5.4 Scenarios for improvement of district heating control

Test scenarios considering the system functionalities of the network including control strategies and additional components were analysed. Different scenarios consider possibilities for improvement of heat distribution in order to be able to achieve higher share of renewable waste heat.

For improvement of hydraulic operation of the network control methods for pump and substation of the last consumer of the network was provided. The aim of this scenario was to analyse the advantages of adopting variable speed control for pump and utilization of flow control valve at user substations.

In order to enhance thermal performance of the network to be able to receive distributed heat in a more efficient manner a scenario for controlling the supply temperature at CHDB is provided. The effect of variable supply temperature on consumers and distributed heat integration was further analysed.

5.4.1 Outdoor temperature compensation

Supply temperature of heat fluxes from the plant can be either constant for entire year or adjusted in order to avoid unnecessary heat load on central plant. Commonly supply temperature of plant is regulated by changes in outdoor temperature, because heat demand of buildings are often measured considering outdoor temperature. Hence, outdoor temperature could be the link between users demand and temperature of the water that plant is supplying.

Both constant and variable supply temperature are considered in separate simulations in order to compare the effect of outdoor temperature compensation. According to DH energy monitoring platforms of university campus, supply temperature is defined as a linear function of outdoor temperature as shown in Figure 5-17 and constant supply temperature is assumed 75°C.

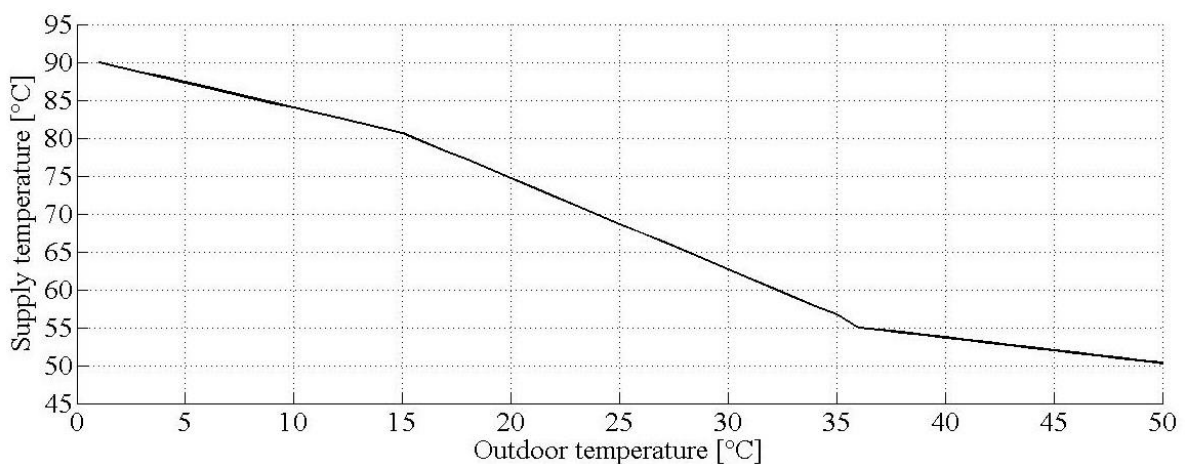


Figure 5-17 Adjustment of supply temperature proportional to outdoor temperature

5.4.2 Pressure difference control

Minimum pressure difference at the users ΔP_{USER} were assumed to be 0.7 bar. This value however is associated with the pressure differential at the plant between the supply and the return line. The building farthest from the CHDB (no. 24), meets the minimum pressure differential between supply and return line, thus control of this substation is the most crucial. As it was mentioned in preliminary design it is assumed that one heat exchanger receives the total heat requirement of the building for space heating and domestic hot water. This assumption was due to available measured data. A simplified model of a substation could consist of a heat exchanger to receive heat from the primary side and a flow control valve as shown in Figure 5-18.

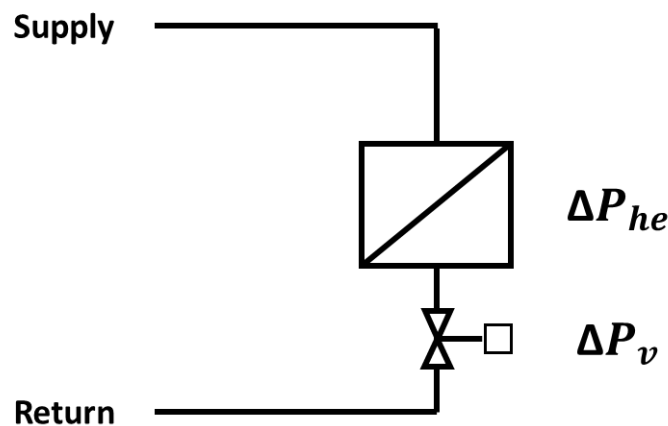


Figure 5-18 Hydraulic resistances due to additional components

The flow of the water in heat transfer section of heat exchanger is associated with a pressure drop proportional to square of mass flow rate. The valve is located after heat exchanger in order to compensate necessary pressure drop and in order to maintain pressure balance at CHDB by the pump. In this method pump updates the rotation speed according to the outputs of pressure drop from substation and hydraulic losses in supply.

$$\Delta P_{USER} = \Delta P_{he} + \Delta P_v \quad 5-28$$

ΔP_{he} and ΔP_v are defined as a function of mass flow rate as follow:

$$\Delta P_{he} = kG^2 \quad 5-29$$

$$\sqrt{\Delta P_v} = \frac{G}{k_v} \quad 5-30$$

where K in 4-29 is considered to be constant and is determined for design condition.

K_v Determines the capacity of the valve and is defines how much volumetric flow rate m^3/h flows through the valve with pressure differential of 1 bar. K_v is proportional to opening position of the valve.

In order to have a better control on performance of the substation the ratio “valve authority” was introduced as:

$$N = \frac{\Delta P_v}{\Delta P_{he} + \Delta P_v} \quad 5-31$$

Valve authority shows how much pressure drop in the whole circuit is due to valve.

In order to achieve satisfactory pressure drop in the whole circuit mass flow rate through the valve remains constant. Therefore by closing the valve velocity of water in the valve due to reduction of cross section area increases and causes extra pressure drop. Valve sensor applies inputs of the pressure differential between plant and the substation in the supply line and controls the position of the valve in order to maintain constant 3 bar pressure difference between the supply and return line at the plant.

5.4.3 Pump control

Pressure rise due to pump directly affect the hydraulic balance and energy investment of the network. Pumps are commonly controlled by adjusting flow rates or/and adjusting the rotation speed according to characteristic curve. Affinity laws express relationships between several variables involved in pump performance such as flow rate, impeller diameter, head and power. There are two ways to express these relationships: either holding the impeller diameter or the rotation speed constant. Affinity laws for a constant impeller diameter are:

$$\frac{G_1}{G_2} = \frac{n_1}{n_2} \quad 5-32$$

$$\frac{\Delta P_{pump,1}}{\Delta P_{pump,2}} = \left(\frac{n_1}{n_2}\right)^2 \quad 5-33$$

$$\frac{p_1}{p_2} = \left(\frac{n_1}{n_2}\right)^3 \quad 5-34$$

where n is the rotation speed. The pump used in this network rotates at 2620 rpm in design condition.

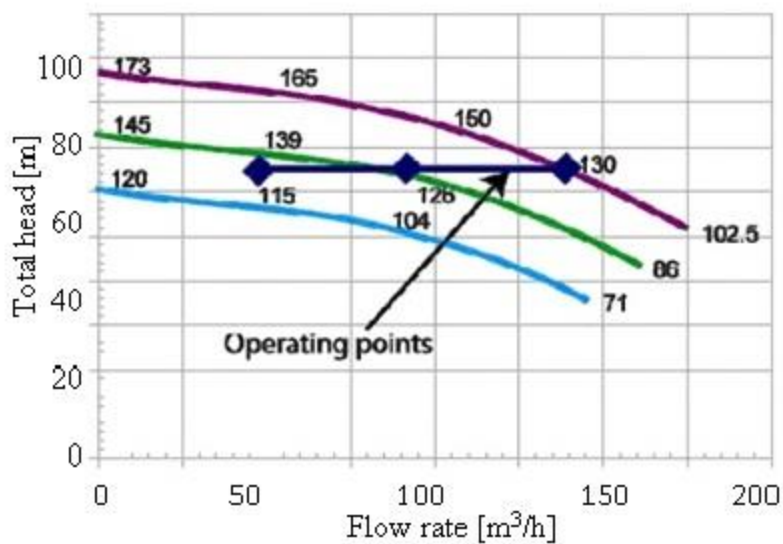


Figure 5-19 Working points of variable speed controlled pump

The pump used in first branch maintains constant pressure rise of 3 bar by pump, therefore is controlled by adjusting rotation speed.

Assume that due two decrease in costumers' heat demand plant must reduce the flow rate into the system. Therefore working point of the pump is subjected to change. By using affinity laws rotation speed of the pump is then changed in order to reach pressure to the desired value. Consequently power consumption of the pump will change.

5.5 Waste heat integration measurement cases

Integration of waste heat from datacentre was illustrated in 5.1.2. Cooling demand of datacentre during the year is fairly constant. Therefore the amount of available waste heat and the mass flow rate of the water for heat recovery purposes was assumed constant. Variations of heat pump power consumption are neglected. Extracting higher mass flow rates means relying more on waste heat source. On the other hand, differing from heat exchanger design value could dramatically affect the heat transfer efficiency (equation 4-4). Heat exchanger was designed for injecting maximum 1 MW heat power into the main grids of the network (Case 1). Two other Cases was also dedicated to higher percentages of total mass flow rate in the network (G_{\max}) which lead to increase in maximum heat load. In addition mass flow rate of the refrigerant needs to increase proportionally in order to maintain constant thermal efficiency (equation 4-4). Summary of design setups for different cases are shown in Table 5-4.

Table 5-4 Test cases for reflecting different share of renewable energy source

Case	$G_{c,des}$ kg/s	$G_{c,des} / G_{\max}$ %	$G_{h,des}$ kg/s	ΔT_{\max} K	r	η_t %	Q_{\max} MW
Case 1	10.2	9.6	8.56	35	0.58	65	1
Case 2	12.7	11.5	10.27	35	0.56	65	1.2
Case 3	15.5	14.6	11.13	35	0.50	65	1.3

Three scenarios are defined in order to evaluate the effect of change in functionality in the network such as:

- Reference scenario: In order to have a better comparison between possible situations, reference scenario is defined as the condition where 2620 rpm for pump rotation speed and 75°C supply temperature is constant.

Other possible scenarios are:

- Outdoor temperature compensation (OTC) scenario: Supply temperature was adjusted as explained in Figure 5-17.
- Pump control (PC) scenario: The only pump in the network is of a variable speed control (VSC) type. In this scenario pump was controlled in order to maintain 3 bar pressure difference between supplies and return pipes in first node. This is done by synchronizing the pump with flow control valve at end user substation.

Pressure drop at consumer substations is due to pressure drop in the heat exchanger and flow control valve as discussed before. In this scenario pump receives information about hydraulic losses within supply pipe and ΔP_{USER} .

$$\Delta P_{PUMP} = 2\Delta P_{MAX} + \Delta P_{USER} \quad 5-35$$

The chapter results includes representation of main physical characteristics of the system, pressures, temperatures and further analysis of the network for three waste heat integration cases. Finally the advantage and disadvantage of pump and supply temperature control methods were discussed.

CHAPTER 5

Results

Simulations were done for different cases with different contributions of datacentre. All cases were tested for the entire year in order to give an overall knowledge of network performance in heating seasons. Possibility of efficient integration of the waste heat was further analysed through suggested scenarios. The model is verified once it is able to present pressure and temperature distribution in the nodes. Further analysis of the network could be resulted from pressure and temperature of the nodes. The model was first assembled for reference scenario and later modified for OTC and PC scenario. In this chapter for each scenario, pressure and temperature distribution and related characteristics of the system such as maximum pump power is first shown to be reliable to result further analysis.

6.1 Reference scenario

6.1.1 Thermal characteristics of the network

Steady state temperature distribution of 11 MW heat rate in the network at design condition was shown in Figure 6-1. Users at substations experience average temperature difference of 25K between supply and return line in their substations. 10.2 kg/s of return water is then redirected to datacenter building and reheated from 49°C to 70°C in order to recover 1 MW heat power from cooling the servers. Introducing such heat causes temperature gradients from datacenter building and propagates toward the first node which is the heat production centre is

Results

the farthest point in the return line. therefore temperature of return water at central heat production center slightly increases.

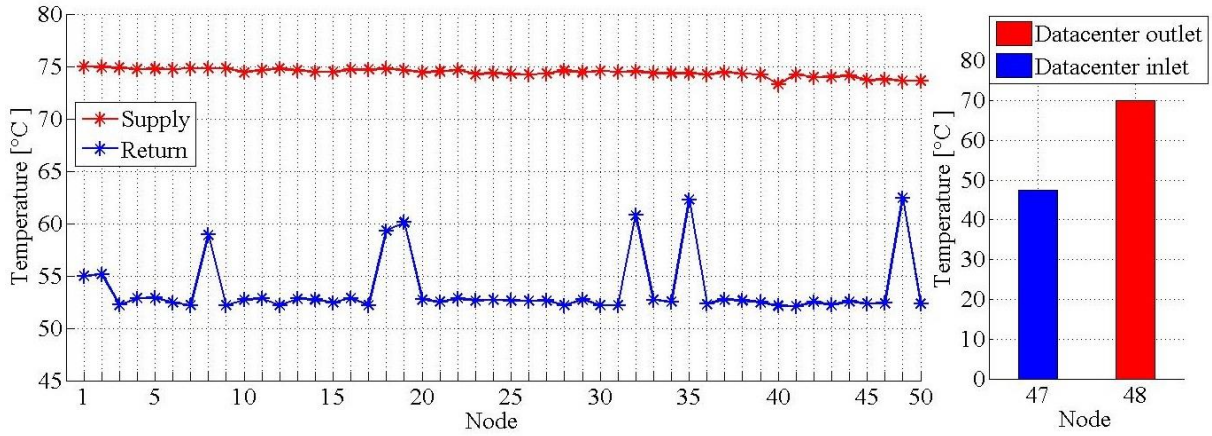


Figure 6-1 Temperature distribution for Reference scenario

Temperature drop at the last user substations is shown in Figure 6-2 for the entire year. Since waste heat is connected to the return line temperature drop in substations was not considerably affected by waste heat source.

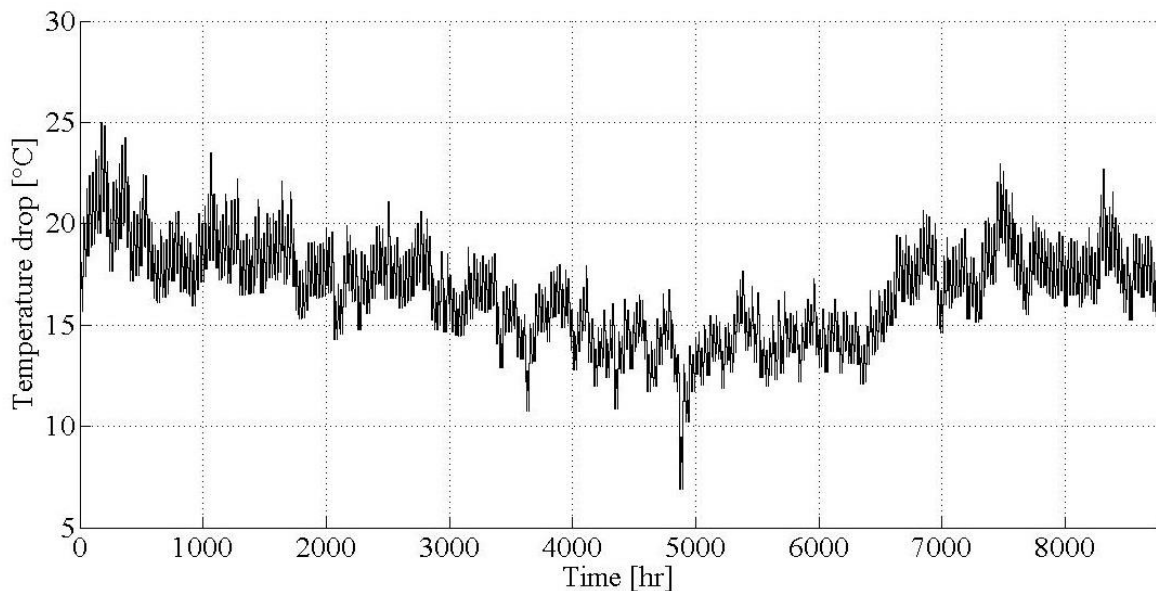


Figure 6-2 Hourly temperature drop variation at user substation no. 24

During the high demand days temperature difference was higher in order to ensure required heat transfer. This value however decreases in low demand condition which causes the water to return with higher temperature and consequently lower heat absorption from waste heat

source. Figure 6-3 shows heat rate from the waste heat source in the entire year for three described cases.

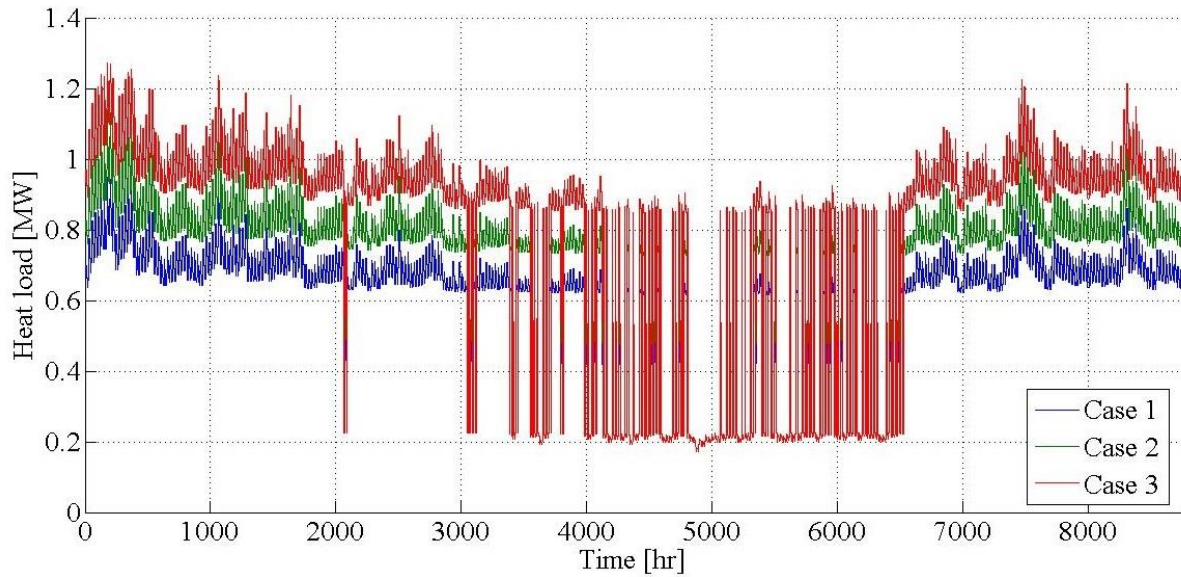


Figure 6-3 Hourly heat power from waste heat source (Reference scenario)

Waste heat integration was successful for most of the hours of the year with average loads from 0.7 MW in Case 1 to 0.95 MW in Case 3. Increasing share of the integrated waste heat source lead to higher annual energy production from 5.1 GWh in Case 1 to 6.94 GWh in Case 3. Duration curve of heat production by the waste heat in three cases is shown in Figure 6-4.

Table 6-1 Waste heat recovery in Reference scenario

Case	G [kg/s]	G/G _{max} [%]	Min. Temperature of hot water [°C]	Max.heat power [MW]	Annual thermal energy production [GWh/year]	Average heat power [MW]
Case 1	10.2	9.6	70	0.98	5.1	0.6
Case 2	12.7	11.5	70	1.18	5.9	0.68
Case 3	15.5	14.6	70	1.26	6.9	0.79

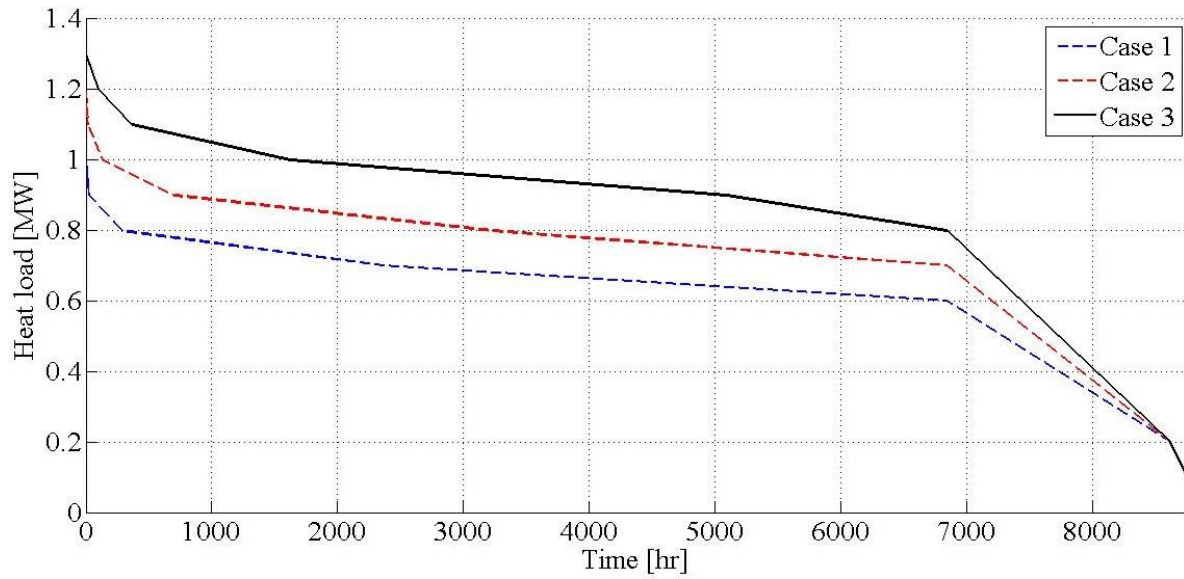


Figure 6-4 Duration curve of heat power at datacenter substation (Reference scenario)

Increasing the amount of reheated water lead to an increase in peak load of waste heat from 0.98 MW in Case 1 to 1.26 MW in Case 3. This 30% increase is followed by approximately 50% increase of reheated water mass flow rate.

Temperature of the waste heat source inlet for entire year is shown in Figure 6-5. Due to lower temperature drop at substations in low demand hours, temperature of water to be reheated by waste heat source was higher and consequently caused reduction of heat load from datacentre to near 0.2 MW as shown in Figure 6-3.

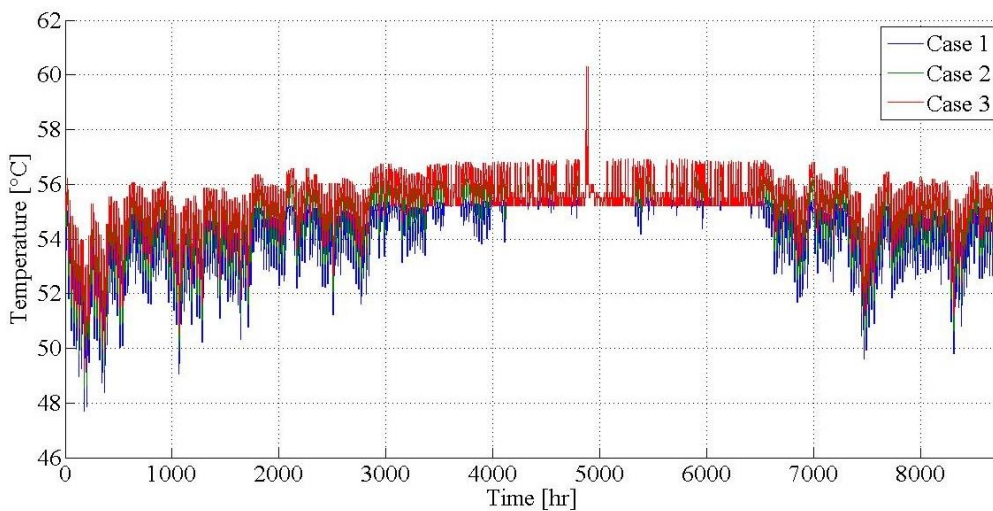


Figure 6-5 Temperature of the return water redirected to datacenter substation for all the cases of waste heat share (Reference scenario)

The supply and return temperature at CHDB is shown in Figure 6-6. Integrating waste heat to network grids lead to a higher return temperature, this effect was more significant when the higher share was adopted.

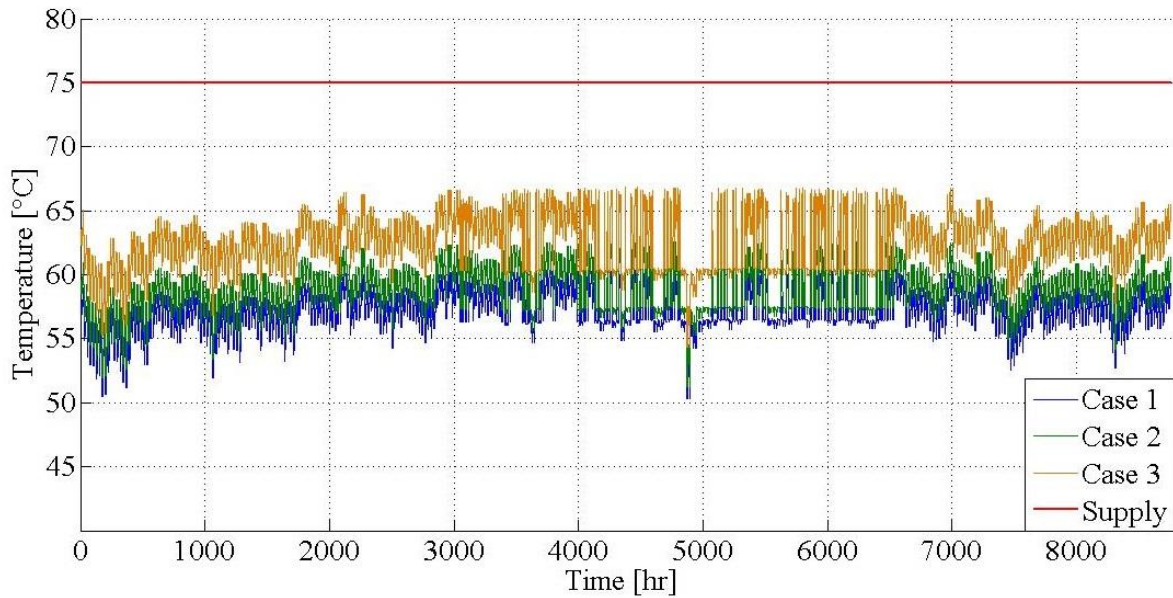


Figure 6-6 Hourly temperature levels at main heat production building

Increasing share of integrated waste heat source in the network in different cases could effect on heat losses within distribution pipes as shown in Figure 6-7. Increasing share of waste heat increases temperature levels within the network, therefore thermal energy loss in pipes occurs with higher rates.

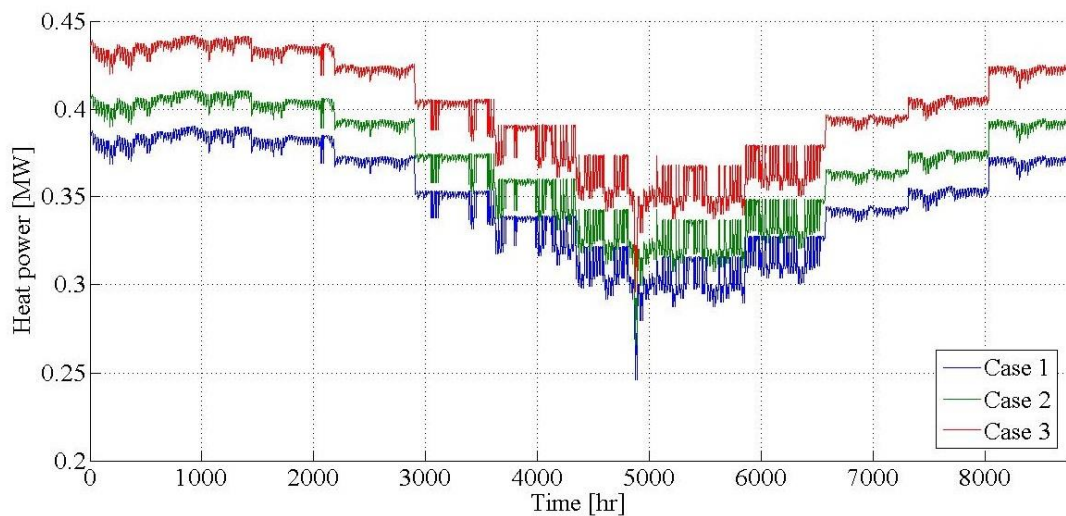


Figure 6-7 Hourly variation of heat power loss in the pipes (Reference scenario)

During the high demand hours higher amount of heat was lost however comparing to the total heat demand includes lower percentage. Increasing share of distributed renewable heat source in Case 2 and Case 3 was resulted in higher annual heat losses in general , from 12% in Case 2 to 14% in Case3. Table 6-2 summarises result of heat loss in three cases.

Table 6-2 Distribution energy losses in three cases

Case	Annual thermal energy loss [GWh/year]
Case 1	2.9
Case 2	3.2
Case 3	3.5

6.1.2 Hydraulic analysis of the network

Results of pressure distribution in supply and return lines from main distribution unit to furthest point of the network for design condition is shown in Figure 6-8. As the flow moves toward the farthest point of the network pressure gradients due to friction and hydraulic losses cause pressure drop in supply and return lines. If there is no additional pump in distribution network pressure in the pipes from first point in supply to return to first point constantly decreases by circulating. Fluctuations in the return line are due to injection of hot water from datacentre which specifically effects on pressure balance in nearby point in return line.

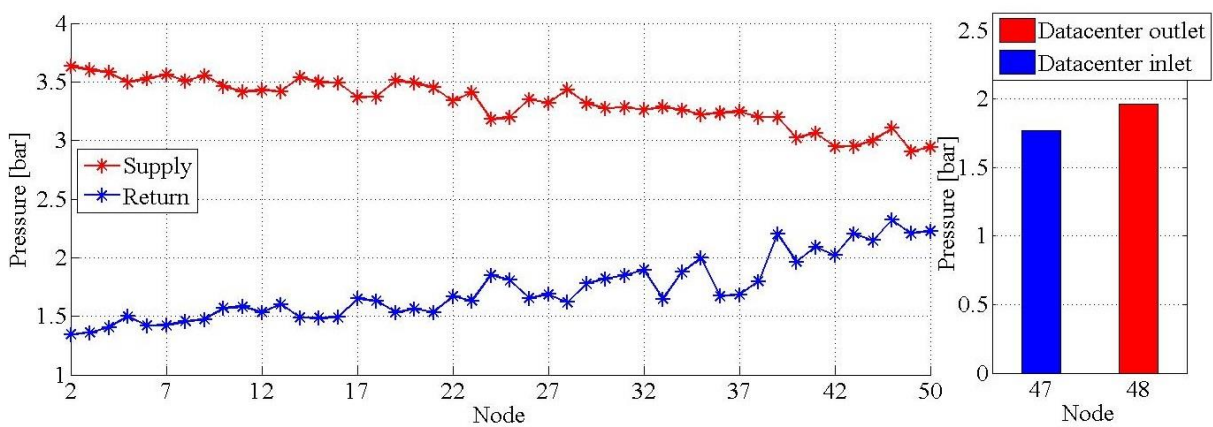


Figure 6-8 Pressure distribution Vs. nodes arranged by distance in design condition (Reference scenario)

Results

On average the pressure drop in the network was 127 Pa/m in supply line and 163 Pa/m in return line. Pump input power of 40 kW at constant rotation speed of 2620 rpm was required for overcoming overall 1.8 bar pressure drop in distribution and 0.7 bar in last user substation. Duration curve of pump power in Figure 6-9 shows the number of hours in the year pump required a certain minimum power.

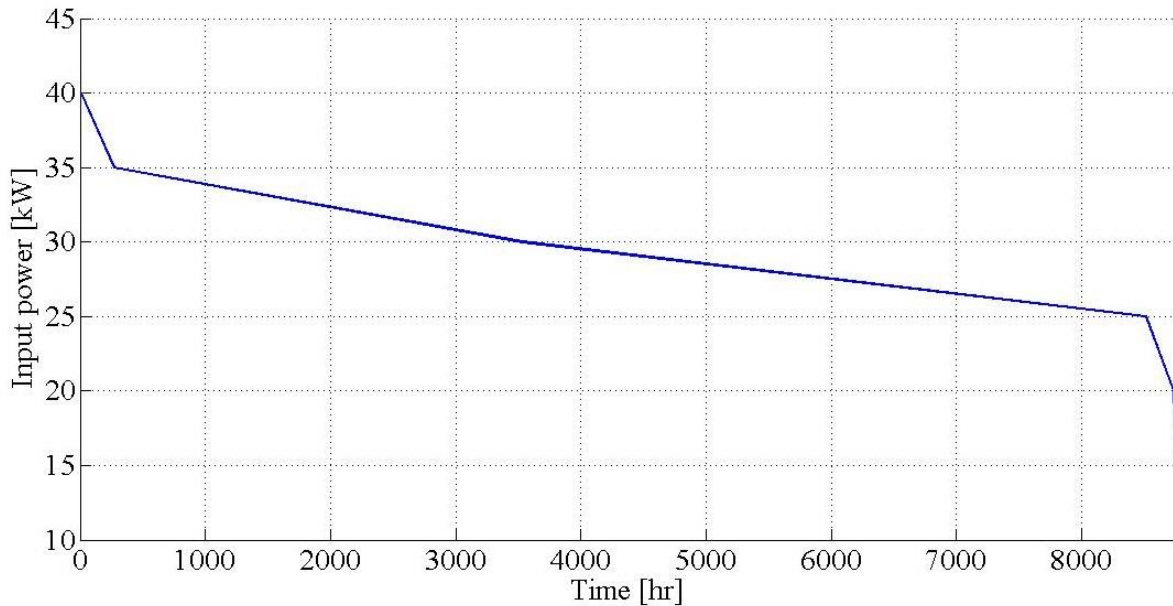


Figure 6-9 Pumping power vs. number of hours

Pressure of supply water at main heat production centre for entire year is shown in Figure 6-10. These pressures for supply are result of pressure increase by pump with electric input powers shown in Figure 6-11. Annual energy consumption of pump was 257 MWh/year.

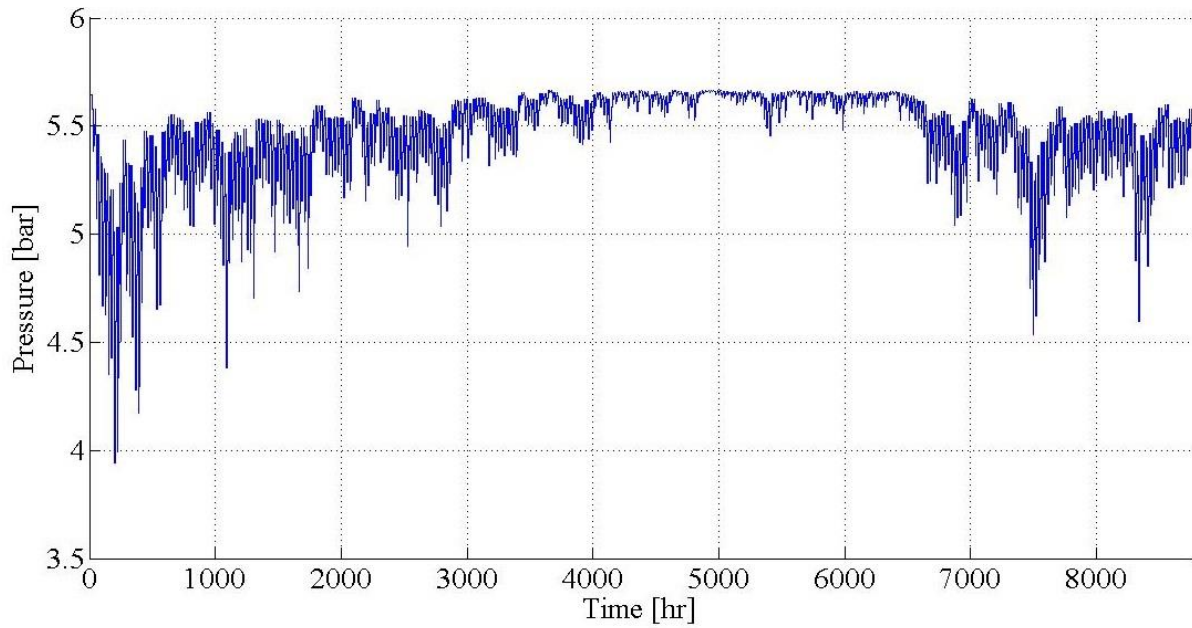


Figure 6-10 Hourly supply pressure variations at CHDB

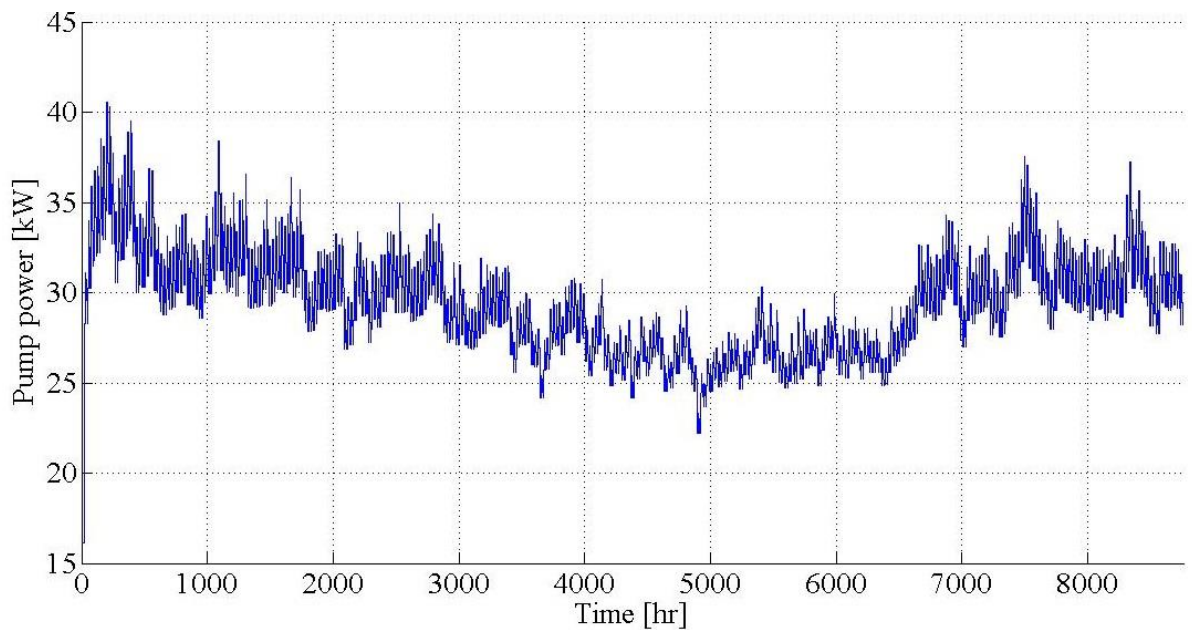


Figure 6-11 Hourly variation of pumping power required by network (Reference scenario)

Pressure drop at a user close to datacentre building is shown in Figure 6-12 for three cases in entire year. During high demand hours pressure drop in the network and in the consumer substation was higher. This is due to higher mass flow rate in the network which increases hydraulic losses. Minimum 0.7 bar pressure drop due to efficient heat transfer was assumed for user substations, however Figure 6-12 reveals that pressure drop at this user falls below the

limit in some hours of the year for Case 2 and Case 3. Figure 6-13 shows the frequency of this problem in the year.

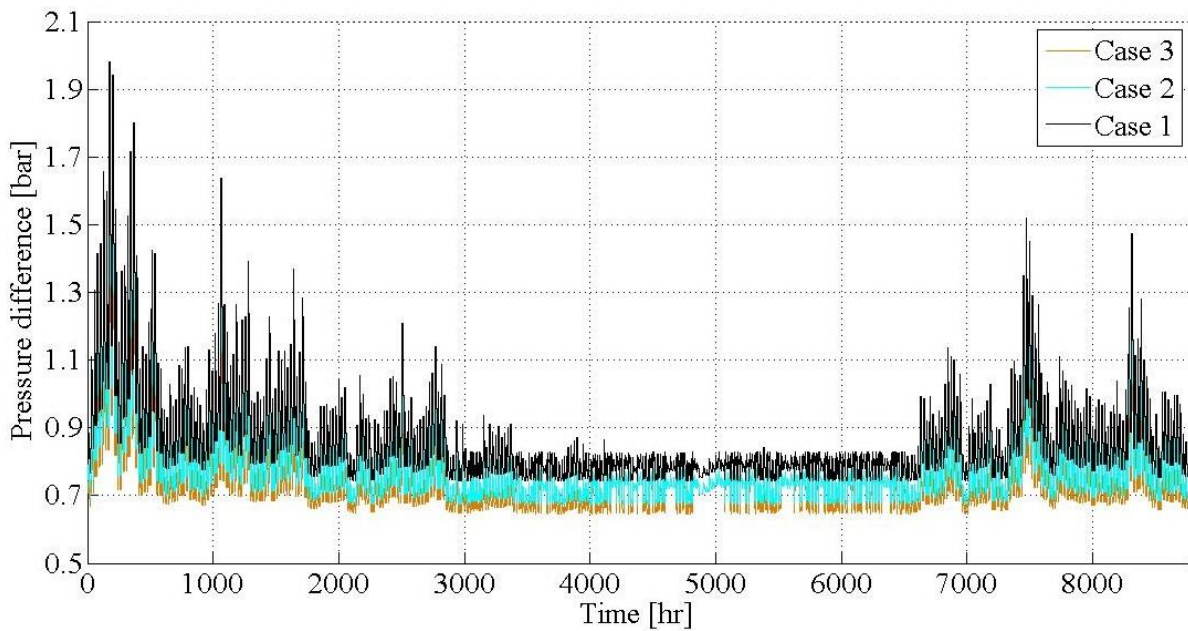


Figure 6-12 Hourly Pressure gradient at node 37 (user substation no. 17) in reference scenario

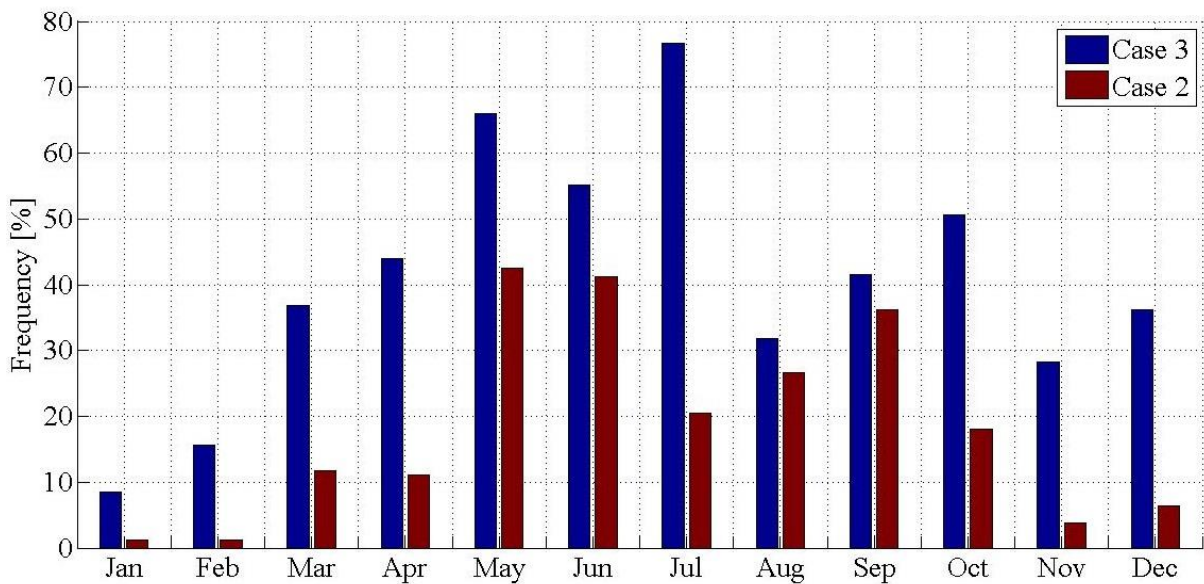


Figure 6-13 Frequency of fail hydraulic balance at node 37 (user substation no. 17)

During the low demand months pressure drop problem is more often evident, in both Case 2 and Case 3. This is due to lower mass flow rate in the network which makes the pressure of flow from datacentre to disturb hydraulic balance of the users nearby more than in high demand conditions. A constant mass flow rate for recovering waste heat was dedicated. Lower mass

flow rates in the network due to lower heat demand. This means in low demand conditions hydraulic balance of the network depends more on waste heat source interaction with main grids. Therefore in warmer month failure is more evident. Figure 6-14 shows pressure of the outlet from the datacentre. In high demand conditions reduction of pressure of injected hot water from waste heat source is followed by general pressure drop in the system. Higher pressure of supply in low demand condition is due to absence of any control on pressure difference at last user substation. Pressure of the water at datacentre inlet is shown in Figure 6-15. Higher pressure levels in low demand hours is followed by constant speed operation of the pump and lower hydraulic losses. This leads to higher pressure level of return water also in datacentre operation.

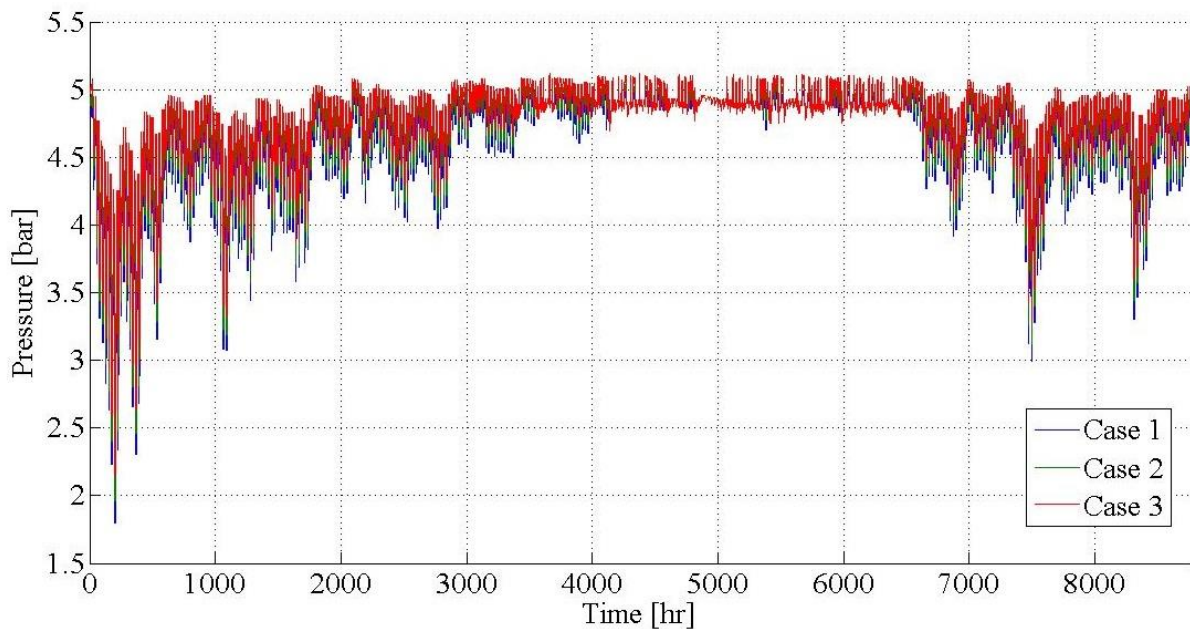


Figure 6-14 Hourly variation of waste heat outlet connection pressure

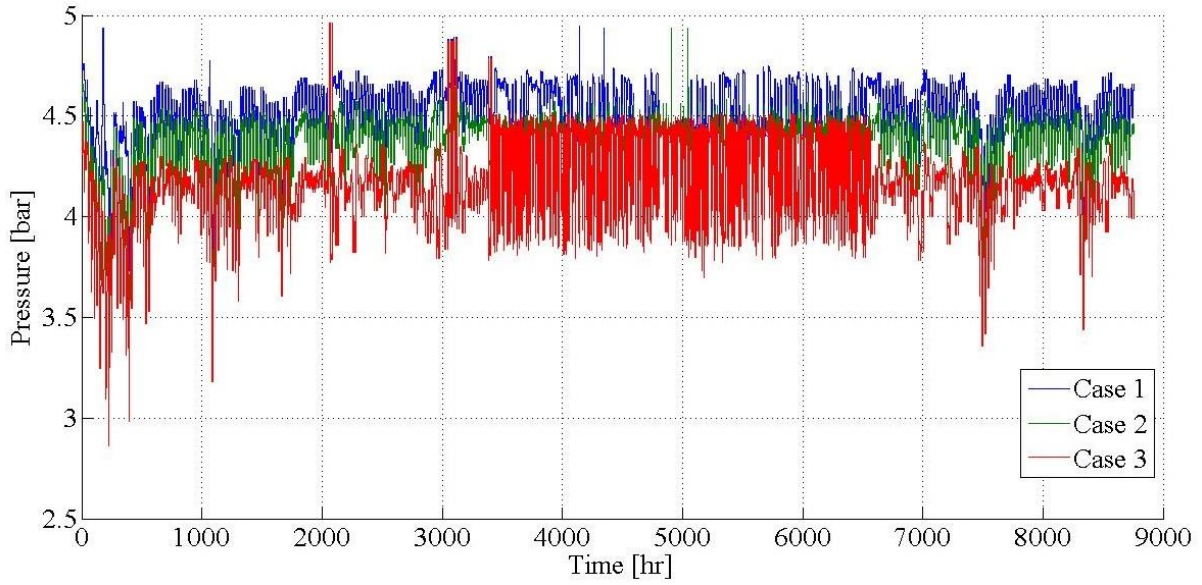


Figure 6-15 Hourly variation of waste heat inlet connection pressure

6.2 Outdoor temperature compensation scenario

Temperature distribution in design condition for OTC scenario is shown in Figure 6-16. Higher supply temperature in this condition leads to higher temperature level for datacentre substation and consequently lower heat load from waste heat source.

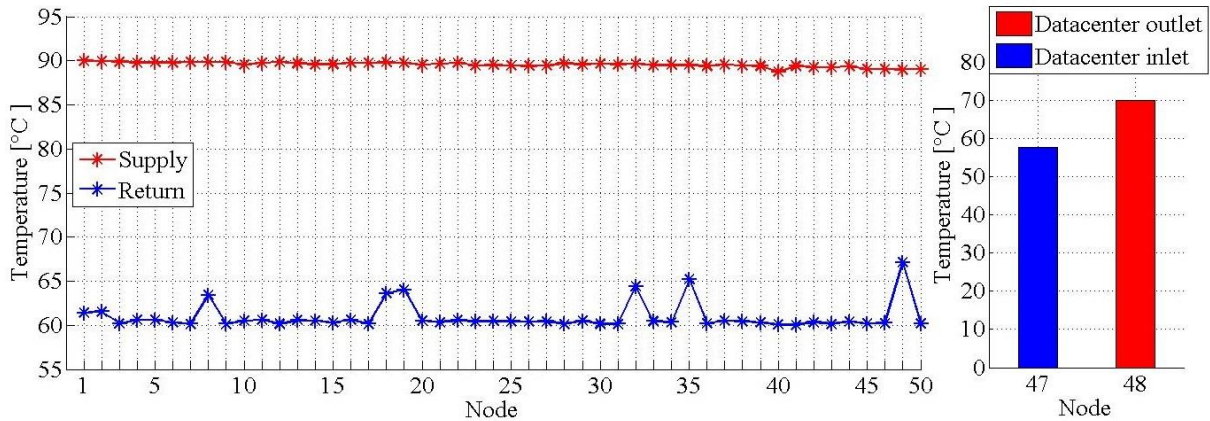


Figure 6-16 Temperature distribution vs. distance in OTCscenario

Figure 6-17 shows Temperature drop at a user substation for entire year.in this scenario variation of temperature drop due to heat transfer in user substations is higher due to variation of supply temperature.

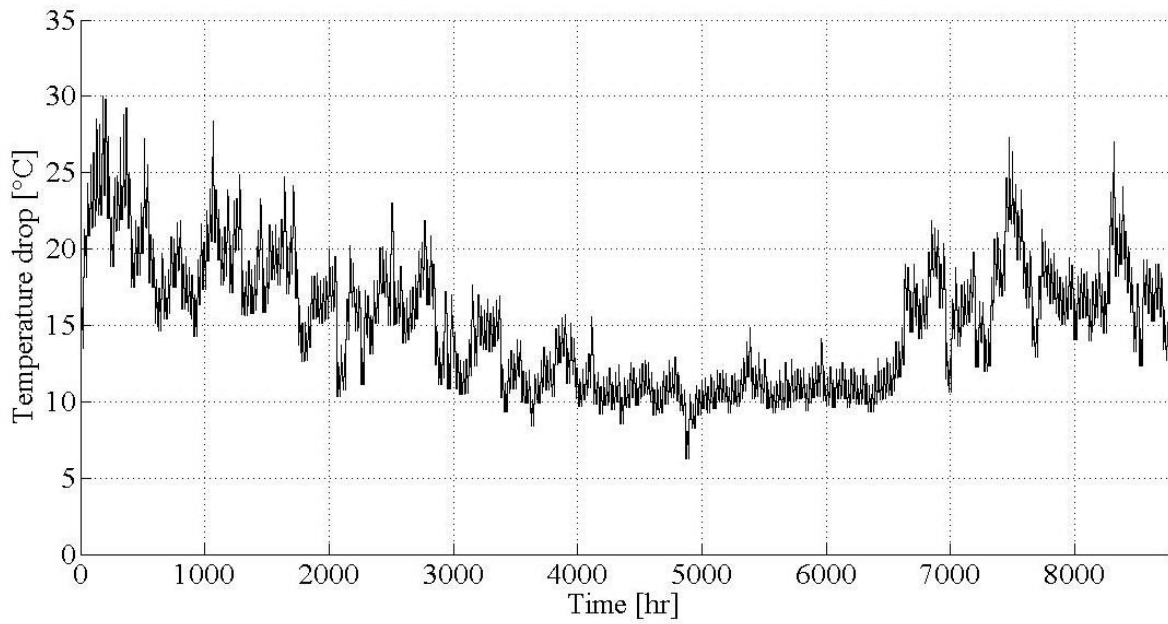


Figure 6-17 Hourly variation of temperature drop at user substation no.50

In colder hours of the year when heat request of buildings is higher, user substations work with higher temperature difference, however in warmer hours of the year temperature difference becomes lower than Reference scenario. Lowering supply temperature has considerable effect on efficiency of heat exchangers in consumer buildings. Figure 6-18 compares response of heat exchanger at a substation during the year.

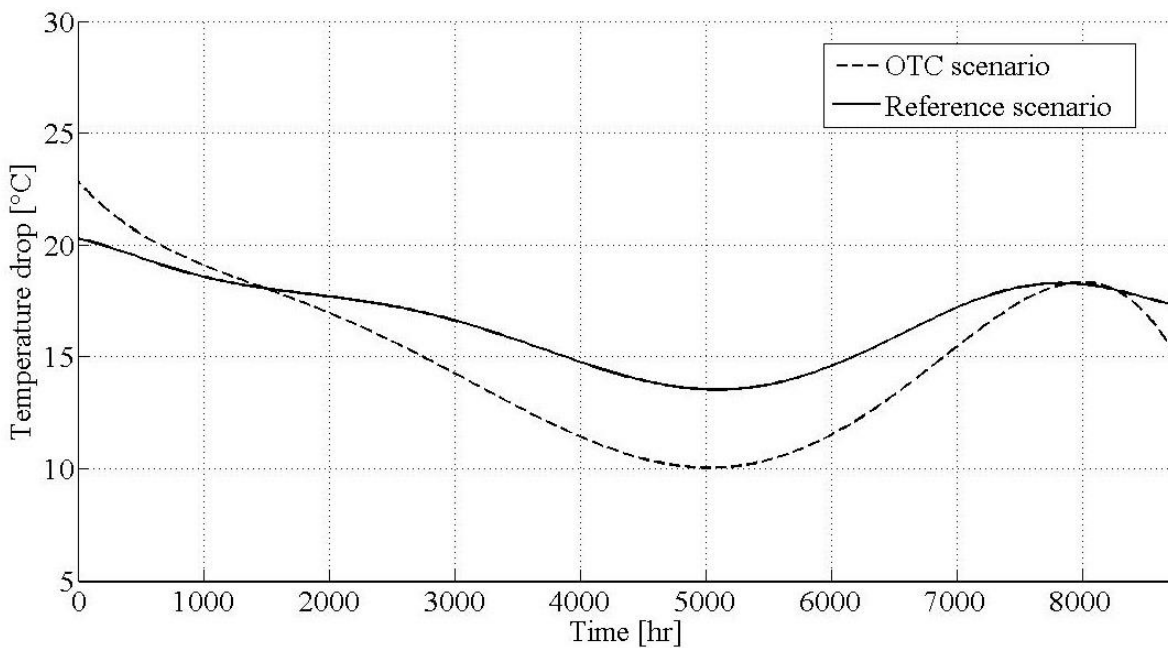


Figure 6-18 Temperature drop variation at user substation no.50

Heat production at datacentre substation in this scenario is shown in Figure 6-19. The effect of regulating temperature level of supply is clearly visible in heat recovering process. During high demand conditions higher supply temperature is adopted and consequently temperature level in return is higher. Despite the high demand hours which are associated with greater amount of temperature drop at user substations the heat load in these conditions is at its lowest values.

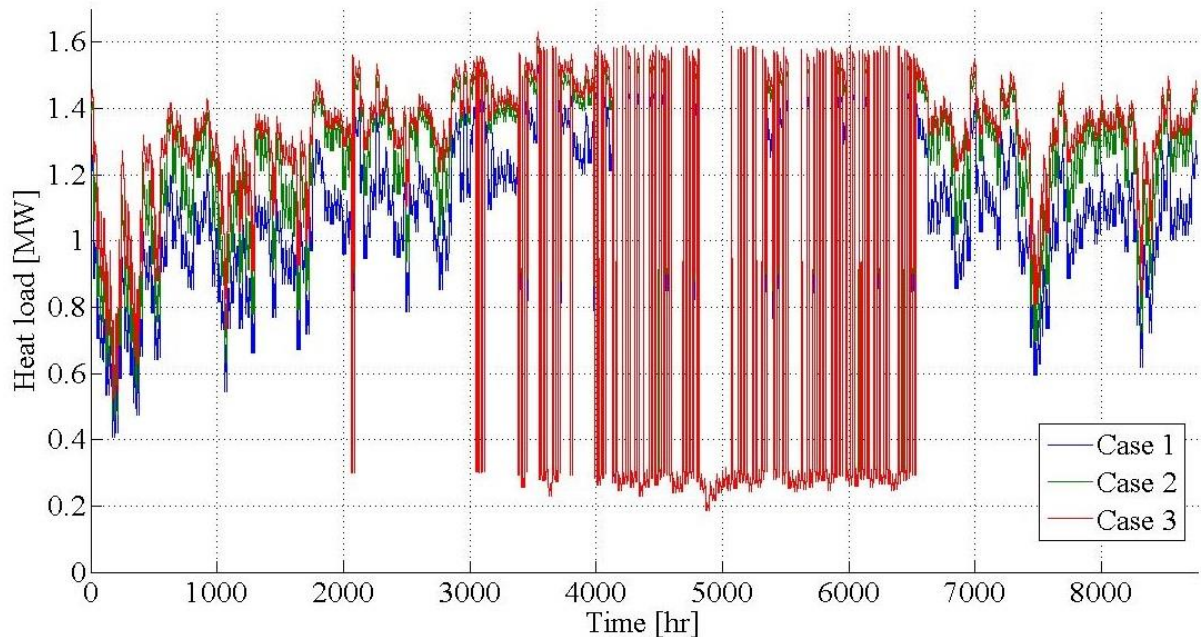


Figure 6-19 Hourly variation of heat power absorbed by waste heat source for OTC scenario

Lower heat requirement of building corresponds to lower supply temperatures. Despite of lower temperature drop, low supply temperature provides reasonably cooled water in return line to feed the datacentre substation. As a result, heat recovery from datacentre hits the peak of near 1.6 MW in Case 3. Figure 6-20 shows temperature at the inlet of waste heat source.

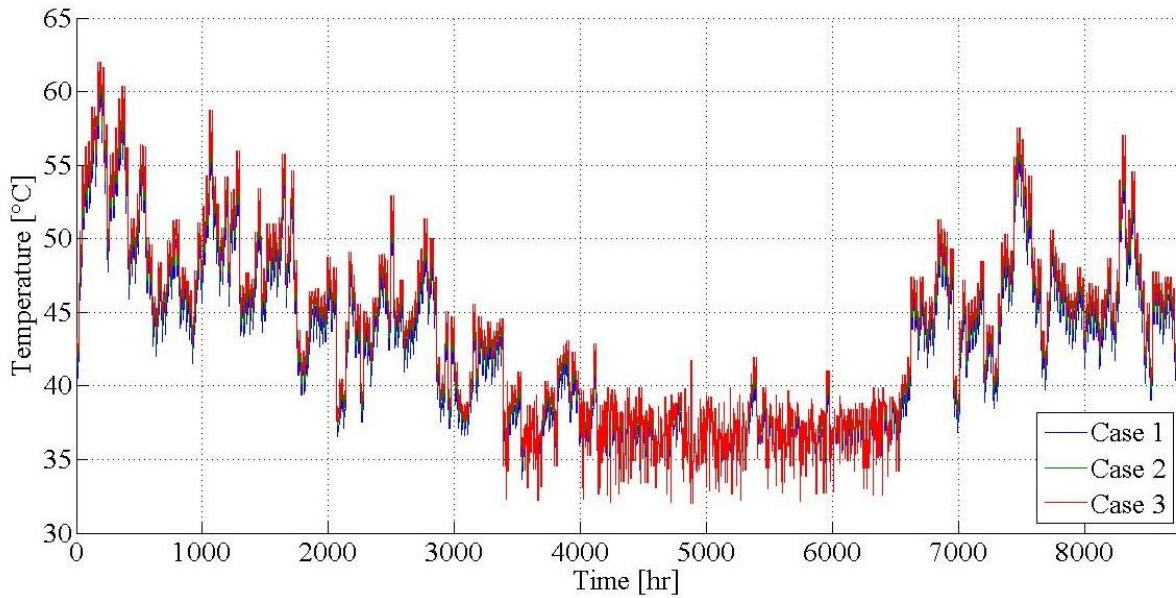


Figure 6-20 Hourly variation of temperature of redirected water to waste heat source

Duration curve of waste heat source contribution in the network is shown in Figure 6-21. Peak load for all case is increased. Also annual heat production is significantly increased, which is mostly due to reduction of temperature according to outdoor temperature. Integration of waste heat source is achieved for almost 6800 hours in the year with higher average heat load.

Case	G [Kg/s]	G/G _{max} [%]	Min. Temperature of hot water [°C]	Max. Heat power [MW]	Annual thermal energy production [GWh/year]	Average heat power [MW]
Case 1	10.2	9.6	70	1.5	7.9	0.9
Case 2	12.7	11.5	64.2	1.58	9	1.03
Case 3	15.5	14.6	60	1.6	9.5	1.09

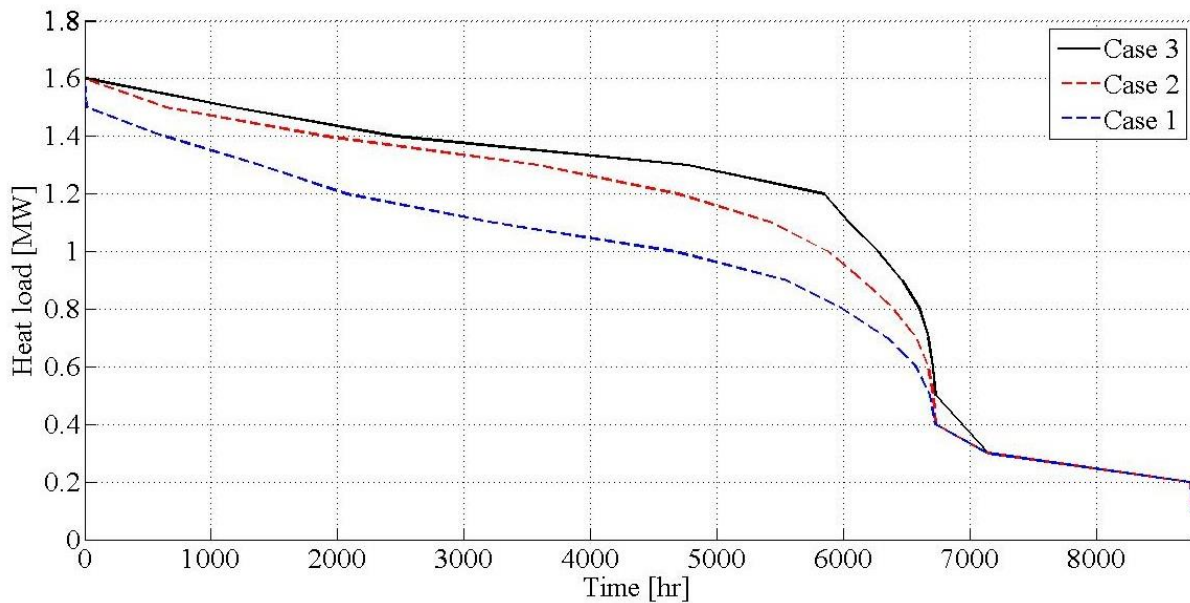


Figure 6-21 Heat power vs. number of hours

Adopting OTC lead to remarkable increase in peak load of waste heat source, however increasing the share of reheated water wasn't resulted in considerable increase in peak load from Case 1 to Case 3. This was due to capacity of the waste heat source and maximum temperature of the hot water.

Temperature of the water supplied by waste heat source is shown in Figure 6-22. In Case 1 for the whole year return water reheated to its maximum 70°C. In Case 2 and Case 3 despite of high heat production temperature of water supplied by waste heat source falls to minimum 61°C and more frequently in low demand hours. This is due to lower temperature levels in the network.

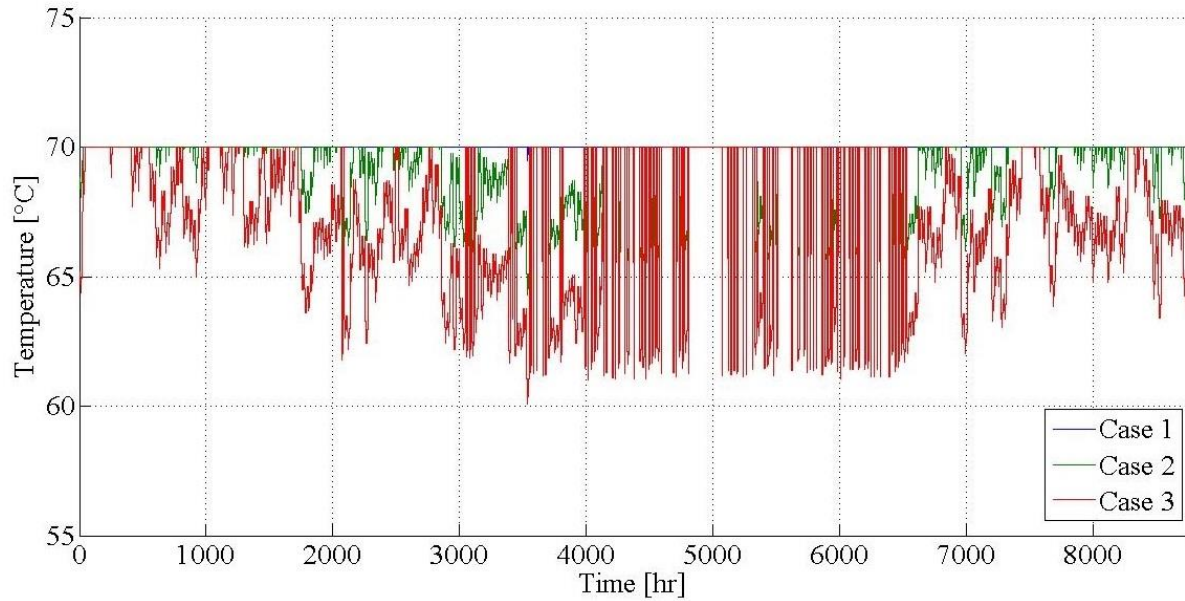


Figure 6-22 Hourly variation of water temperature at the outlet of waste heat source

Figure 6-23 compares energy performance of distributed heat energy source in the network. First of all, the effect of regulating temperature levels is clearly visible in heat production by this unit. In Reference scenario possibility of integrating waste heat source from datacentre is limited to 20% of annual heat request of campus in Case 3, some problems with hydraulic balance near waste heat source when higher share of waste heat is dedicated was diagnosed though. On the other hand, lowering temperature levels when outdoor temperature is higher in OTC scenario leads to providing colder water for heat recovery, as a result contribution of waste heat source in meeting heat request of campus gradually increases to 24% in Case 1 to 28% in Case 3. Despite of considerable increase in the amount of heat produced annually in OTC scenario, due to limited capacity of heat pump cycle at waste heat source substation, reheated water is introduced often with lower temperature grades which makes it difficult to utilize such heat.

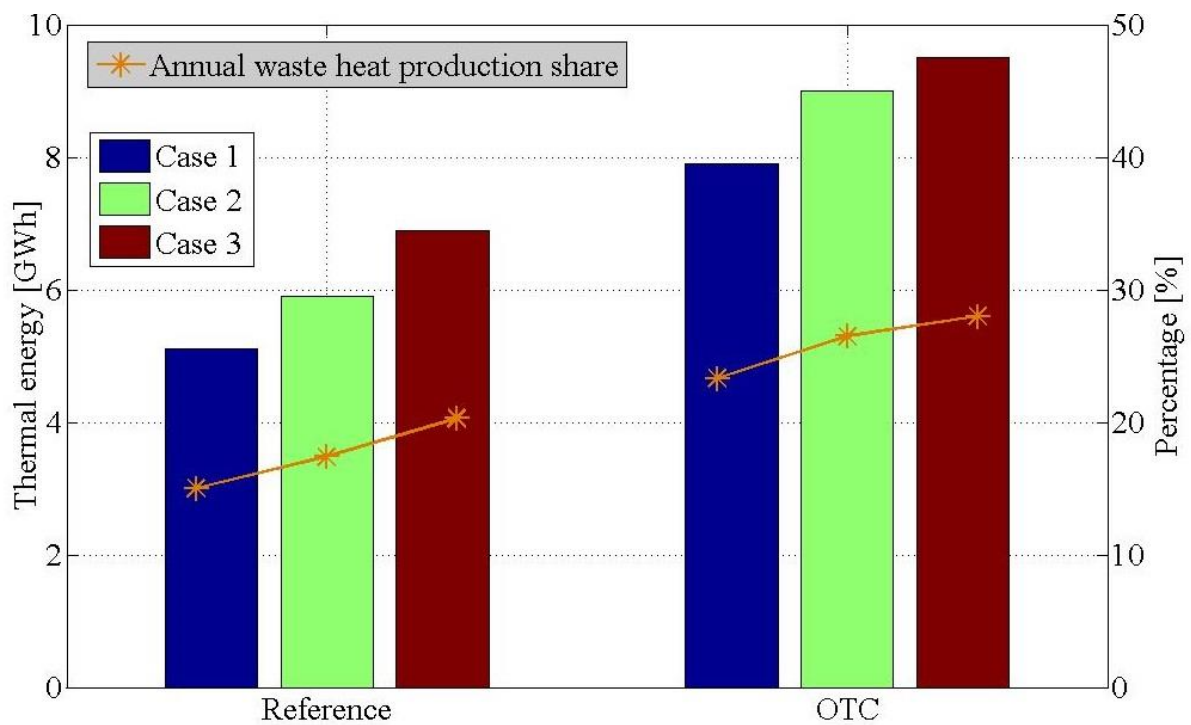


Figure 6-23 Annual renewable waste heat production comparison

Figure 6-24 shows supply and return temperature at main heat distribution building. Difference between supply and return temperature at first node in this scenario is lower, specifically in low demand hours. Integrating waste heat source to return line in this scenario together with regulating supply temperature makes the temperature difference at main distribution building to tend to be lower. For few hours of the year temperature of the return is higher than supply, which shows limitation for adopting higher share of renewable energy source combined with low temperature levels.

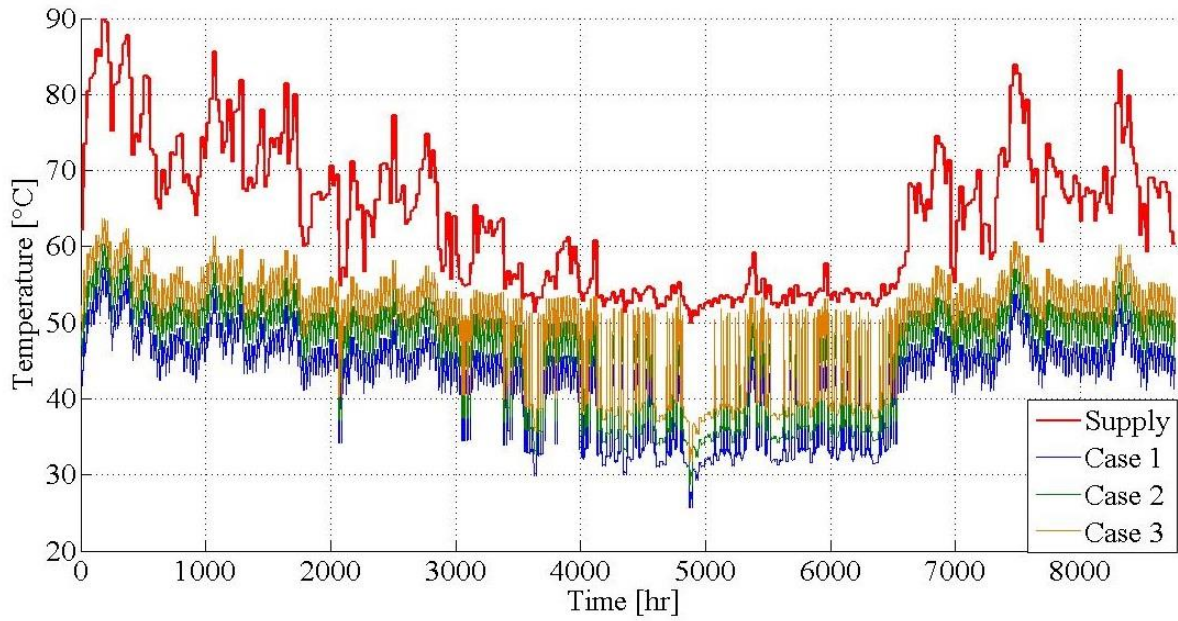


Figure 6-24 Hourly variation of supply and return temperature at main heat production building OTC scenario

Heat loss in pipe lines is shown in Figure 6-25 . Adjusting supply temperature significantly affects the overall heat loss in distribution process. During the low demand hours which are associated with lower supply temperatures, considerable decrease in heat loss is evident.

Table 6-3 Distribution energy losses in three cases OTC scenario

Case	Annual thermal energy loss [GWh/year]
Case 1	2.5
Case 2	2.7
Case 3	2.9

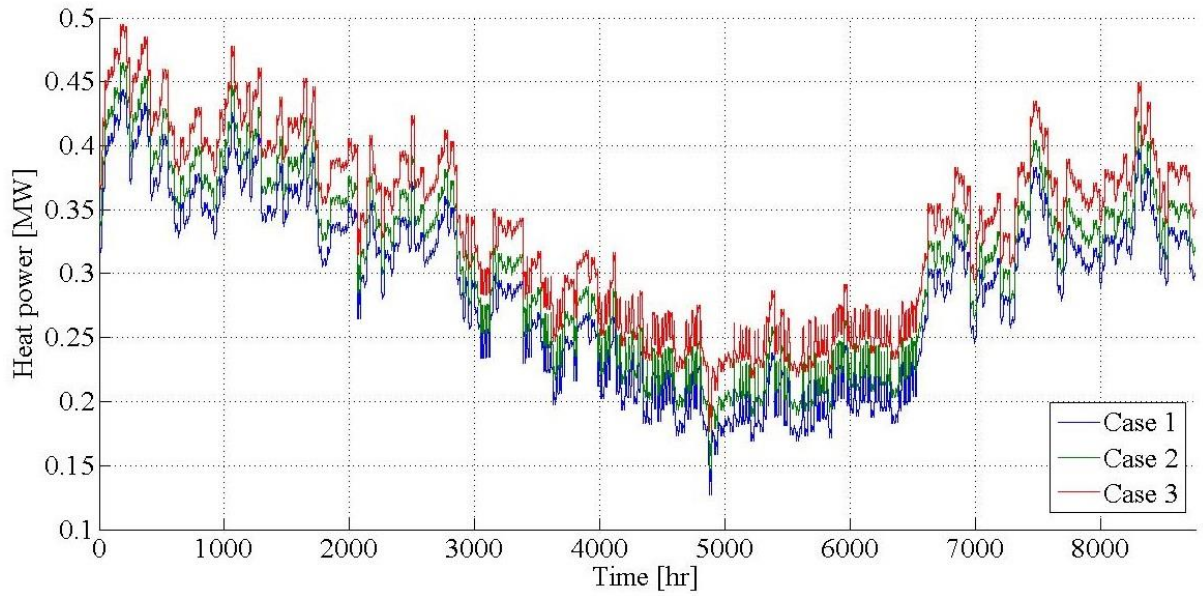


Figure 6-25 Hourly variation of heat power loss in the pipes OTC scenario

Comparison between the annual amounts of heat energy loss is shown in Figure 6-26. Considerable reduction of heat loss when adopting temperature compensation adjustment is one of the advantages of lowering temperature levels in district heating networks. However, regardless of temperature levels in the network by increasing share of renewable heat source slight increase in heat loss is evident.

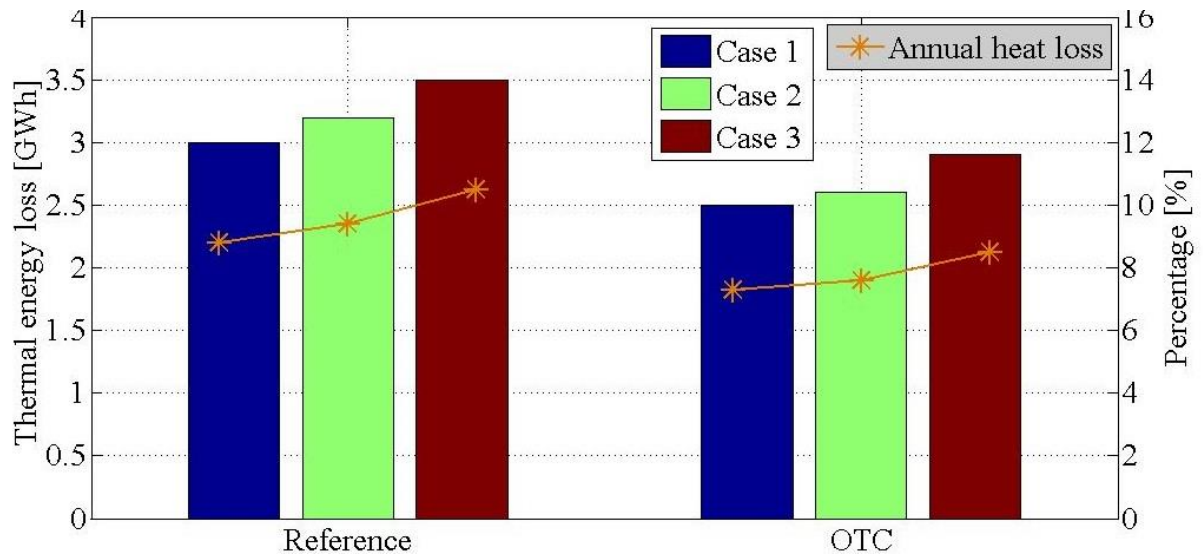


Figure 6-26 Annual heat loss comparison

6.3 Pump and valve control scenario

Pressure distribution in the network for design condition is shown in Figure 6-27. In this scenario pressure drop at the last user substation increased to 1.6 bar by closing the valve (Equation 4-30). Decreasing the pressure of return line leads to less pressure increase due to activity of waste heat source and consequently pressure at nearby nodes are less effected. Lowering pressure of return line is also affected the pressure at datacentre substation as shown in Figure 6-28.

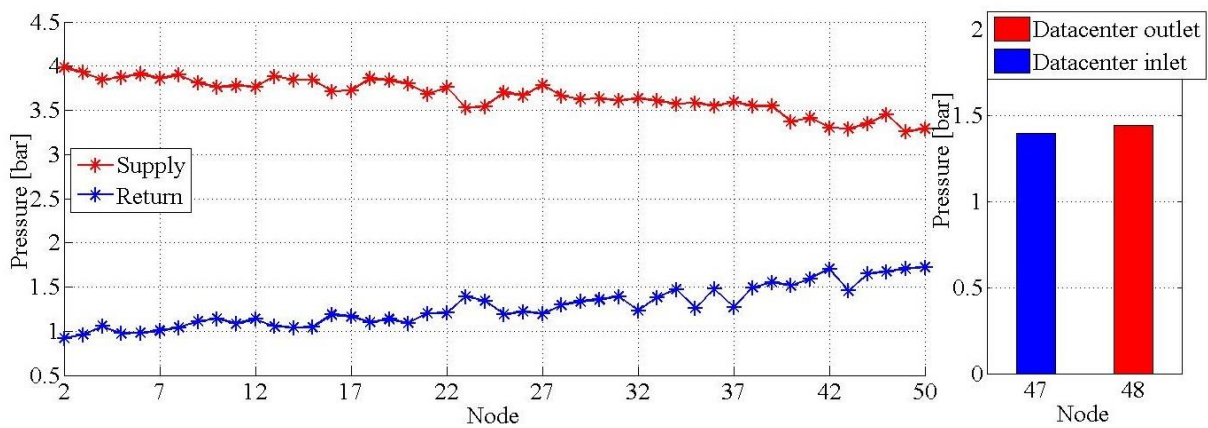


Figure 6-27 Pressure distribution in design condition for PC scenario

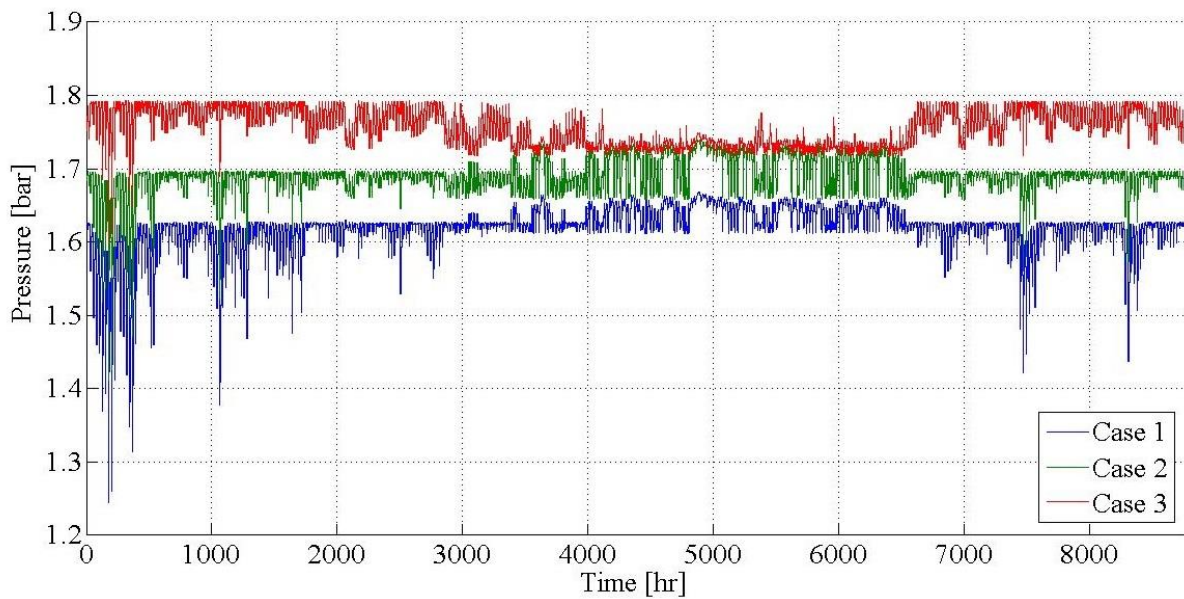


Figure 6-28 Waste heat inection pressure for PC scenario

Pump rotation speed has increased to 2808 rpm in order to ensure 3 bar pressure difference between supply and return lines in first node. In the Table 6-4 pump input power and annual energy consumption of pump is shown. Adopting control option for pump shows potentials for saving power of annual 33%.

Table 6-4 Pump energy consumption in two scenarios

Scenario	Maximum power kW	Annual consumption kWh/year
Reference	40.5	257.55
PC	41.2	172.78

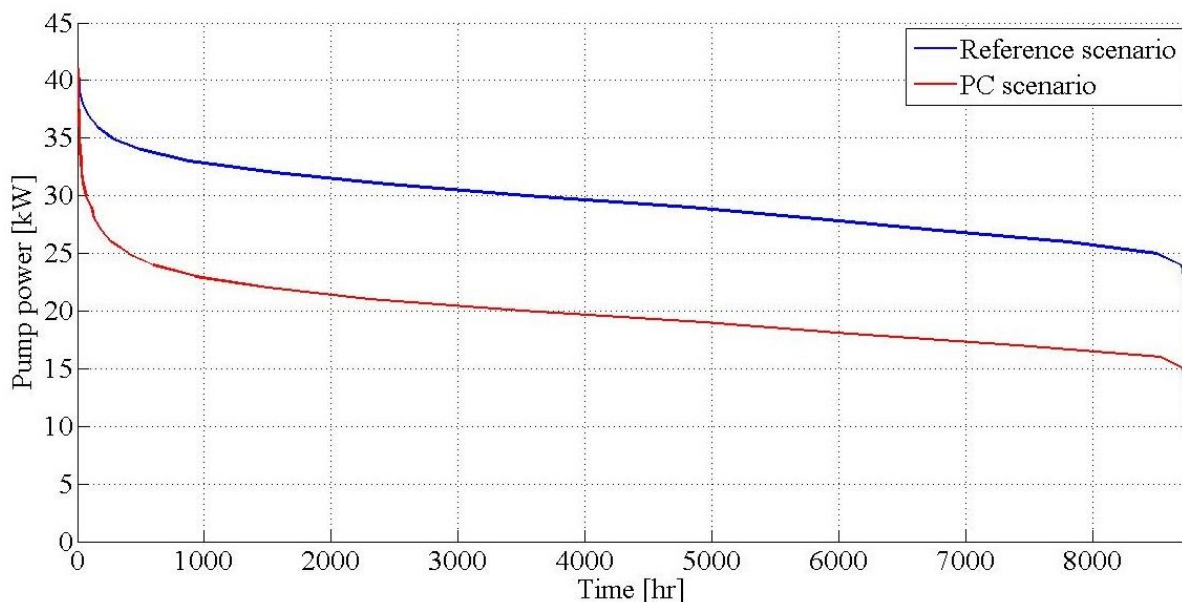


Figure 6-29 Duration curve of pump input power for reference and PC scenario

Comparing duration curves of input power in Figure 6-29 reveals that despite of a slight increase in maximum power, energy use of pump is dramatically reduced. This could also be an advantage for controlling pressure cones o waste heat source specifically when heat demand of the network is low and effect of waste heat source is more considerable in nearby nodes. Figure 6-30 compares pressure drop at a user near waste heat source in three cases in this scenario.

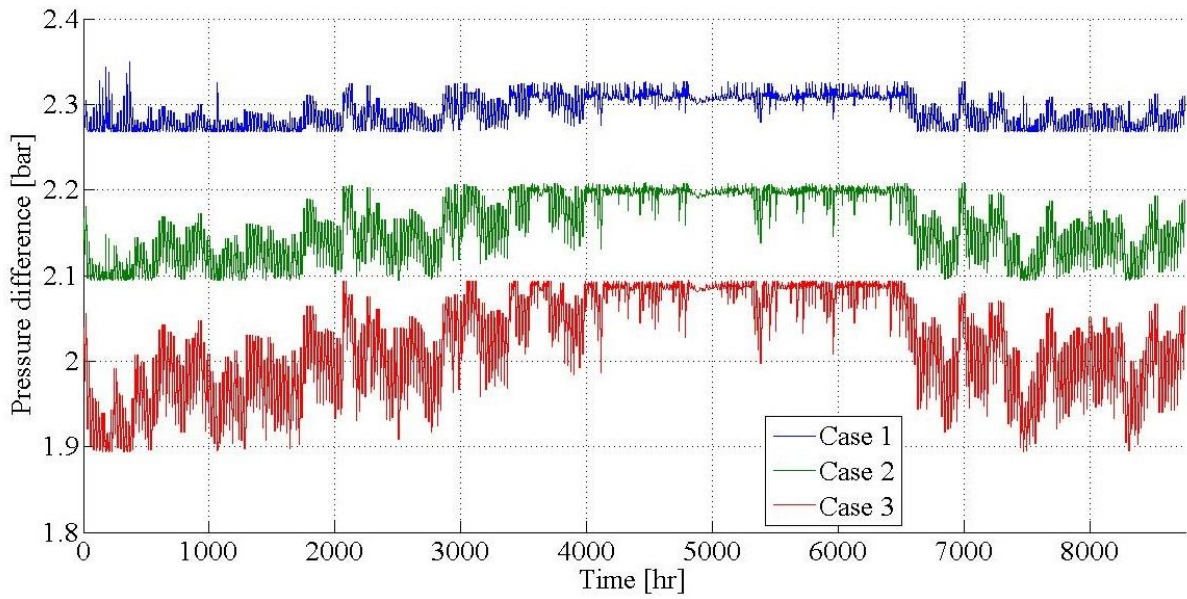


Figure 6-30 Hourly pressure gradient at user substation (PC scenario)

Like in the reference scenario pressure drop at user substation is reduced by increasing the share of waste heat source, however by controlling the pressure difference based on last substation higher pressure difference at users not far from datacentre was evident. In this scenario minimum pressure drop requirement for user substations was maintained in all three cases for the whole year.

CHAPTER 6

Discussion

Studying the DHS generally requires great deal of consideration in different parts of the network. Dealing with various consumer behaviour, presentation of proper model for thermo-mechanical components working in the network, and availability of information are examples of aspects to be considered within a model in which describes thermal and hydraulic behaviour of the application of district heating systems.

Thermal energy use and prediction of energy demand for building is one of the most influential motives for studying DHS. For the presented research thermal behaviour of the last one year was compared and actual data for overall thermal energy consumption of each consumer (including space heating and hot tap water) were used for simulation purpose. Relying only on statistical data might result in errors on outcome, however the reality of the behaviour of district heating network in Gløshaugen campus of NTNU is sufficiently illustrated. The network analysed with heat load capacity of 11 MW. Energy consumption of buildings depend on the type could be explained in detail by considering thermal losses due structural aspects, solar heat gain, hot water consumption, users activity, etc. moreover heat energy demand of the buildings in short and long term could be taken into account more delicately.

Hydraulic part of district heating model is highly effected by the quality of information and approaches dedicated for pipes. Selection of proper type and diameters for design purpose could be coupled with great number of detailed calculation and motivations. Also proper information

of configuration of the pipe connections in the network effects the quality of hydraulic balance in the network. In this study information provided by pipe manufacturers are used with only limit for maximum velocity on 1.5 m/s in pipes. The amount of pressure loss in the network was in the range of 120-170 Pa/m which seems to be reasonable, however precision in designing pipes directly leads to more efficient design of pumping system for network. From this point of view result of hydraulic balance in the network might be eclipsed by rough selection of pipes.

Connection of primary and secondary side is often a challenge when studying district heating systems. As a result of collecting data of overall thermal consumption of each consumer, simultaneously design of secondary substation is reduced to considering overall heat request of buildings. Consumer substations were modelled as a heat exchanger that receives all the requirement of the building. Design criteria of design of heat exchanger was influenced by adopting compensation solution for supply temperature. Temperature drop at consumer substations vary from 8°C to near 30°C in high demand hours. Lowering temperature levels demands heat exchangers to have a control method for temperature levels in secondary side.

Another substation which plays an important role in this network is waste heat source in datacentre building. Utilizing distributed heat pumps in district heating systems needs mechanical and economical justifications. Connection configuration that adopted in this network was done for reheating return water in order to feed return water. Heat capturing procedure in datacentre facility was modelled through design of a heat exchanger in which refrigerant vapour is cooled up to condensation temperature. Heat pump cycle could be defined by considering cooling demand of datacentre. In this study heat load capacity of reference network was assumed to be 1 MW, however increasing share of water circulated in heat pump cycle resulted in capturing more than 1.5 MW but in some cases with lower temperatures. The amount of heat loss had a considerable reduction when OTC scenario was adopted and a reduction of 3% in annual heat energy loss was evident, however increasing share of waste heat had a 16% negative impact on annual heat loss in the same scenario. This was due to increase in temperature of the main grids in return line.

CHAPTER 7

Conclusion

Integrating distributed renewable heat energy sources to district heating systems were discussed in previous chapters. A simulation study of district heating ring of Gløshaugen campus of NTNU which has integrated a waste heat source from datacentre were done in order to analyse the impact of this possible clean energy source. Heat load capacity of the CHDB was near 11 MW heat power for coldest weather condition. Utilizing distributed heat sources in conventional district heating systems comes with considerable advantages and also certain limits. Design and simulation of this network was done by dividing hydraulic and thermal aspects apart.

In calculation of hydraulic part presence of waste heat source played the role of a secondary source of energy, which means produced its own pressure cone. Interfering supply pressure of this waste heat source was shown that had negative effect on pressure balance of nearby consumer substations. This effect was bigger when the share of waste heat source heat production was bigger. Using the variable speed control for pump the pressure cone of the CHDB was maintained constantly 3 bar. Adopting appropriate control mode for pumping system together with simultaneous control of valve in consumer substation at farthest point of the network resulted in covering the pressure balance in consumer substation. Lowering pressure level however may cause extra pressure drop at users which are not affected by waste heat source. The variable speed control shown to be significantly cost efficient for the network, therefore importance of business planning for these type of networks is of a great importance.

The annual energy consumption of the pump was controlled from 258 MWh to 173 MWh which shows 33% cost saving potential.

In thermal part due to the type of integration of waste heat source (Return-Return) consumer substations were not affected by presence of secondary heat source, however dependency of waste heat source on user substation was more evident. Through reference scenario where constant supply temperature of 75°C was assumed for all heat demands it was revealed that higher temperature levels for supply water together with variable temperature drop at consumer substation which is often lower than expected leads to higher temperature of water redirecting to waste heat source. Higher mass flowrates of reheated water if it is agreed by hydraulic part can bring higher thermal efficiency and higher average annual heat load. Within the outdoor temperature compensation scenario possibilities for utilizing lower temperature levels were studied. Remarkable reduction of thermal losses due to distribution by 3% could be the most important economic advantage of lowering temperature levels. Furthermore, lower temperature levels by 20°C in summer resulted in higher waste heat recovery, however it was revealed that higher share of circulating water in datacentre substation causes reduction of water temperature to 62°C introduced by waste heat source. Generally return temperature at the CHDB should be lower, however it is increased by introduction of hot water from datacentre to return line.

Finally, integrating renewable thermal energy sources could be advantageous if necessary considerations are taken into account. Hydraulic balance of district heating system integrated renewable energy sources should take into account the weight and fluctuation of heat source as well as coping with the requirements of consumers so that the introduction of heat from distributed source is done both with required pressure and with respect to consumers affected by. For existing networks which majority of heat requirement is provided at CHDB hydraulic balance is highly depends on main pumping system. Variable speed control for pumping system was shown to be both cost saving and beneficial for controlling the pressure disturbances from utilizing distributed waste heat source. Lowering temperature levels in the network was shown to be effective in reduction of heat losses from 10% to 7% and improvement of integrating waste heat source. Reduction of temperature level however had drawbacks such as increasing influence of waste heat introduction to return line on temperature difference at the CHDB, reduction of harvested heat and inefficiency of consumer substation.

CHAPTER 8

Further work

Utilizing renewable heat sources are still challenging in different aspects. The introduction of prosumer to business models together with applying high tech. methods for efficient integrating distributed renewable energy sources requires further researches. Depending on size of the network and available renewable heat sources proper models and definitions should be established. Low grade heat produced from waste heat sources in specific, is still a main reason why penetration of this type of renewable energy source in practice and market is slight. High temperature levels existing DHS, must transit to LTDH in order to accommodate future energy sources. In order to improve integrity and stability of available distributed energy sources in the future district heating systems smart utilizing storage systems plays an important role.

Connection of distributed heat to the main network grids should be optimized according to availability of the source and temperature levels of the DHS. Distributed sources if could meet the planned heat demand with reasonable reliability could be connected to supply line. Control and adapting existing consumers to new thermo-mechanical characteristics of district heating systems using distributed heat sources seem to have a great impact on satisfactory integrating renewable heat sources, especially when prosumers production is supplied directly by nearby demands. Improvements in order to maintain hydraulic balance of the network when distributed sources are introducing heat is suggested.

Further work

Future district heating consumers request less heat due to energy saving measures. Delicate study of energy requirement of consumers and optimum distribution of heat power from distributed sources could result in a more efficient solution toward national and international clean energy goals.

Reference

- [1] Union I. Communication from the Commission to the European Parliament, the Council, the European Economic and Social Committee and the Committee of the Regions. An EU Strategy on Heating and Cooling.: Brussel, 2016.
- [2] Lund H, Möller B, Mathiesen BV, Dyrelund A. The role of district heating in future renewable energy systems. *Energy*. 2010;35(3):1381-90.
- [3] Nord N. Simple district heating scheme. 2012.
- [4] Union E. Proposal for a directive of the European Parliament and the council on the promotion of the use of energy from renewable sources (recast). *Official Journal of the European Union*. 2016;final/2:767.
- [5] Lund H, Werner S, Wiltshire R, Svendsen S, Thorsen JE, Hvelplund F, et al. 4th Generation District Heating (4GDH): Integrating smart thermal grids into future sustainable energy systems. *Energy*. 2014;68:1-11.
- [6] Lake A, Rezaie B, Beyerlein S. Review of district heating and cooling systems for a sustainable future. *Renewable and Sustainable Energy Reviews*. 2017;67:417-25.
- [7] Nord N, Schmidt D, Kallert A, Svendsen S. Improved Interfaces for Enabling Integration of Low Temperature and Distributed Heat Sources—Requirements and Examples.
- [8] sentralbyrå NS. Statistical yearbook of Norway/District heating: Statistisk sentralbyrå, 2016.
- [9] Brand L, Calvén A, Englund J, Landersjö H, Lauenburg P. Smart district heating networks—A simulation study of prosumers' impact on technical parameters in distribution networks. *Applied Energy*. 2014;129:39-48.
- [10] Grosswindhager S, Voigt A, Kozek M. Efficient physical modelling of district heating networks. *Modelling and Simulation*. 2011.
- [11] Haiyan L, Valdimarsson P. District heating modelling and simulation. Conference District heating modelling and simulation.
- [12] Hassine IB, Eicker U. Simulation and optimization of the district heating network in Scharnhäuser Park. Conference Simulation and optimization of the district heating network in Scharnhäuser Park, vol. 49. p. 1-18.
- [13] Ancona M, Branchini L, De Pascale A, Melino F. Smart District Heating: Distributed Generation Systems' Effects on the Network. *Energy Procedia*. 2015;75:1208-13.
- [14] Brand L, Lauenburg P, Englund J. DISTRICT HEATING COMBINED WITH DECENTRALISED HEAT SUPPLY IN HYLLIE, MALMÖ.
- [15] Sciacovelli A, Verda V, Borchiellini R. Numerical design of thermal systems. Clut, Torino. 2013.

Reference

- [16] Frederiksen S, Werner S. District heating and cooling: Studentlitteratur, 2013.
- [17] Guan J, Nord N, Chen S. Energy planning of university campus building complex: Energy usage and coincidental analysis of individual buildings with a case study. *Energy and Buildings*. 2016;124:99-111.
- [18] Standard N. S-002 Working environment, rev. 4. 2004.

Appendix

Implementation of SIMPLE algorithm and FIXED-POINT loop

A Matlab code has been implemented in order to obtain the pressure at each node and the mass flow rate for each branch. A “while” cycle is used to solve the SIMPLE algorithm that contains inside another “while” for the fixed-point method, which solves the nonlinear equation. The results of this procedure are the real mass flow rates and pressures. Together with the while loops it is defined for the SIMPLE and Fixed-Point algorithms a function which calculates the corresponding values for hydraulic conductance of each branch of the network. The calculation of the error of the SIMPLE Algorithm has been performed considering the maximum between the values of the corrections on the pressure and the mass flow rate. The truncation criterion used for the Fixed-Point consisted in calculating the error on the value of the mass flow rate by considering the difference between the i^{th} and the $(i-1)^{\text{th}}$ step. The value of the error to be compared to the tolerance has been chosen to be the maximum of the values calculated for each branch.

Tolerances of 10^{-3} and 10^{-6} are used to verify convergence in the SIMPLE algorithms and Fixed-Point respectively.

The boundary conditions have been imposed modifying properly the \mathbf{H} matrix and the \mathbf{b} vector, in order to avoid the correction of the element which corresponds to it.

From the guessed values of pressure, the SIMPLE loop performs its iterations, thanks to the "while" cycle, until it reaches the convergence using the concepts of Residuals coming from Momentum Equation that must be lower than the tolerance. The new values are obtained from correction of updated residuals using the defined under-relaxation coefficients. The chosen values are 0.1 for the SIMPLE (for both pressure and mass flow rate) and 0.3 for the Fixed-Point.

The calculations are organized in a main script that is the only one to launch. The first section “data input” is devoted to the initialization of the main data such as geometrical data, thermo-physical data and logical data like the numeration of the nodes, definition of user nodes and inner nodes and the build of the incidence matrix \mathbf{A} for both the supply and return configurations.

Matrix \mathbf{A} is built in a proper function that require as input the number of node, the number of branches, and two logical vector containing one the inlet nodes for each branch and the other the outlet nodes of each branch.

The second section of the main code solve the fluid-dynamic problem. This function requires as input the numbers of node and the number of branches, the prevalence of the pump, the matrix \mathbf{A} and the vector of the requested flow rate at the user; and give as output the number of iterations of the simple algorithm the final vectors of pressure at nodes and mass flow rate in the branches, and two vectors containing the error behavior of \mathbf{P} and \mathbf{G} during calculation.

The function, first build the vector \mathbf{t} , then after the definition of the necessities vectors and data solve two while cycles, the inner one is devoted to the solution of the fixed point algorithm and once the mass flow rates related to the guessed pressures is found, the outer while cycle, evaluate the correction on the pressures. Conductance matrix \mathbf{Y} is built in another function that receive as input the only a flow rate vector.

Once the FD problem is solved and the mass flow rates are available, all the point regarding thermal problem are solved directly in the main code.

In this part firstly the code builds the matrix \mathbf{K} and vector \mathbf{f} for the supply circuit:

two “for” cycles and an “if” one analyze matrix \mathbf{A} in order to find which branch send its flow rate to the node i and which one receive is flow rate from node i and consequently compile the vector \mathbf{f} and the proper cells of matrix \mathbf{K} .

Then the boundary conditions for the inlet node (the plant) and for the outlet ones (users) of the network are imposed: another for-for-if cycle is built in order to modify properly diagonal and non-diagonal elements of matrix \mathbf{K} .

The return cycle is built in the same way, only inverting the user’s nodes and the plant’s node boundary condition. Another inlet and outlet nodes in return cycle are associated with decentralized production node.

